Sedimentary microplastic contamination in a Bavarian river system – Alz

Bachelor thesis to graduate for

Bachelor (U)

Bachelor of Science (BSc)

UNIVERSITY OF VIENNA

Presented by:	Mario Bubl
Matriculation number:	01502454
At:	September 24, 2018
Supervisor:	ao. Univ.-Prof. Dr. Michael Wagreich

Abstract

Sedimentary microplastic contamination of the German river Alz was analysed with the aim to acquire further information about how high the concentration of plastic in Alpine catchment is. Furthermore, it was a goal to find out whether anthropogenic influence from bigger cities (wastewater treatment plants) and factories affects the accumulation rate of plastic, especially in smaller river systems.
Along the Alz, 24 (19 sandy, 5 clayey) samples were collected. The 19 sandy river bank sediments were visually subdivided with a binocular microscope - every inferred plastic particle was sought out. Extrapolated onto one kilogram/sediment a total amount of 659555 objects ($<$5 mm) were separated – categorised in fibres, microbeads, fragments and films. Sample site "After Truchtlaching" with 81604 particles/kg contains most pieces found per sample.
To figure out whether the objects that were found really consisted of plastic and also as a method for polymer indification, Raman-spectroscopy was conducted. It was feasible to ascertain a organic pigment phthalo green (copper phthalocyanine) used for colouring thermoplastics in a green-gray microbead at the site "After Trostberg" as well as blue pigments in fragments at the sites "After Burgkirchen" and "Runoff, Marktl". Additionally the origin of a fibre as p-(Ethylene terephthalate) was measured. The accumulation of fibres is especially noticeable around the bigger cities and the greatest abundance of microbeads was estimated at public hot spots.
In context to obtain superior knowledge of sedimentary microplastic contamination in smaller river systems, which are contributory to larger rivers ending in the world's oceans, more studies are needed to be done in the future.

Contents

List of Figures

List of Tables

1 Introduction

Humanity is using synthetic organic polymers, which are better known and combined with the therm “plastic”, on a global scale. The benefits of these materials are well known but the bad impact on the global terrestrial and marine environment, because of poor recycle systems and failure in policy, makes the short and long term risks alarming. From the year 1950 with a global plastic production of 10 million tonnes, there has been an increase to around 335 million tonnes in 2016 [1] [2]. An international research team published, that in the year 2010, 192 coastal countries produced 275 million metric tons waste consisting of plastic. 4.8 to 12.7 million tons of this plastic waste entered the oceans [3]. Scientists ascertained in 2014 more than 5.25 trillion particles are drifting in the sea [4].
Sedimentary microplastic contamination of smaller rivers in Alpine catchments has received little attention in the past, therefore the survey on the river Alz is conducted with the aim to find out the concentration of plastic particles compared to those consisting of minerals and organic material.
The river Alz is one of the contributory of the Danube (Inn $\rightarrow$ Danube $\rightarrow$ Black Sea). According to a survey over two years, when stationary driftnets where placed in the Austrian Danube, it was detected, that the abundance of plastic was higher than the larval fish floating in the river [5]. The amount of all the plastic that flows from the second largest river of Europe into the Black Sea is estimated to be about 4.2 metric tons per day [5].
The microplastic data will give us a better idea about how high the contamination of those small plastic particles especially in smaller river systems is. In addition, my goal is to point out a relation between samples with higher contaminations and public hotspots like cities and factories. Furthermore, the analyses using Raman-spectroscopy should point out the amount of different polymers, such as Polyethylene or Polystyrene.

2 Background information

2.1 River Alz

Figure 1: River Alz

The study area is a river in Southern Germany which is called Alz. It originates from Lake Chiemsee, the largest lake of Bavaria with 79.9 km^2 [6], which is mainly fed by the Tiroler Ache (Ostalpin) [7]. The main influx of the observed river apart from the lake is from the river Traun. The river Alz runs through the Molasse basin of the German State Bavaria with a length of about 63 km and terminates close to the city Marktl where it merges with the river Inn.

The river can be divided into two parts. The so called upper Alz (obere Alz) and the lower Alz (untere Alz). The upper part reaches from the city of Seebruck to the town of Emmerting. In this section of the river one can observe a higher anthropogenic influence than in the lower part.

Mean water level in summer amounts 84.0 cm (1970 - 2013) at Seebruck, 115.0 cm (1970 - 2013) at Trostberg and 51.0 cm (1975 - 2013) at Burgkirchen with a volumetric flow rate in summer of $60.5 m^3/s$ (1931 - 2013) at Seebruck, $25.5 m^3/s$ (1951 - 2013) at Trostberg and $16.9 m^3/s$ (1951 - 2013) at Burgkirchen [8].

2.2 Microplastic

Since the 1970s plastic has been contaminating the environment and especially marine ecosystems. In the year 1972 Carpenter and Smith revealed with the help of neuston nets a surface occurrence of small plastic particles on the Sargasso Sea [9] [10] [11].
Microplastic contamination is pervasive all over the planet. Likewise in every marine ecosystem such as the deep sea and the polar regions. Not only in water column of the open ocean, however even in terrestrial environments and on shorelines of remote islands the plastic particles accumulate [12] [13] [14] [15].
Recent publications and the press report from 2013 of the marine strategy framework directive (MSFD) technical subgroup on marine litter, it is recommended to categorise plastic in context of size as follows. Macroplastic should be determined >25 mm, mesoplastic from 5 - 25 mm and everything less than 5 mm as microplastic [16] [17]. Furthermore, MSFD Guidance subdivides microplastic in large (1 - 5 mm) and small (<1 mm) [17].
The large surface to volume ratio of plastics consisting of different types of polymers enables them a great absorbing capacity for persistent, bioaccumulative, toxic compounds (PBTs) as well as persistent, organic pollutants (POPs) and metals [18] [19]. Additionally, plastics generally speaking contain additives such as plasticizers (dibutyl phthalate or diethylhexyl phthalate), which affect several hormone systems of fishes, amphibians and invertebrates [20]. Furthermore, these particles can consist of fillers, stabilizers or pigments, which are according to literature as frequently toxic [20] [21].
In context of global warming, scientists found out, that microplastics which have been enriched and frozen in the Arctic Sea ice is melting into the world‘s oceans. The amount of these objects conserved in the ice is calculated to be higher than those of the surface water of the greate plastic gyres [22]. Because of gobal distribution likewise in remote environments (polar regions, deep sea floor), microplastics represent on the one hand an expedient for biostratigraphical correlation in the geological archive and on the other hand a good indicator of Anthropocene strata [23].

3 Setting and methods

3.1 Setting

(a) Before Emmerting (b) After Emmerting

Figure 2: Setting

When planning the fieldwork, I was searching for convenient spots to take samples of different river sediments. As a first testable hypothesis, after the river passes cities, the amount of microplastic is expected to be higher. Thus, I chose these particular areas to take samples. Examples of these "Down-City-Areas" are for instance, Altenmarkt with approximately 4.300, Trostberg with roughly 11.500, Garching with about 8.500 and Burgkirchen with around 10.500 inhabitants [24] [25] [26] [27].
The lower Alz is a nature reserve with 7.6 km^2 and thus the largest protected area in the administrative district of Altötting [28]. As a second hypothesis, since nature reserves are supposed to be cleaner than non- protected areas it was also important to collect samples in this part of the river. The aim was to draw comparisons between the upper and the lower Alz, which reflect a non-protected and a protected area.

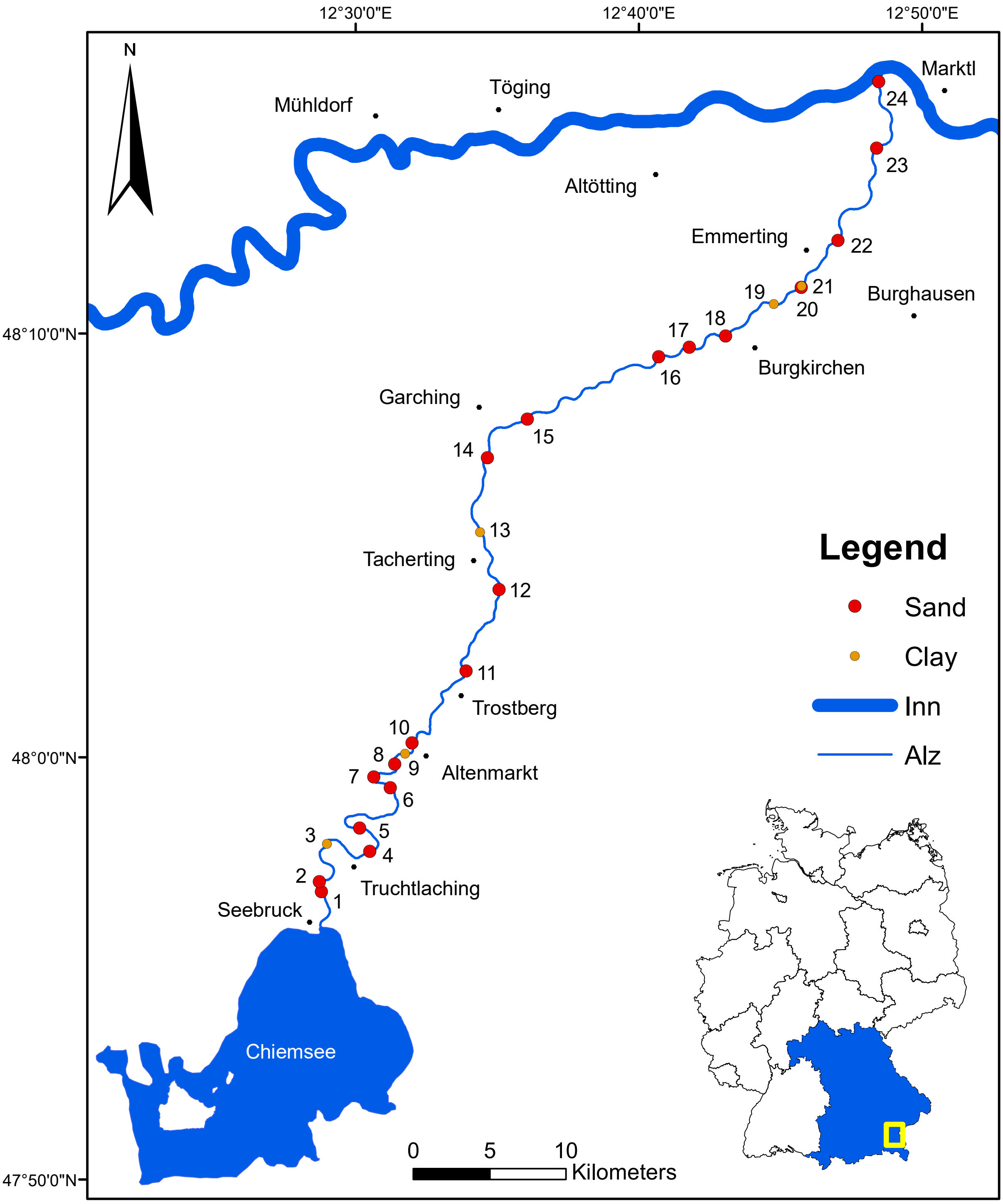

Coordinate System: WGS 1984 Web Mercator Auxiliary Sphere
Projection: Mercator Auxiliary Sphere

3.2 Sample collection

(a) Apple seed engraver (b) Stainless steel spoon

Figure 3: Sampling techniques

The survey was conducted in August 2017. In anticipation of finding sandy and clayey sediments at the river shores, I was trying to find the best way of collecting and storing the samples. Sediments with a variation in grain size were collected with a stainlesssteel-spoon (Shovel-lenght: 7 cm). For sediments with smaller grain size such as clay and silt, a stainlesssteel-appleseedengraver *SAE* (∅ 1.7 cm; lenght: 7 cm) was used. With this technique, I was able to have a constant withdrawal of the top 7 cm of surface sediment. Along the 63 km course of the Alz, 24 samples of bank material under the water surface were taken, which correspond on average one setting spot every 2.6 km. All samples were kept in distilled brown laboratory vials (100 ml) with glass or natural cork plug, at temperatures around 10°C during the whole survey and the transport from Bavaria to Vienna/Austria. The sediments are then stored at a constant temperature of 8°C (Dept. Palaeontology; Uni Vienna).

Table 1: Setting and methods

Sample	Site	Environ.	Type	Year	Month	Lat. (°)	Long. (°)	Dry Sediment-Weight [g]	Found pieces per kg
$S01$_0817	Tributary,Chiemsee	Molasse basin	Spoon	2017	Aug	47.947	12.480	153.622	78173
$S02$_0817	Pullach	Molasse basin	Spoon	2017	Aug	47.951	12.479	115.624	41077
$S03$_0817	Before Truchtlaching	Molasse basin	SAE	2017	Aug	47.966	12.483	20.399	NM
$S04$_0817	After Truchtlaching	Molasse basin	Spoon	2017	Aug	47.963	12.508	107.15	81604
$S05$_0817	Seeon-Seebruck	Molasse basin	Spoon	2017	Aug	47.972	12.502	126.488	20759
$S06$_0817	Roit	Molasse basin	Spoon	2017	Aug	47.988	12.520	128.106	25553
$S07$_0817	Massing	Molasse basin	Spoon	2017	Aug	47.992	12.511	194.291	24341
$S08$_0817	Laufenau	Molasse basin	Spoon	2017	Aug	47.997	12.523	168.513	31685
$S09$_0817	Barrage Altenmarkt	Molasse basin	SAE	2017	Aug	48.001	12.530	18.512	NM
$S10$_0817	After Altenmarkt	Molasse basin	Spoon	2017	Aug	48.006	12.533	175.104	15349
$S11$_0817	After Trostberg	Molasse basin	Spoon	2017	Aug	48.034	12.565	156.176	57171
$S12$_0817	Before Tacherting	Molasse basin	Spoon	2017	Aug	48.066	12.584	123.226	26429
$S13$_0817	After Tacherting	Molasse basin	SAE	2017	Aug	48.089	12.573	46.012	NM
$S14$_0817	Before Garching	Molasse basin	Spoon	2017	Aug	48.118	12.578	114.834	69945
$S15$_0817	After Garching	Molasse basin	Spoon	2017	Aug	48.133	12.601	117.152	48134
$S16$_0817	After Hirten	Molasse basin	Spoon	2017	Aug	48.157	12.678	188.558	5898
$S17$_0817	After Hirten	Molasse basin	Spoon	2017	Aug	48.161	12.696	144.869	13458
$S18$_0817	Before Burgkirchen	Molasse basin	Spoon	2017	Aug	48.166	12.718	147.828	48501
$S19$_0817	After Burgkirchen	Molasse basin	SAE	2017	Aug	48.178	12.746	29.938	NM
$S20$_0817	After Burgkirchen	Molasse basin	Spoon	2017	Aug	48.185	12.762	221.695	18957
$S21$_0817	Before Emmerting	Molasse basin	SAE	2017	Aug	48.185	12.763	15.582	NM
$S22$_0817	After Emmerting	Molasse basin	Spoon	2017	Aug	48.203	12.784	106.339	32596
$S23$_0817	Nature reserve	Molasse basin	Spoon	2017	Aug	48.239	12.807	236.782	5614
$S24$_0817	Runoff, Marktl	Molasse basin	Spoon	2017	Aug	48.270	12.814	202.781	14311

4 Analytical methods

4.1 Smear Slides

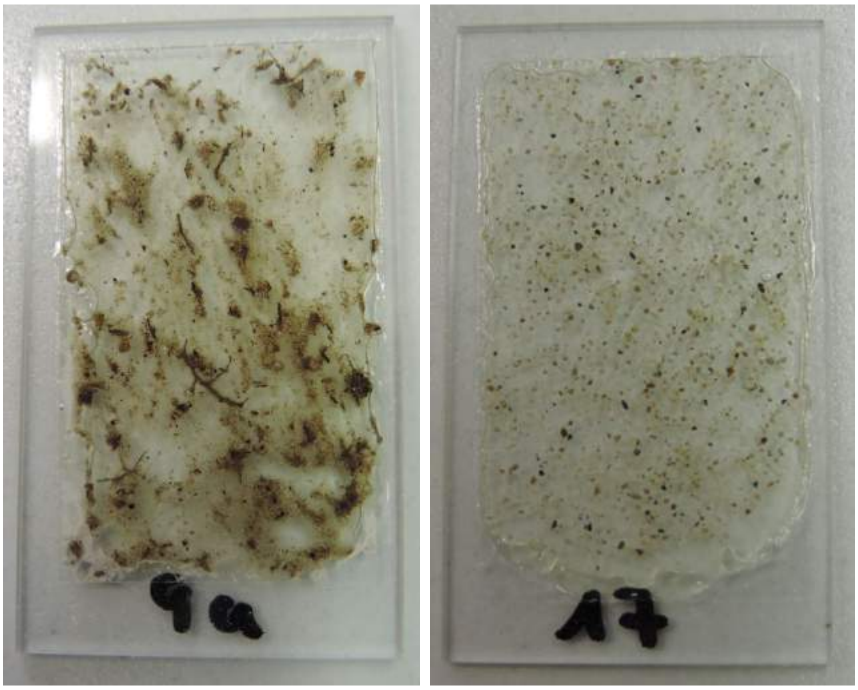

(a) Clay (b) Sand

Figure 4: Smear-Slide

In order to visualise the samples with a transmitted light microscope (Department of Geodynamics and Sedimentology; Uni. Vienna), the sediment samples were prepared on smear slides. This gives an idea about concentration of different minerals, organic amount and in the context of searching for microplastic especially the incidence of fibres, films, fragments and flakes.
Furthermore, this analysis assist to glean further analytic procedure, such as cleaning the sediments of organic material, by severally conditioning with hydrogen peroxide (H_2O_2).

Preparation

Avoiding contamitaion by plastic, like fibres from clothes, a laboratory coat was worn, during the preparation of the smear slides. For each individual operation all the instruments were cleand with Aceton ($(CH_3)_2CO$).

(a) Petri dishes (b) Hotplate

Figure 5: Preparation

Sand: With a small spatula, a representative as possible amount of the coarser sediments were taken, put into Petri dishes and kept 24 houres by 40°C in the dry cabinet. The Microscope Slides 28 x 48 mm thickness 1.55 mm ± 0.05 mm were put on a hot plate with around 120°C. Once the heat build-up, Canada Balsam for clinical diagnosis is melted on the Slide. Subsequently the samples are interspersed straight into the resin and coverd with Cover Slips 24 x 40 mm. During refrigeration the Slides are hardened and prepared for visualising.

Clay/Silt: In almost the same manner such as the process of sandy samples, a prestigious amount of dried clay respectively silt is taken from the Petri dishes put directly on the Cover Slips and is streaked with a pin in a drop of purified water. After considerable time the Slips are placed on the Microscope Slides with the melted Canada Balsam. The Slides were cooled and stored for visualising with a transmitted light microscope (Department of Geodynamics and Sedimentology; Uni. Vienna).

4.2 Sediment-Splitter

(a) Sediment-Splitter (b) Laboratory Vial

Figure 6: Splitting

Using an electronic Sediment-Splitter (Department of Geodynamics and Sedimentology; Uni. Vienna), the samples were separated into small representative amounts (1-4 g) of the total quantity and stored in laboratory vials (20 ml) with a natural cork plug. This method was used to prepare them for the visual sorting and separation.

The focus of this thesis was on samples with variation in grain size > 63 μm. All clayey and silty samples (S03_0817, S09_0817,S13_0817, S19_0817, S21_0817) are no longer in use, because the particles are too small for accurate visual sorting and seperation.
Furthermore, in context of this bachelor-thesis the decision of using visual sorting has been made, since it is easy to accomplish and cheap [16].

4.3 Visual sorting and separation

(a) Binocular (b) Storage bin

Figure 7: Sorting and Separation

Visual sorting and separation of plastic particles was done with a binocular microscope (Department of Geodynamics and Sedimentology; Uni. Vienna). The splitted samples were spread out into a ceramic bin. With a pin all particles which purports to consist of different kind of polymers were seperated and put into paleontologic storage bins. Meanwhile the found pieces were counted and categorised into fibres, microbeads, fragments and films.
All collected data was projected onto kg and visualized in graphics. (6.2 Measurement and morphology of found particles: Table 4 and bar diagram below)

4.4 Grain size analysis

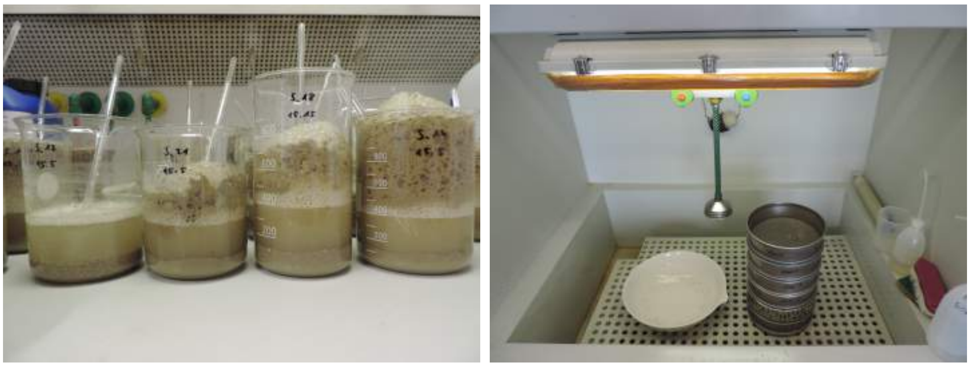

(a) Preparation with H_2O_2 (b) Sieving

Figure 8: Grain size analysis

Initially the collected samples were filled into graduated beakers and the weight was measured. Samples with a variation in grain size contain a various amount of organic material. Preparing them for sieving, all sands needs to be dosed with hydrogen peroxide (H_2O_2). Furthermore, a 400 watt ultrasonic bath was used to avoid the cohesion of particles.
Samples were washed through successively decreasing sifters. Mesh size of the sieves ranges from 2 cm to 63 µm. The fractions have been dried and weighed (Table 2, 3).
Objective target was to find out, if there is a correlation between grain size and abundance of fibres. Thus, the amount of small particles like fibres may be higher in corser or finer sands - greater in well sorted or poor sorted or rather dependent on the location.

4.5 Raman spectroscopy

Raman spectroscopy was used to analyse the different types of polymers the microplastic particles consist of.

Functional principle: All Raman measurements were implemented with a HORIBA JOBIN YVON LabRAM HR 800 spectrometer (Dept. Mineralogy and Crystallography; Uni. Vienna). Monochromatic light in form of a laser (green: 532 nm, red: 633 nm, infrared: 785 nm) is put on the material which needs to be analysed. The molecules absorb a part of the laser energy. Thereby light can be observed which has less energy,

what is visualised in a graph. During elastic collision of the photones with the molecules a change in energy can be estimated, which is specific for each material.
Based on the main bands of the phases, the spectra can be compared with the database (Thermo Fisher Scientific Inc.: Spectral IR Database; Bio-Rad's Spectral Databases version 9.00 R2) what should reveal of which material the particles consist of.

Instrument settings: All found pieces were measured at room temperature with infrared excitation laser (785 nm), using 50x and 100x objective - 600 groves/mm - 5, 40 and 60 s integration time - different steps of intensity (25%, 50%, 100%). Spectral range was set on -15 - 4000 cm^{-1}.

Regarding the high amount of particles found in all samples it was not manageable to analyse all seperated types of inferred plastic objects in context of this bachelor thesis. Therefore I concentrated on the most promising examples.
All photos were taken by my own with a Canon PowerShot G15 and a Nikon COOLPIX P520. GPS data was meassured with mobile app Locus Map.

5 Error range and uncertainties

Airborne contamination of fibres is one of the greatest problems of analysing sediments on microplastic. During sample collection and all analytic steps I tried to minimise the risk of extra contamination as effectively as possible. While working with the sandy samples exclusively clothes produced out of 100% cotton and a laboratory coat was worn as well as using only plastic-free material. More precise investigations concerning this study need to be probed in special facilities, such as cleanrooms. Otherwise it is not possible to prove that, all founded particles originate from the taken samples. Normal chemistry lab of the Faculty of Earth Sciences/Vienna are not designed to avoid extra contamination of microplastic, hence a certain proportion of the findings in the samples of the riverbanks can be airborne contamination.

Furthermore, no strict protocol or guideline in context of searching and analysing sediments on microplastic exist in the scientific community in general (measurements, sample techniques, analytic methods and so forth). Therefore the resulting data from the different studies are hardly or only with caution comparable with each other [16].

6 Results

6.1 Analytical methods

Visual sorting and seperation: Whilst working with the binocular, it became apparent that, the smaller grain size of samples was, the higher the amount of discovered fibres was. Challenges during visual sorting and seperation were the reason for the very fine grain to cohere. Samples with corser grain size were estimated with an decreasing number of fibres.

Grain size analysis: The elicited reaction of the sandy material with H_2O_2 was categorized into vigorous, mean and poor reaction. Concentration of organic material in samples $S05\_0817$, $S06\_0817$ and $S14\_0817$ was estimated with the highest and in samples $S16\_0817$, $S17\_0817$, $S23\_0817$ and $S24\_0817$ with the lowest amount.
Folk and Ward method resulted in, that $S07$ (1816.9 μm) is on average the coarsest and $S22$ (157.1 μm) the finest sample. Most poorly sorted sample is $S06$ (3.615 μm), whereas $S17$ (1.475 μm) is the best sorted.
In the following tables detailed data to all samples is given. The sedimentary environments have been classified and vizualised with Gradistat [29]. Extensive results of the grain size analysis is attached in the appendix.

Data from table 2 shows the amount-factor of the respective categories from the total amount of dried sediment used for this analysing method. The histogram below visualizes the distribution of the grain fraction in every sample.

Table 2: Grain size analysis

Sample	Category1 >2 mm	Category2 2-1 mm	Category3 1-0.5 mm	Category4 0.5-0.25 mm	Category5 0.25-0.125 mm	Category6 0.125-0.063 mm
$S01$	0.437	0.136	0.111	0.113	0.076	0.044
$S02$	0.010	0.019	0.049	0.167	0.469	0.158
$S04$	0.176	0.094	0.155	0.250	0.129	0.027
$S05$	0.387	0.074	0.068	0.160	0.148	0.058
$S06$	0.325	0.046	0.085	0.138	0.125	0.125
$S07$	0.667	0.194	0.080	0.022	0.015	0.008
$S08$	0.559	0.105	0.132	0.122	0.042	0.014
$S10$	0.349	0.174	0.244	0.160	0.035	0.010
$S11$	0.323	0.017	0.019	0.190	0.286	0.090
$S12$	0.005	0.001	0.009	0.258	0.486	0.150
$S14$	0.032	0.008	0.072	0.443	0.230	0.093
$S15$	0.042	0.002	0.013	0.333	0.424	0.105
$S16$	0.363	0.079	0.188	0.330	0.028	0.003
$S17$	0.012	0.004	0.144	0.738	0.086	0.005
$S18$	0.308	0.027	0.033	0.207	0.286	0.086
$S20$	0.423	0.086	0.066	0.256	0.125	0.020
$S22$	0.007	0.007	0.032	0.259	0.360	0.219
$S23$	0.514	0.215	0.170	0.077	0.010	0.002
$S24$	0.574	0.054	0.021	0.154	0.107	0.041

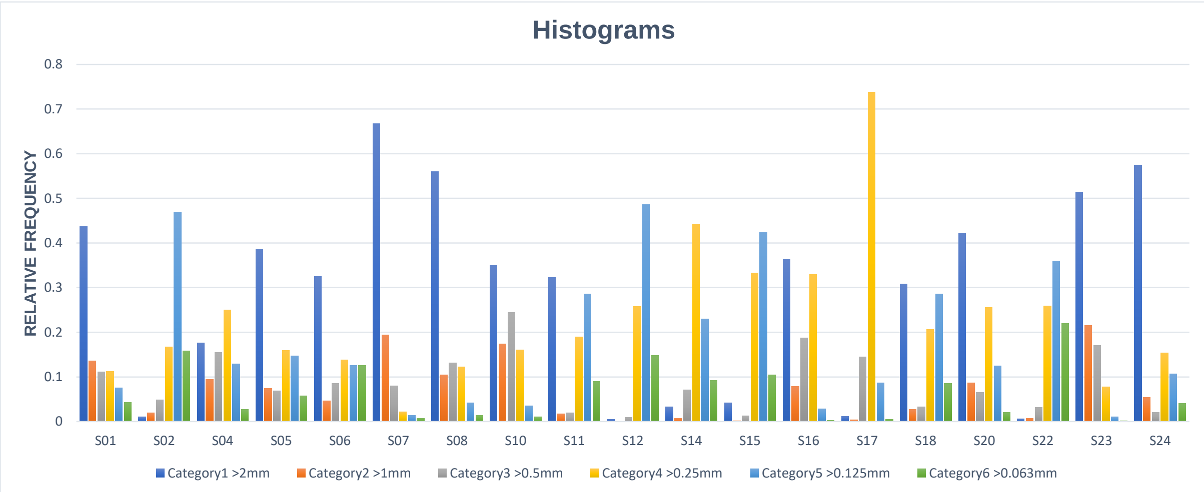

Table 3 grades the different samples in context of total fibres amount from highest (top) to lowest (bottom) count. Furthermore, the correlation between mean and sorting (in μm) of the sandy samples and the fibres number is given. All data is measured with Folk and Ward method (μm).

Table 3: Grain size analysis

Sample	**Fibres total**	**Mean**	**Description**	**Sorting**	**Description**
$S01$	55658	966.8	Coarse Sand	2.769	Poorly Sorted
$S14$	49726	234.0	Fine Sand	1.777	Moderately Sorted
$S15$	34896	192.1	Fine Sand	1.753	Moderately Sorted
$S04$	33885	572.1	Coarse Sand	2.978	Poorly Sorted
$S18$	33786	457.7	Medium Sand	3.498	Poorly Sorted
$S11$	32096	455.7	Medium Sand	3.526	Poorly Sorted
$S08$	24714	1210.3	Very Coarse Sand	2.534	Poorly Sorted
$S02$	24242	161.1	Fine Sand	1.931	Moderately Sorted
$S22$	19208	157.1	Fine Sand	1.911	Moderately Sorted
$S05$	15458	740.3	Coarse Sand	3.390	Poorly Sorted
$S06$	14905	564.8	Coarse Sand	3.615	Poorly Sorted
$S20$	11708	879.5	Coarse Sand	2.778	Poorly Sorted
$S24$	9660	1110.8	Very Coarse Sand	2.836	Poorly Sorted
$S10$	9028	937.6	Coarse Sand	2.372	Poorly Sorted
$S12$	8629	160.9	Fine Sand	1.716	Moderately Sorted
$S17$	8074	339.9	Medium Sand	1.475	Moderately Well Sorted
$S07$	6954	1816.9	Very Coarse Sand	1.610	Moderately Well Sorted
$S23$	4728	1437.6	Very Coarse Sand	2.015	Poorly Sorted
$S16$	4718	763.5	Coarse Sand	2.434	Poorly Sorted

6.2 Measurement and morphology of found particles

Table 4: Found pieces per kg

Sample	Fibres	Fibres coloured	Microbeads	Microbeads coloured	Fragments	Films	Other	Total
*S*01	46278	9380	0	0	7504	10631	4377	78173
*S*02	20202	4040	0	0	7407	7407	2020	41077
*S*04	31811	2074	0	0	18672	17980	11065	81604
*S*05	13692	1766	0	1325	3091	883	0	20759
*S*06	14054	851	0	0	10221	425	0	25553
*S*07	6954	0	0	0	7948	5464	3974	24341
*S*08	23447	1267	0	0	5703	0	1267	31685
*S*10	8577	451	1354	0	4514	0	4514	15349
*S*11	31093	1003	0	2507	19558	0	3009	57171
*S*12	8090	539	0	539	16181	539	539	26429
*S*14	49180	546	0	0	19125	1092	0	69945
*S*15	32490	2406	1203	601	9626	1203	601	48134
*S*16	4718	0	0	0	393	786	0	5898
*S*17	6729	1345	0	0	4934	448	0	13458
*S*18	31062	2724	0	1089	10899	2179	544	48501
*S*20	11430	278	836	1951	4181	278	0	18957
*S*22	18044	1164	0	2328	11059	0	0	32596
*S*23	4728	0	0	0	886	0	0	5614
*S*24	9660	0	0	0	3577	1073	0	14311

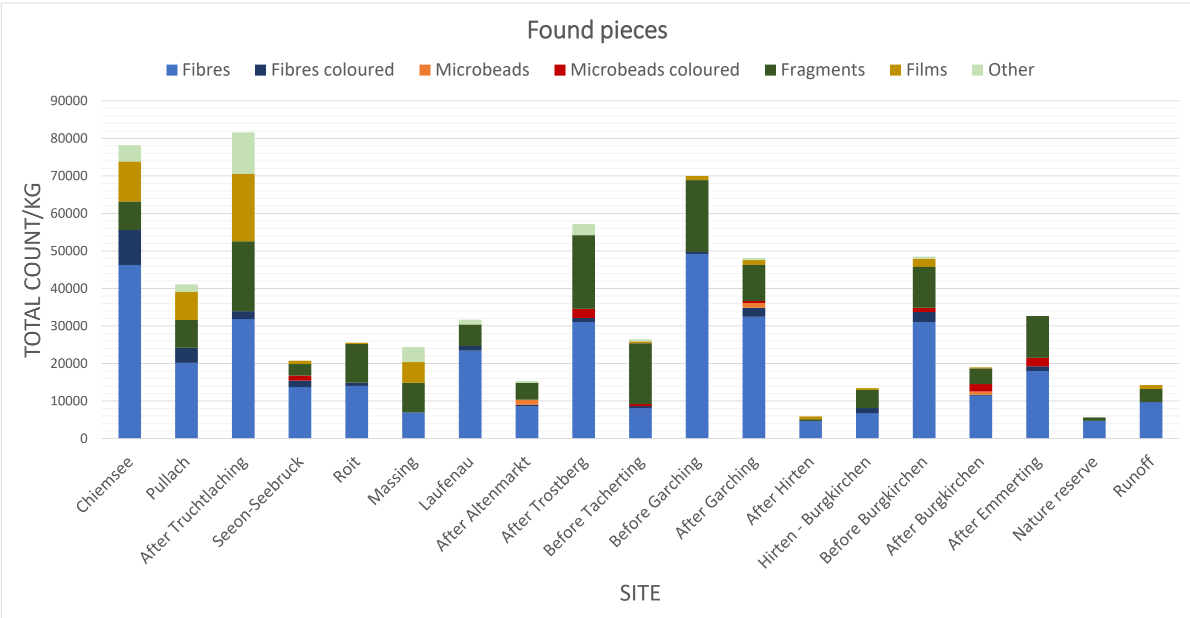

Figure 9 represents each object type category of the most interresting particles found in all 19 sand samples. The photos were taken with a camera system including a binocular microscope (Department of Geodynamics and Sedimentology; Uni. Vienna).

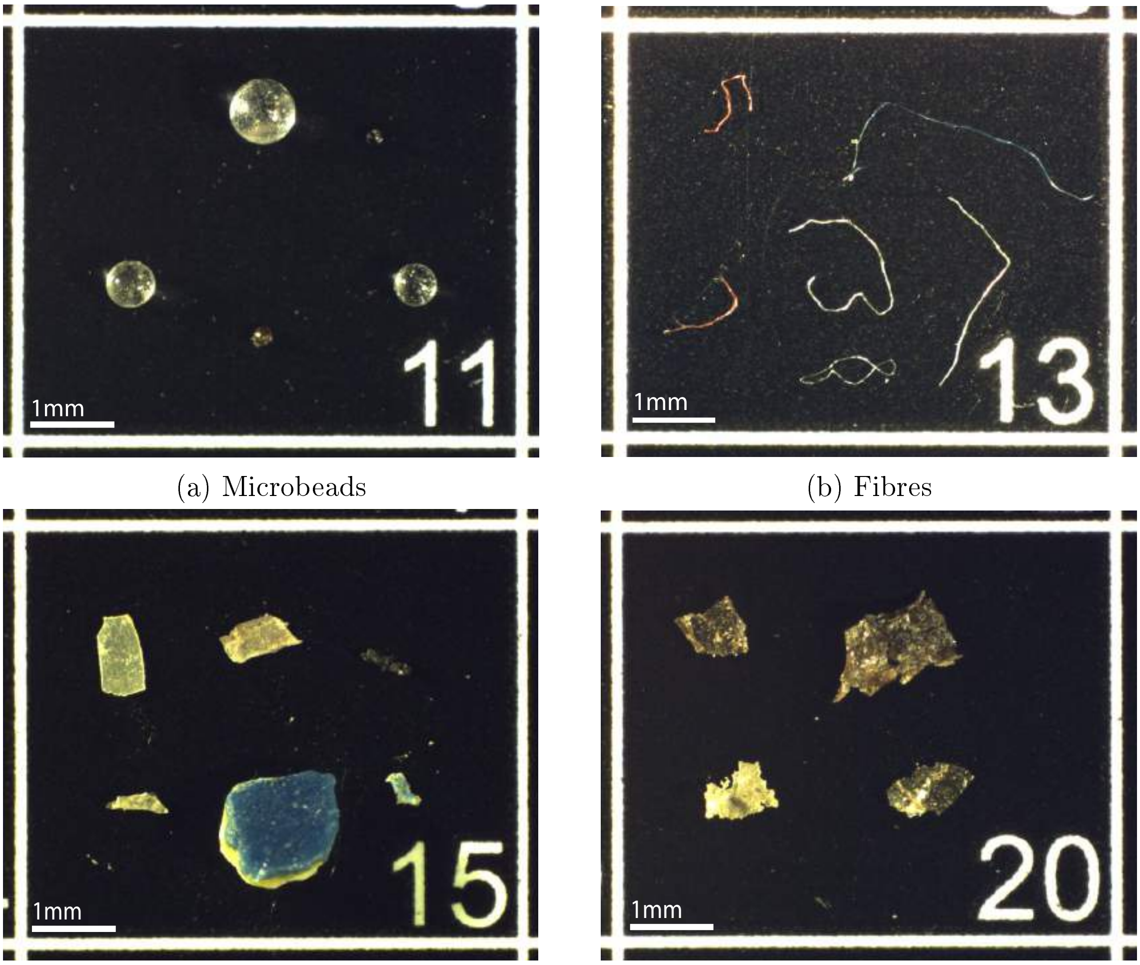

(a) Microbeads (b) Fibres

(c) Fragments (d) Films

Figure 9: Found pieces

Measurement: All discovered particles separated from the splitted samples were extrapolated on 1 kg sediment, numerated in table 4 and illustrated in bar diagram below it (Found pieces). A estimated total amount of 659555 objects were visually picked out of the sandy samples, which purports to consist of plastic. The maximum of particles found in the sediments is at site "After Truchtlaching" ($S04$) with 81604 particles/kg. The smallest number of pieces (5614/kg) was counted in site "Nature reserve" ($S23$).

Maximum fibres count with 55658 is estimated in sample $S01$ - lowest tally was found in sample $S16$ with a total number of 4718 fibres. Around the public hotspots, the cities Trostberg and Garching, a high gathering of fibres can be estimated with a peak at site "Before Garching" ($S14$ - 49726 fibres/kg).
First appearance of microbeads is in the sediment of site "Seeon-Seebruck" ($S05$; 1325 microbeads/kg). Maximum count is after city Garching $S20$ with 2787 microbeads/kg. Alonge the river Alz microbeads abundance is upmost after cities of Altenmarkt ($S10$; 1354 microbeads/kg), Trostberg ($S11$; 2507 microbeads/kg) Garching ($S15$; 1804 microbeads/kg) and Emmerting ($S22$; 2328 microbeads/kg).
In all samples pieces were found and catigorized as fragments. Maximum number is in sample $S11$ with 19558 and lowest in sediment at site "After Hirten" ($S16$) with 393 fragments per kilogram.
On average, the first 6 sample spots close to Lake Chiemsee contain the majority of seperated films, with a maximum of 17980 at site "After Truchtlaching" ($S04$).

Morphology: All found pieces were less than 5 mm in size. Fibres seperated from the riverbank sediments of the Alz had a variation in lenght from about 1 mm up to maximum 4 mm. A blue fibre from sample $S01$ as demonstrated in figure 9 ((b) Fibres) is the longest with 4 mm. Almost exclusively all fibres manifest a constant diameter, however they had a great variation in colour, size and shape.
The most interesting microbeads are shown at (a) Microbeads. The biggest discovered bead with 0.75 mm in diameter is transparent and was estimated in sample $S10$. Whereas a black microbead from sample spot $S05$ has a diameter of 0.2 mm and is considered as the smallest one seperated. All beads were black, brown, red, white and transparent in colour with a great variation in diameter.
Sample spots $S24$ with a small (0.5 mm) blue-white and $S23$ with a blue-yellow-white fragment (1.5 mm) contain the most special found pieces. Most typical shape caracter is shown by a transparent example ($S07$; 0.9 mm) in the upper left corner of image (c) Fragments (Figure 9).
Films almost exclusively possess a light brown-yellow colour, which is given in the upper left corner in (d) Films of Figure 9 ($S12$). Fragments as well as films feature numerous variations in shape and size.

6.3 Polymer identification

All spectra identified with Bio-Rad's Spectral Databases as well as unidentified spectra plotted with QtiPlot 0.9.9.12 Win is attached in the appendix.
The graphs show the scattered light intensity (y-axis) for every energy (frequency: wavenumber in cm^{-1}) of the monochromatic laser light (x-axis). The unknown spectra is given smoothed and without background.

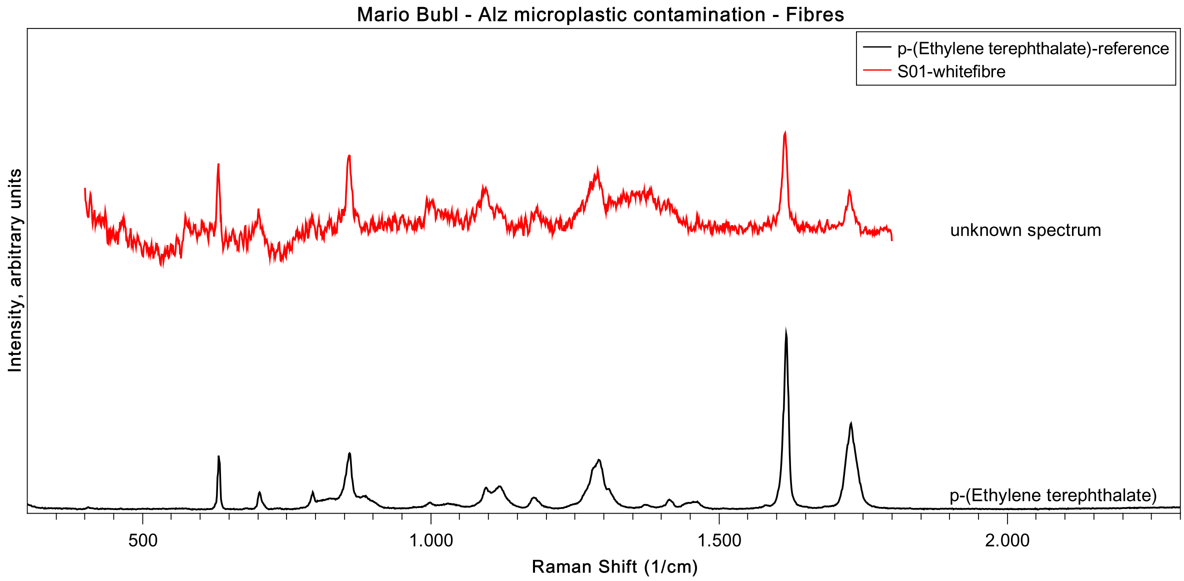

Figure 10: Fibre-Spectrum plotted with QtiPlot 0.9.9.12 Win

Figure 10 illustrates the spectrum of a white fibre (red) and its closest database match (black). Highest band of bending vibration (around 600) is at a frequency of 631.47 cm^{-1}, maximum band of stretching vibrations (>700) at 1614.55 cm^{-1}.

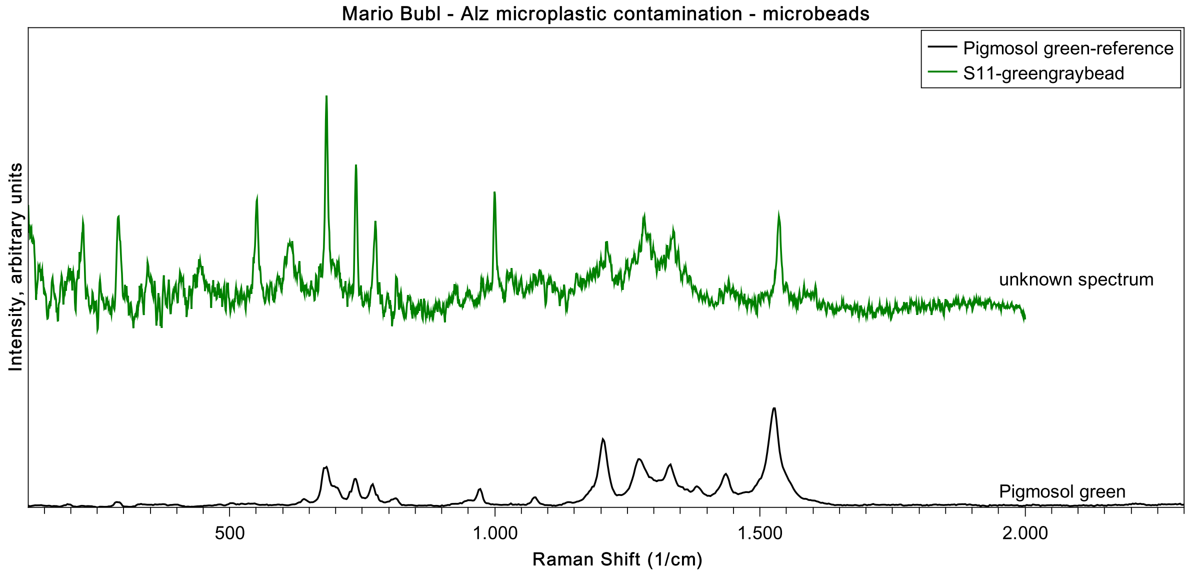

Figure 11: Microbead-Spectrum plotted with QtiPlot 0.9.9.12 Win

Figure 11 shows the spectrum of a green-gray microbead (green) and its closest database match (black). Highest bands of lattice vibration (around 100 - 300) are at a frequency of 223.26 and 290.43 cm^{-1}. Highest bending vibration is 682.72 cm^{-1} and maximum bands of stretching vibrations are 999.45 and 1535.68 cm^{-1} of frequency.

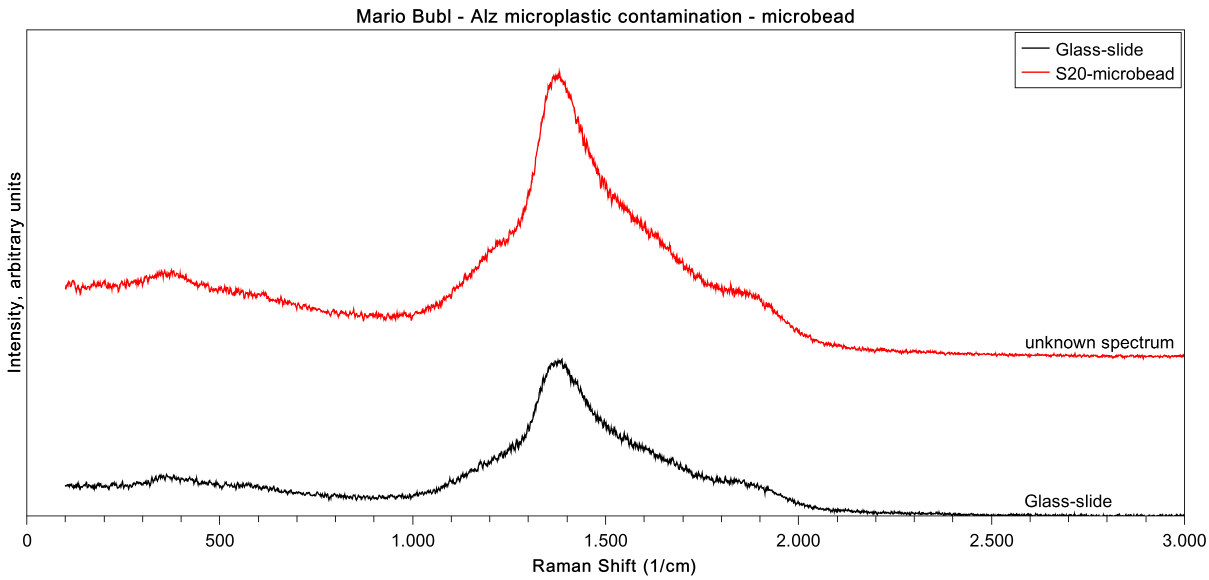

Figure 12: Microbead-Spectrum plotted with QtiPlot 0.9.9.12 Win

Figure 12 illustrates the spectrum of one of the transparent microbeads found in the samples (red) and its closest database match (black). The spectrum consists of a broadened band in a frequency range of 1000 - 2000 cm^{-1}. The peak can be estimated at 1379.11 cm^{-1}.

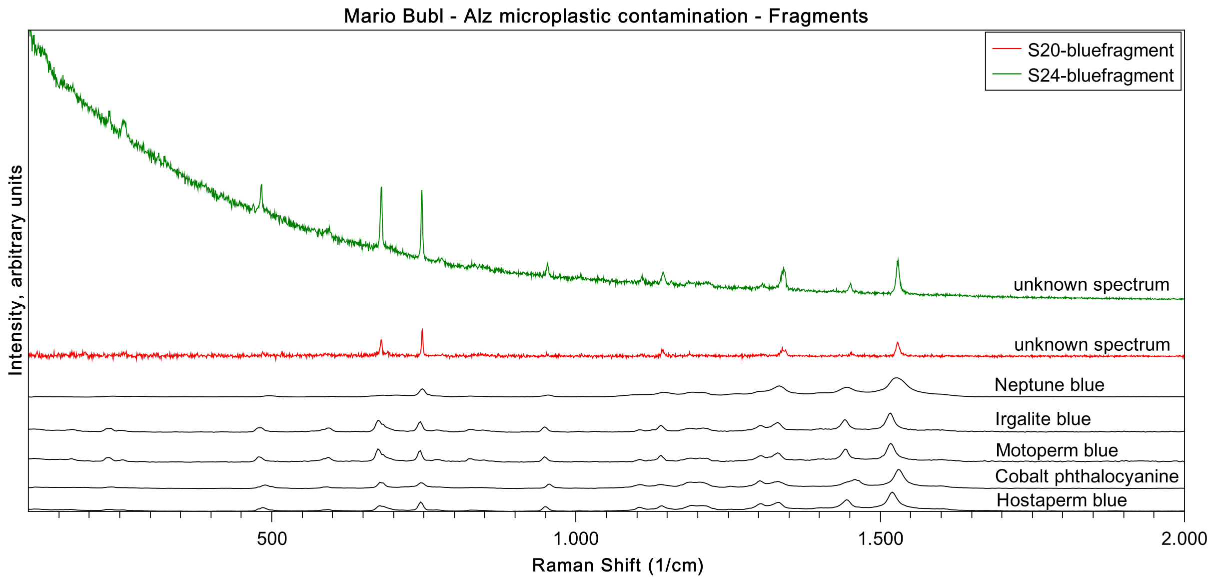

Figure 13: Blue-Fragments-Spectrum plotted with QtiPlot 0.9.9.12 Win

Figure 13 shows the spectra of two blue fragments (red/green) and its closest database matches (black). Main bands from red spectrum can be estimated in a frequency range of 650 - 750 cm^{-1} with a maximum band at 747.51 cm^{-1}. Maximum peak of stretching vibrations is at a frequency of 1528.03 cm^{-1}. The green spectrum shows two bands of lattice vibration at a frequency of 220.80 and 233.66 cm^{-1}. Two maximum peak bands are at 680.46 and 746.78 cm^{-1}. Highest band of stretching vibrations is at 1529.31 cm^{-1}.

7 Discussion

7.1 Analytical methods

Smear-Slides: This bachelor thesis was considered a pilot study at the faculty of Earth Sciences/Vienna, to analyse the German river Alz and the Austrian river Triesting in a similar way [30]. Because no guidelines exist in earth sciences in the context of searching for microplastic in sediments, we found out while evaluating different types of analytical methods that the smear-slides were not auxiliary. The photos below were taken with a camera system included in a transmitted light microscope (Department of Geodynamics and Sedimentology; Uni. Vienna).

(a) Fragment

(b) Grain

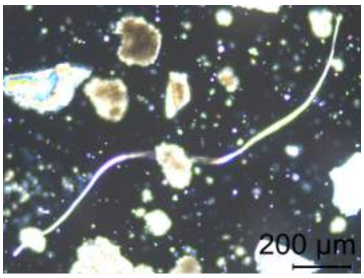

(c) Fibre

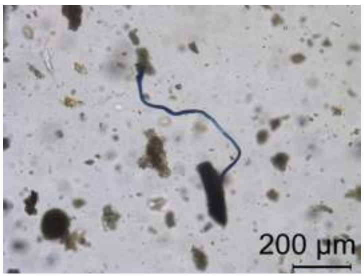

(d) Fibre

Figure 14: Transmitted light microscope findings

With a transmitted light microscope and different indices such as extinction (Analyzer), structure, colour or bevelled edges, it was not possible to distinguish the "plastics" from organic materials or minerals.

Fragments of garnets can be easily mistaken for glass or microplastic particles (Figure 14; (b) Grain). Flat spherical objects such as chlorite are hard to differentiate from plastic particles, because when they have a certain thinness they do not interfere respectively turn black with the analyzer and plastics do not either.
The bevelled edges, which are typical for secondary microplastic broken from larger objects are often rounded due to transportation in rivers (Figure 14; (a) Fragment).
Furthermore, the fibres that were found (Figure 14; (c,d) Fibre) in the Smear-Slides can either consist of polyester, polyamid (nylon) or cotton as well as mineral wool or fiberglass which is used in the shipbuilding industry (Lake Chiemsee).

Visual sorting and separation: While sorting the particles it became clear that separating the particles that consist of plastic from the high amount of particles all together is arduous. The transparent layer of muscovite can be easily confound with a piece of a microplastic film. Calcareous shelled objects, often of white colour, have the potential to be misinterpreted as plastic fragments. In addition very small round compounds consisting of different minerals can be mixed up with plastic-microbeads.

Grain size analysis: The aim of the grain size analysis is to prove that samples with fine sand contain a higher amount of fibres than samples with coarse sand. The transport behaviour of microplastic in the environment is still not very well understood. Table 3 in part 6 (results) shows the grain size analysis and illustrates the correlation between the total amount of fibres found in different samples and the measured data such as the mean or the sorting value. Consequently there is no trend observable. It is a speculation that the accumulation of fibres in marine environments does not only depend on parameters such as the mean value or the sorting, but is also affected by sample spot and anthropogenic influence. The main gathering of fibres were estimated to be around public hot spots (wastewater treatment plants) such as the bigger cities alonge the river Alz and by the first sample spots close to lake Chiemsee. Airborne contamination of fibres in the sandy samples is a great problem, however the high accumulation around sites with the most anthropogenic influence implies that a large amount of fibres were already in the collected samples.

Raman spectroscopy: This analytic method turned out to be challenging. While analysing the most interesting objects, the Raman signal with the identifiable Raman bands was multiplexed with luminescence bands especially when black particles were analysed. Longer integration time up to 60 s and higher laser intensity was sometimes useful to get small Raman bands, which are comparable with the database. Furthermore, the microplastic particles are often not well preserved and strongly weathered, which makes them harder to analyse.

Fibres

Altogether 7 fibres were analysed. The Raman spectrum of a white fibre (2.5 mm) from sample spot $S01$ (Figure 10/ Results - bottom, central) was first compared with the Spectral IR Database. The closest database was p-(Ethylene terephthalate). Bio-Rad's Spectral Databases estimated $S01$_whitefibre as Polyester Film. The same database was ascertained to be the best fit for three further fibres. White fibre from $S17$ was perceived as cellulose, microcrystalline, which tells us that a larger amount of the separated fibres do consist of organic material such as cotton. Furthermore, it was not possible to evaluate four fibres with both databases - spectra is in appendix.

Microbeads

Jointly 30 Microbeads were vetted. The most interesting bead was found in sample $S11$ at the site "After Trostberg". The Raman spectrum of this 0.3 mm small green-gray bead is given in figure 11/Polymere identification. It was not possible to analyse the supporting material, however the closest database from Spectral IR Database of the green colour is Pigmosol green - Bio-Rad's Spectral Database estimates Hostasol Green G-K. These organic pigments are ordinarily termed phthalo green. Phthalogreen 632 among others is used to colour molded thermoplastics. Therefore it stands to reason that the separated green-gray microbead is a microplastic bead produced for the cosmetic industry [31].

Furthermore, 5 microbeads were defined as glassbeads (4 in appendix). In figure 12 the spectrum of a transparent 0.5 mm bead from sample spot "After Burgkirchen" is compared with the closest database - spectra of a laboratory glass-slide. According to this relation, a high amount of the microbeads that were found per kg may consist of glass.

Additionally the spectra of 3 calcite, 3 hematite, 1 quartz and 1 magnetite bead is in the appendix. A considerable proportion of the beads calculated on one kg of sediment are of mineralogical origin. It was not possible to evaluate 16 microbeads.

Fragments

11 fragments were analysed with Raman-spectroscopy.
In figure 13 two objects (Photo - figure 9 - (c) Fragments) coloured with a blue pigment are compared with the best-fitting database. The Bio-Rad's Spectral Database shows that the best-fitting database for the fragment from the site "After Burgkirchen" ($S20$) is the neptune blue 722 spetrum. For the fragment from the site "Runoff, Marktl" ($S24$), it shows that it is the hostaperm blue pigment on a white cellulose supporting material. It stands to reason that these two particles can consist of plastic, since blue pigments such as the examples listed in figure 13 are used to color synthetic polymers.
The blue-yellow-white fragment from sample spot $S22$ (Photo - figure 9 - (c) Fragments) is thought to be ceramic glass, because the Raman spectrum is similar to the measured glass-slide and glassbead spectra. It was not possible to determine the supporting material.
The spectra of three aragonites (figure 9 - (c) Fragments - upper-left) and two hematites is in the appendix. 3 black fragments could not be evaluated ($S10$,$S15$,$S18$).

Films

In total 5 films were attempted to be analysed with Raman-spectroscopy. It was not possible for 4 of them - the spectra are in the appendix. The film from sample $S12$ thought to be aragonite.

According to the results of polymer-identification it seems that a large amount of the listed particles (Table 4) found in all the 19 samples do not consist of different types of polymers. Various are composed of organic material and minerals.

7.2 Potential sources

(a) Children's paddling pool

(b) Stand Up Paddleboard

Figure 15: Macroplastic

Microplastic as a factor of environmental pollution, is categorized into two groups. Primary microplastic, applied for air-blasting technology or resin pellets used in cosmetic products (phthalo green colored thermoplastic microbead – $S11$) and secondary microplastic, which are fragments originating and broken from larger pieces [13] [32]. Small freshwater systems like the evaluated river Alz which are contributory for larger rivers that end up in the world‘s oceans (Inn → Danube → Black Sea), are one of the most important inland sources of plastic pollution inputs [33] [34] [35] [36] [37]. Wastewater treatment plants and factories along these small fluviatile river systems are the source of microplastic fibres which could for example come from synthetic sports clothes. In a survey from 2011, scientists demonstrated with an experiment, that a single piece of clothing can produce over 1900 fibers per wash [35]. Once in the environment, the microplastic fibers can be easily inhaled by humans. Lung tissues absorb them where they can be related with tumors. Furthermore, textile dye allergy (polyester with Disperse Blue 106 and 124) can cause widespread autoeczematization reactions and dermatitis [38] [39].

8 Conclusions and Outlook

Minimizing plastic pollution and its global environmental impact on all ecosystems of our planet should not exclusively be a question for the citizenry and thus the end-consumer of the different countries. Governments of the United Nations need to determine management strategies to diminish the far-reaching consequences of unacceptable waste policy [9] [40].
Not just a fixed scale in optical characters, but rather sample techniques and analytical methods should be optimised and simplified. Worldwide guidelines need to be implemented, to make data from different surveys comparable to eachother [16].
The Press release of the European Commission from Mai 28th this year (2018) predicts that the top 10 single-use plastic products found at sea and beaches of Europe will be banned with new EU-wide rules to reduce marine litter [41]. Targets such as banning these single-use products are important, however the problem hereby is, that this is not the solution of the problem, it is only a small step to reduce European plastic impact. Furthermore, the global plastic pollution is not a European question, it is a problem to be solved globally.
Scientists on every continent are researching for new materials such as biopolymers. The advantages and disadvantages of these products are debatable. New plastics which are environment-friendly need to be developed (green chemistry) [16]. Policy-maker, scientists, the industry and the public need to collaborate in the sense of living a sustainable life on our planet, so that future generations will not suffer because of our deficiency [42].

The significance of microplastic contamination and its environmental impact around the globe is increasing. Many surveys exist in context of finding and analyzing microplastic in water but also in sediments of beaches and larger rivers. Due to the fact that the health of small river systems is essential for the stability of several ecosystems, the focus on these streams, such as the observed river Alz, has to be enhanced in the future.

Acknowledgments

Hereby I want to thank my supervisor Ao. Univ. Prof. Dr. Michael Wagreich (Department of Geodynamics and Sedimentology; Uni. Vienna) for choosing the topic area of this bachelor thesis.
Furthermore, I am indebted to Dr. (Dipl.Min.) Martin Ende (Dept. Mineralogy and Crystallography; Uni. Vienna), for advising me on technical and analytical matters during Raman-spectroscopy.
Dipl.-Ing. Sabine Hruby-Nichtenberger was a great help with laboratory work during the steps of analytical methods.
Special thanks goes to Georg Drexler and Verena Trompa who were a great help during field work as well as to Heidi Steiner (administrative district office - Altötting/ environmental protection - legislation and techniques) for supporting me with legal aspects.

Bibliography

[1] PlasticsEurope. Plastics – the facts 2012, 2012.

[2] PlasticsEurope. Plastics – the facts 2017, 2018.

[3] Jenna R. Jambeck, Roland Geyer, Chris Wilcox, Theodore R. Siegler, Miriam Perryman, Anthony Andrady, Ramani Narayan, and Kara Lavender Law. Plastic waste inputs from land into the ocean. Science, 347(6223):768–771, 2015.

[4] Marcus Eriksen, Laurent C. M. Lebreton, Henry S. Carson, Martin Thiel, Charles J. Moore, Jose C. Borerro, Francois Galgani, Peter G. Ryan, and Julia Reisser. Plastic pollution in the world's oceans: More than 5 trillion plastic pieces weighing over 250,000 tons afloat at sea. PLOS ONE, 9(12):1–15, 12 2014.

[5] Aaron Lechner, Hubert Keckeis, Franz Lumesberger-Loisl, Bernhard Zens, Reinhard Krusch, Michael Tritthart, Martin Glas, and Elisabeth Schludermann. The danube so colourful: A potpourri of plastic litter outnumbers fish larvae in europe's second largest river. Environmental Pollution, 188:177 – 181, 2014.

[6] Global Nature Fund (GNF). Lebendiger see des jahres 2014: Chiemsee, 2014.

[7] Geologische Bundesanstalt (GBA) <Wien>. Geologie von Österreich: Vergrößerung der geologischen Übersichtskarte der republik Österreich 1:1 500 000 aus "rocky austria - geologie von Österreich - kurz und bunt", 2013.

[8] Bayrisches Landesamt für Umwelt Gewässerkundlicher Dienst Bayern. Hauptwerte seebruck , trostberg, burgkirchen/ alz, 2018.

[9] Edward J. Carpenter and K. L. Smith. Plastics on the sargasso sea surface. Science, 175(4027):1240–1241, 1972.

[10] John B. Colton, Bruce R. Burns, and Frederick D. Knapp. Plastic particles in surface waters of the northwestern atlantic. Science, 185(4150):491–497, 1974.

[11] Anika Ballent, Patricia L. Corcoran, Odile Madden, Paul A. Helm, and Fred J. Longstaffe. Sources and sinks of microplastics in canadian lake ontario nearshore, tributary and beach sediments. Marine Pollution Bulletin, 110(1):383 – 395, 2016.

[12] David K. A. Barnes, Francois Galgani, Richard C. Thompson, and Morton Barlaz. Accumulation and fragmentation of plastic debris in global environments. Philosophical Transactions of the Royal Society of London B: Biological Sciences, 364(1526):1985–1998, 2009.

[13] Matthew Cole, Pennie Lindeque, Claudia Halsband, and Tamara S. Galloway. Microplastics as contaminants in the marine environment: A review. Marine Pollution Bulletin, 62(12):2588 – 2597, 2011.

[14] Juliana A. Ivar do Sul, Monica F. Costa, Mário Barletta, and Francisco José A. Cysneiros. Pelagic microplastics around an archipelago of the equatorial atlantic. Marine Pollution Bulletin, 75(1):305 – 309, 2013.

[15] Lisbeth Van Cauwenberghe, Ann Vanreusel, Jan Mees, and Colin R. Janssen. Microplastic pollution in deep-sea sediments. Environmental Pollution, 182:495 – 499, 2013.

[16] Ivleva Natalia P., Wiesheu Alexandra C., and Niessner Reinhard. Microplastic in aquatic ecosystems. Angewandte Chemie International Edition, 56(7):1720–1739.

[17] S. Werner L. Oosterbaan P. Nilsson D. Fleet S. Kinsey R. C. Thompson J. van Franeker T. Vlachogianni M. Scoullos J. M. Veiga A. Palatinus M. Matiddi T. Maes S. Korpinen A. Budziak H. Leslie J. Gago G. Liebezeit F. Galgani, G. Hanke. Msfd technical subgroup on marine litter; guidance on monitoring of marine litter in european seas, publications office of the european union,, 2013.

[18] Karen Ashton, Luke Holmes, and Andrew Turner. Association of metals with plastic production pellets in the marine environment. Marine Pollution Bulletin, 60(11):2050 – 2055, 2010.

[19] Albert A. Koelmans, Ellen Besseling, Anna Wegner, and Edwin M. Foekema. Plastic as a carrier of pops to aquatic organisms: A model analysis. Environmental Science & Technology, 47(14):7812–7820, 2013. PMID: 23758580.

[20] Jörg Oehlmann, Ulrike Schulte-Oehlmann, Werner Kloas, Oana Jagnytsch, Ilka Lutz, Kresten O. Kusk, Leah Wollenberger, Eduarda M. Santos, Gregory C. Paull,

Katrien J. W. Van Look, and Charles R. Tyler. A critical analysis of the biological impacts of plasticizers on wildlife. Philosophical Transactions of the Royal Society of London B: Biological Sciences, 364(1526):2047–2062, 2009.

[21] Delilah Lithner, Åke Larsson, and Göran Dave. Environmental and health hazard ranking and assessment of plastic polymers based on chemical composition. Science of The Total Environment, 409(18):3309 – 3324, 2011.

[22] Obbard Rachel W., Sadri Saeed, Wong Ying Qi, Khitun Alexandra A., Baker Ian, and Thompson Richard C. Global warming releases microplastic legacy frozen in arctic sea ice. Earth's Future, 2(6):315–320.

[23] Jan Zalasiewicz, Colin N. Waters, Juliana A. Ivar do Sul, Patricia L. Corcoran, Anthony D. Barnosky, Alejandro Cearreta, Matt Edgeworth, Agnieszka Gałuszka, Catherine Jeandel, Reinhold Leinfelder, J.R. McNeill, Will Steffen, Colin Summerhayes, Michael Wagreich, Mark Williams, Alexander P. Wolfe, and Yasmin Yonan. The geological cycle of plastics and their use as a stratigraphic indicator of the anthropocene. Anthropocene, 13:4 – 17, 2016.

[24] Gemeinde Altenmarkt a. d. Alz. https://www.altenmarkt.de/ - einwohnerzahl, 2018.

[25] Stadt Trostberg an der Alz. https://www.stadt-trostberg.de - bevölkerungsentwicklung, 2018.

[26] Gemeinde Garching a.d.Alz. https://www.garching-alz.de/startseite/ortsbeschreibung/ - ortsbeschreibung, 2018.

[27] Gemeinde Burgkirchen a. d. Alz. http://www.burgkirchen.de - heimatverbunden - gemeindeinformationen - zahlen & daten -, 2018.

[28] Landratsamt Altötting. https://www.lra-aoe.de/landkreis/landschaft/naturschutzgebiete - untere alz.

[29] Blott Simon J. and Pye Kenneth. Gradistat: a grain size distribution and statistics package for the analysis of unconsolidated sediments. Earth Surface Processes and Landforms, 26(11):1237–1248.

[30] Paris Konstantinides. Untersuchung der mikroplastik-kontamination im sediment des flusses triesting/nÖ. 2018.

[31] Steinwall Inc. Pigments used to color molded thermoplastics.

[32] Charles James Moore. Synthetic polymers in the marine environment: A rapidly increasing, long-term threat. Environmental Research, 108(2):131 – 139, 2008. The Plastic World.

[33] GESAMP Report and Studies N° 82. Proceedings of the gesamp international workshop on micro-plastic particles as a vector in transporting persistent, bio-accumulating and toxic substances in the oceans, 2010.

[34] Fatehi Dubaish and Gerd Liebezeit. Suspended microplastics and black carbon particles in the jade system, southern north sea. Water, Air, & Soil Pollution, 224(2):1352, Jan 2013.

[35] Mark Anthony Browne, Phillip Crump, Stewart J. Niven, Emma Teuten, Andrew Tonkin, Tamara Galloway, and Richard Thompson. Accumulation of microplastic on shorelines woldwide: Sources and sinks. Environmental Science & Technology, 45(21):9175–9179, 2011. PMID: 21894925.

[36] Michiel Claessens, Steven De Meester, Lieve Van Landuyt, Karen De Clerck, and Colin R. Janssen. Occurrence and distribution of microplastics in marine sediments along the belgian coast. Marine Pollution Bulletin, 62(10):2199 – 2204, 2011.

[37] Kimberly Ann V. Zubris and Brian K. Richards. Synthetic fibers as an indicator of land application of sludge. Environmental Pollution, 138(2):201 – 211, 2005.

[38] J L Pauly, S J Stegmeier, H A Allaart, R T Cheney, P J Zhang, A G Mayer, and R J Streck. Inhaled cellulosic and plastic fibers found in human lung tissue. Cancer Epidemiology and Prevention Biomarkers, 7(5):419–428, 1998.

[39] Melanie Pratt and Victoria Taraska. Disperse blue dyes 106 and 124 are common causes of textile dermatitis and should serve as screening allergens for this condition. 11:30–41, 04 2000.

[40] Roland Geyer, Jenna R. Jambeck, and Kara Lavender Law. Production, use, and fate of all plastics ever made. Science Advances, 3(7), 2017.

[41] European Commission Fact Sheet. Single-use plastics: New eu rules to reduce marine litter, 2018.

[42] Richard C. Thompson, Charles J. Moore, Frederick S. vom Saal, and Shanna H. Swan. Plastics, the environment and human health: current consensus and future trends. Philosophical Transactions of the Royal Society of London B: Biological Sciences, 364(1526):2153–2166, 2009.

Appendix

In the appendix detailed data of the analytical methods is given. Several observed Raman spectra and their comparison with spectra of Bio-Rad's Spectral Database are attached primarily.
Additionally all spectra, which were not possible to estimate are plotted with QtiPlot 0.9.9.12 Win and attached.
Furthermore, multiple data of the grain size analysis, measured with Gradistat is attached.
Finally the waiver by the government of the federal district of Bavaria is appended.

Bio-Rad Laboratories
Informatics Division

06.07.2018 16:04

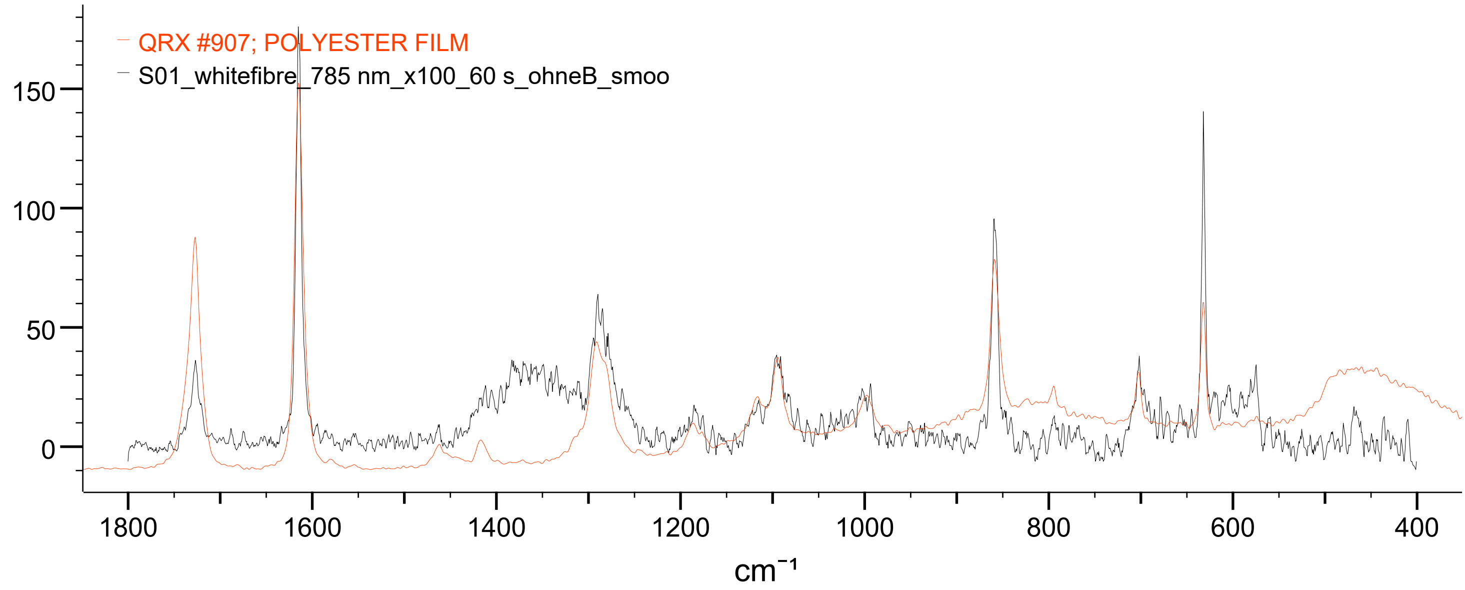

Manuelle Korrekturen: Basislinie
Suchbereiche: Voll
Suchalgorithmus: Korrelation
Pfad des Suchspektrums: C:\Users\installuser\Desktop\Bachelorarbeit\Microplastic Bachelorarbeit [work]\Raman\Bubl\Fasern\S01weiß\weiß2_polyesterfilm\S01_whitefibre_785 nm_x100_60 s_ohneB_smoo.l6s

Name:	Wert
Ergebnis-HQI	68.09
Datenbankabkürzung	QRX
Datenbanktitel	Raman - Polymers & Monomers (Basic) - Bio-Rad Sadtler
Datensatzkennung	907
Name:	POLYESTER FILM
Classification	POLYESTERS
Instrument Name	Bio-Rad FTS 175C with Raman accessory
Raman Corrections	Referenced to internal white light source; Baseline subtracted
Raman Laser Source	Nd:YAG
Raman Laser Wavelength	1064
Source of Sample	ICI Americas, Inc.
Synonyms	MELINEX TYPE S/92 GAUGE
Technique	FT-Raman

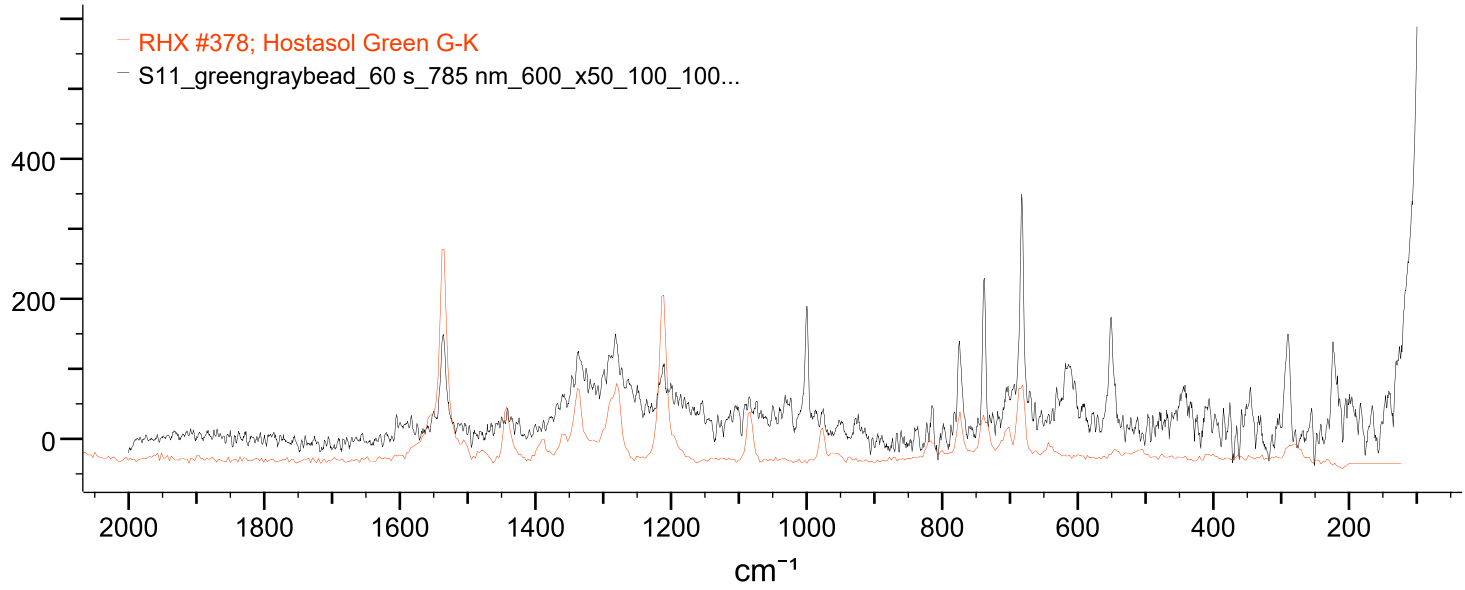

Manuelle Korrekturen: Keine
Suchbereiche: Voll
Suchalgorithmus: Korrelation
Pfad des Suchspektrums: C:\Users\installuser\Desktop\Bachelorarbeit\Microplastic Bachelorarbeit [work]\Raman\Bubl\Kugeln\fertig\S11\Kugel grau\S11_greengraybead_60 s_785 ...

ereinstimmu	Info	Gewicht	Name:	Chemische Struktur	Spektrum
		0.54	Hostasol Green G-K		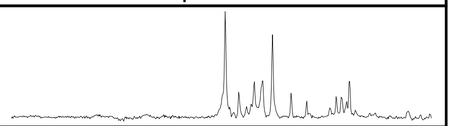

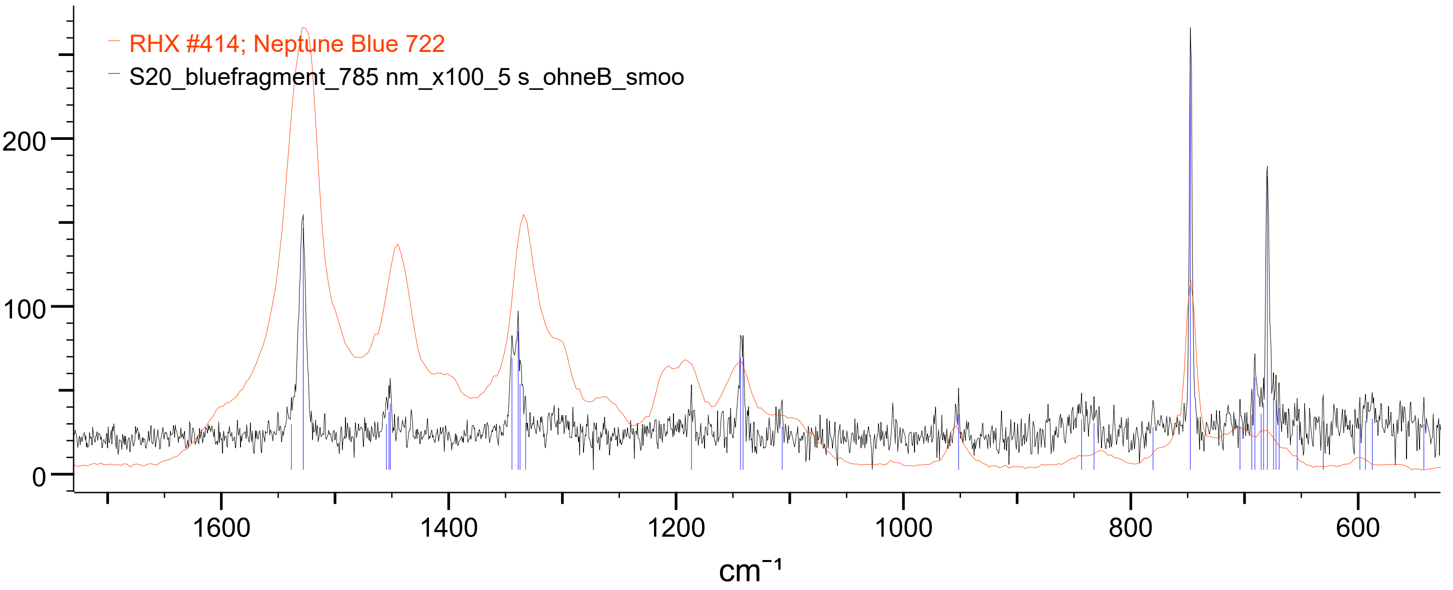

Manuelle Korrekturen: Keine

Suchbereiche: Voll

Suchalgorithmus: Korrelation

Pfad des Suchspektrums: C:\Users\installuser\Desktop\Bachelorarbeit\Microplastic ...

Klassifikation	Gruppe	Bindur	Bereich	Intensität	Modus	Bemerkungen
Miscellaneou	Plasticized Poly (vinyl					

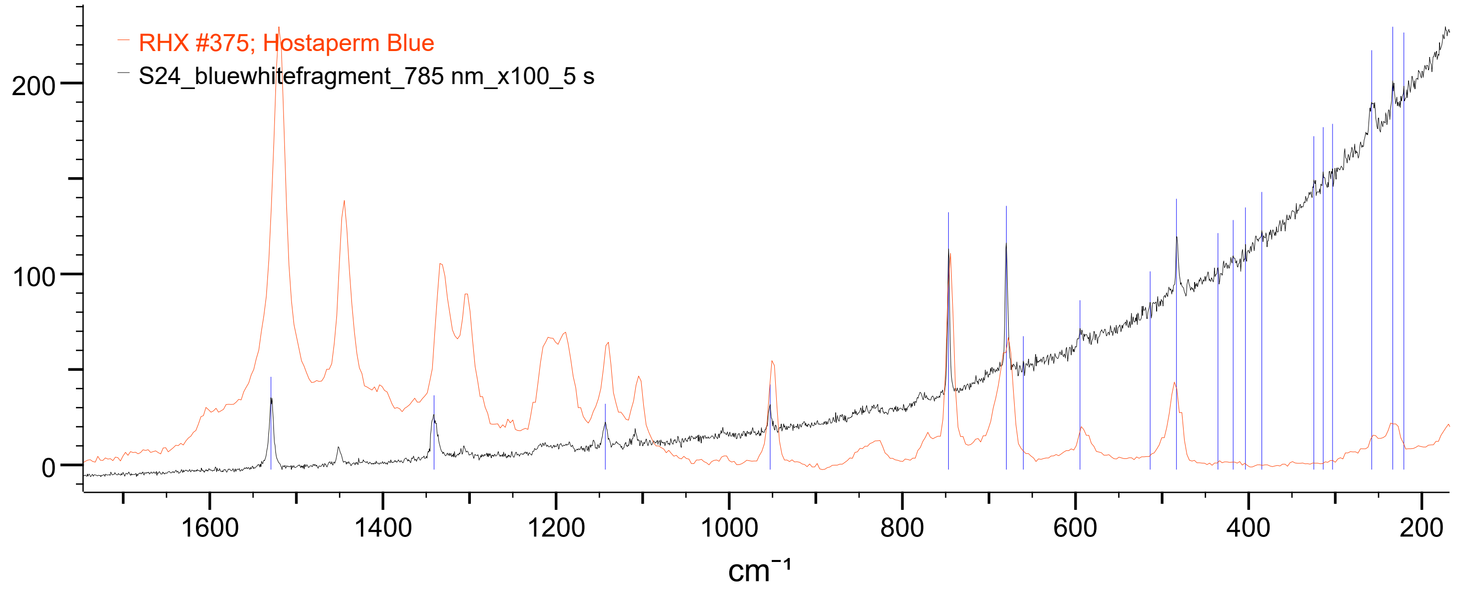

Manuelle Korrekturen: Keine

Suchbereiche: Voll

Suchalgorithmus: Korrelation

Pfad des Suchspektrums: C:\Users\installuser\Desktop\Bachelorarbeit\Microplastic ...

Klassifikation	Gruppe	Bindun	Bereich	Intensität	Modus	Bemerkungen
Nitro Compou	C-NO_2					

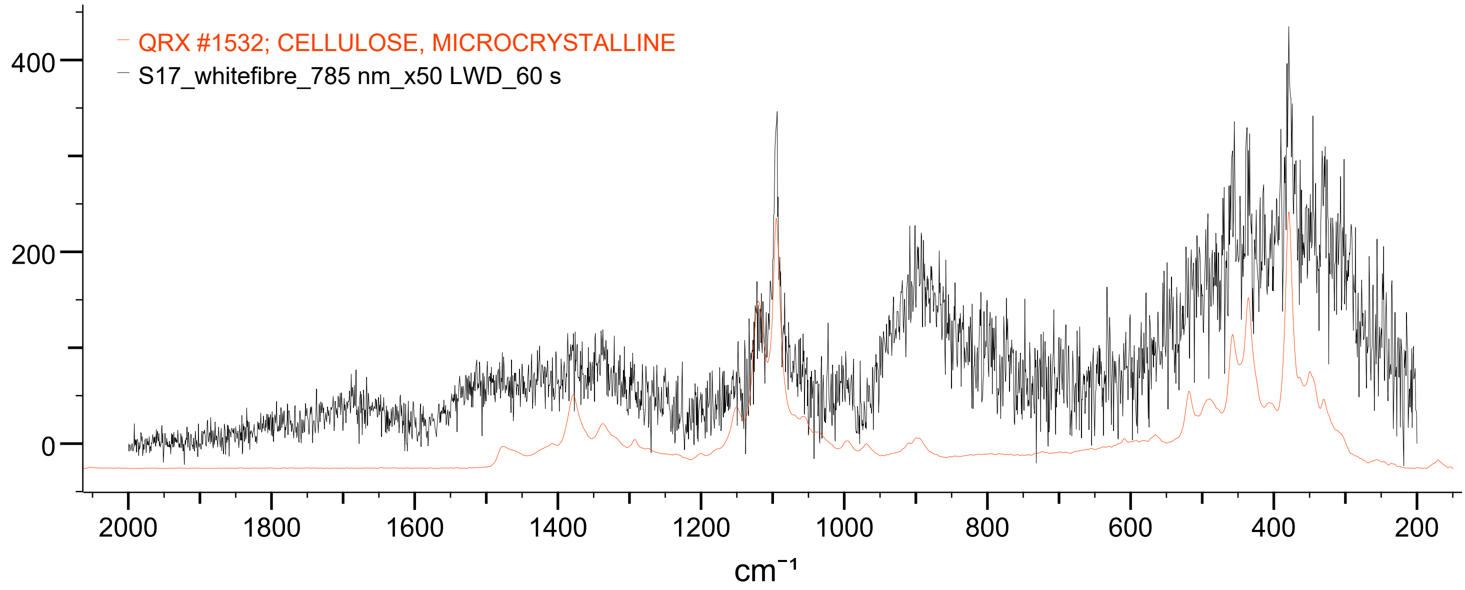

Manuelle Korrekturen: Basislinie
Suchbereiche: Voll
Suchalgorithmus: Korrelation
Pfad des Suchspektrums: C:\Users\installuser\Desktop\Bachelorarbeit\Microplastic Bachelorarbeit [work]\Raman\Bubl\Fasern\S17 weiß\2. Versuch\S17_whitefibre_785 nm_x50 LWD_60 s.ngs

ereinstimmu	Info	Gewicht	Name:	Chemische Struktur	Spektrum
		0.51	CELLULOSE, MICROCRYSTALLINE	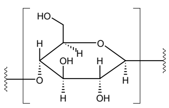	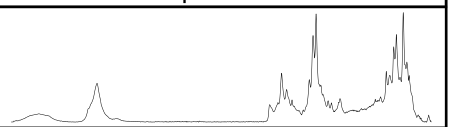

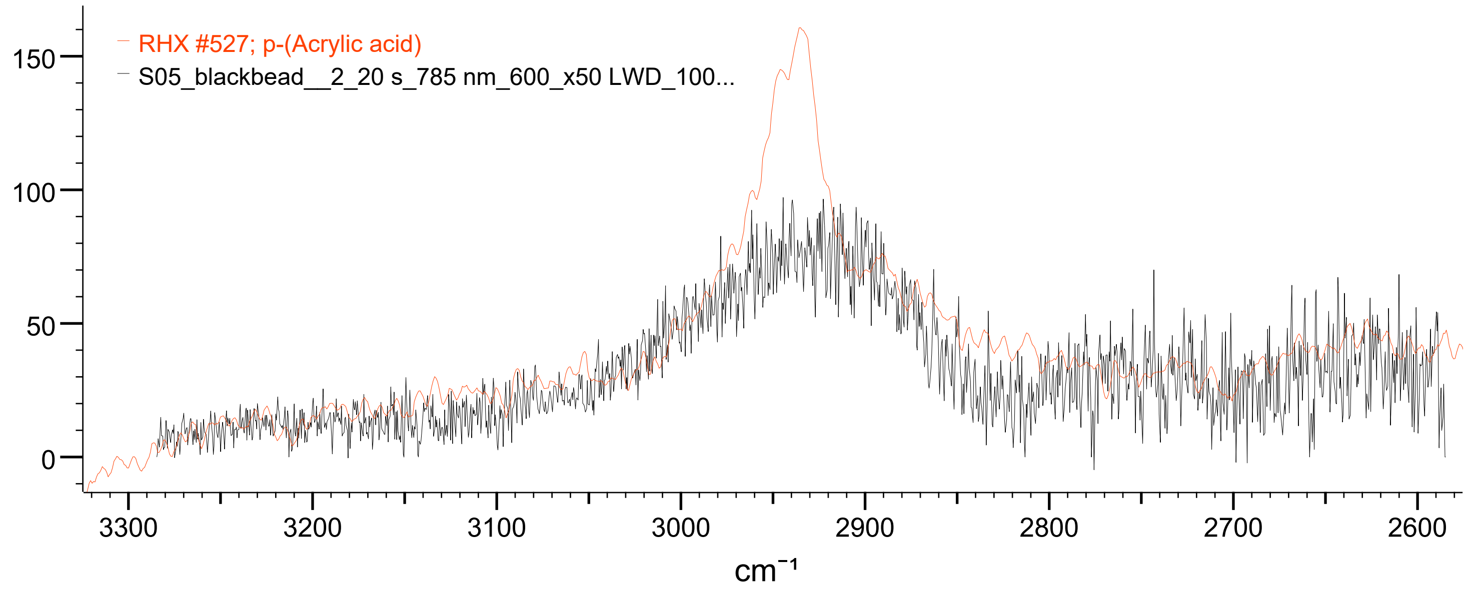

Manuelle Korrekturen: Basislinie
Suchbereiche: Voll
Suchalgorithmus: Korrelation
Pfad des Suchspektrums: C:\Users\installuser\Desktop\Bachelorarbeit\Microplastic Bachelorarbeit [work]\Raman\Bubl\Kugeln\S05_schwarze Kugel\schwarzeKugel1\S05_blackbead__2_20 s_785 nm_600_x50 ... LWD_100_100_300 pgs

Name:	Wert
Ergebnis-HQI	96.23
Datenbankabkürzung	RHX
Datenbanktitel	Raman - Forensic - HORIBA
Datensatzkennung	527
Name:	p-(Acrylic acid)
CAS Registry Number	9003-01-4
Classification	polymer
Comments	MW 4 000 000; powder
Formula	C3H4O2
Instrument Name	HORIBA
Laser Power	632.8
Source of Sample	Jobin Yvon
Source of Spectrum	HORIBA Scientific
Substance Type	p-(acryl)

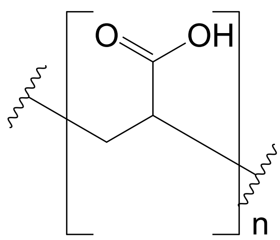

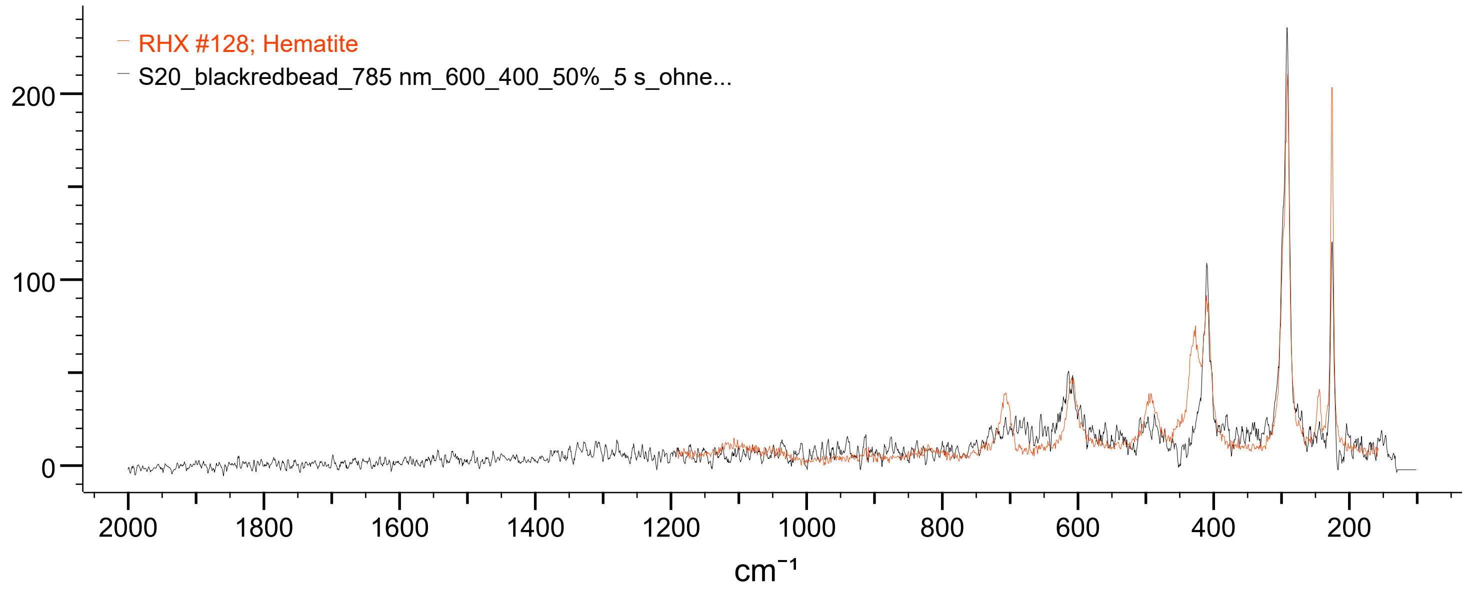

Manuelle Korrekturen: Keine
Suchbereiche: Voll
Suchalgorithmus: Korrelation
Pfad des Suchspektrums: C:\Users\installuser\Desktop\Bachelorarbeit\Microplastic Bachelorarbeit [work]\Raman\Bubl\Kugeln\fertig\SBE\Kugel schwarz kaputt mit rotem schimmer\S20_blackredbead_785 ... nm_600_400_50%_5 s_ohneB_smoo l6s

Name:	Wert
Ergebnis-HQI	82.03
Datenbankabkürzung	RHX
Datenbanktitel	Raman - Forensic - HORIBA
Datensatzkennung	128
Name:	Hematite
CAS Registry Number	1317-60-8
Classification	mineral
Comments	varieties: Oligiste - Specularite
Formula	alpha-Fe2O3
Instrument Name	HORIBA LabRAM
Laser Power	632.8
Source of Sample	Bersani, Parma, Italy
Source of Spectrum	HORIBA Scientific
Synonyms	C.I. Generic name: Pigment Red 101; PR101; C.I. Constitution No: 77491; Iron oxide

Bio-Rad Laboratories
Informatics Division

06.07.2018 15:50

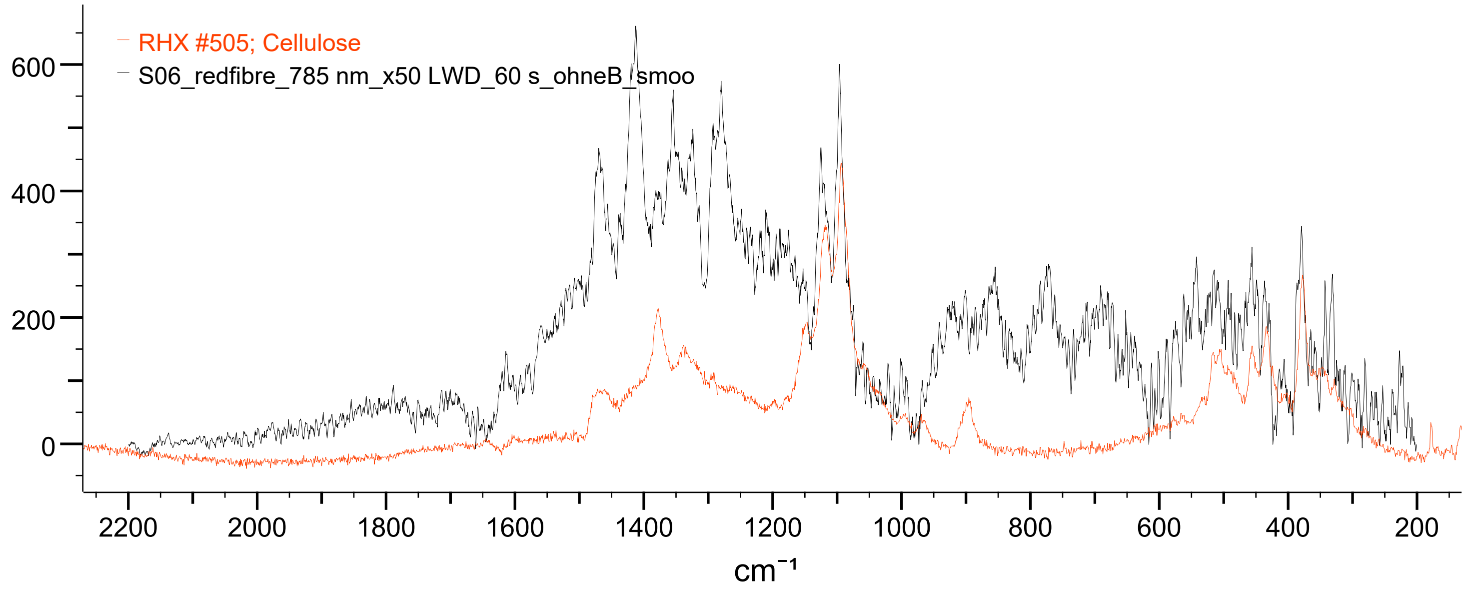

Manuelle Korrekturen: Keine
Suchbereiche: Voll
Suchalgorithmus: Korrelation
Pfad des Suchspektrums: C:\Users\installuser\Desktop\Bachelorarbeit\Microplastic Bachelorarbeit [work]\Raman\Bubl\Fasern\S06 Faser rot\2.Versuch\S06_redfibre_785 nm_x50 LWD_60 s_ohneB_smoo.l6s

ereinstimmu	Info	Gewicht	Name:	Chemische Struktur	Spektrum
		0.38	Cellulose	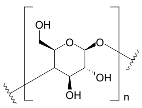	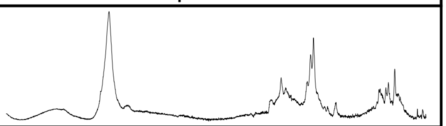

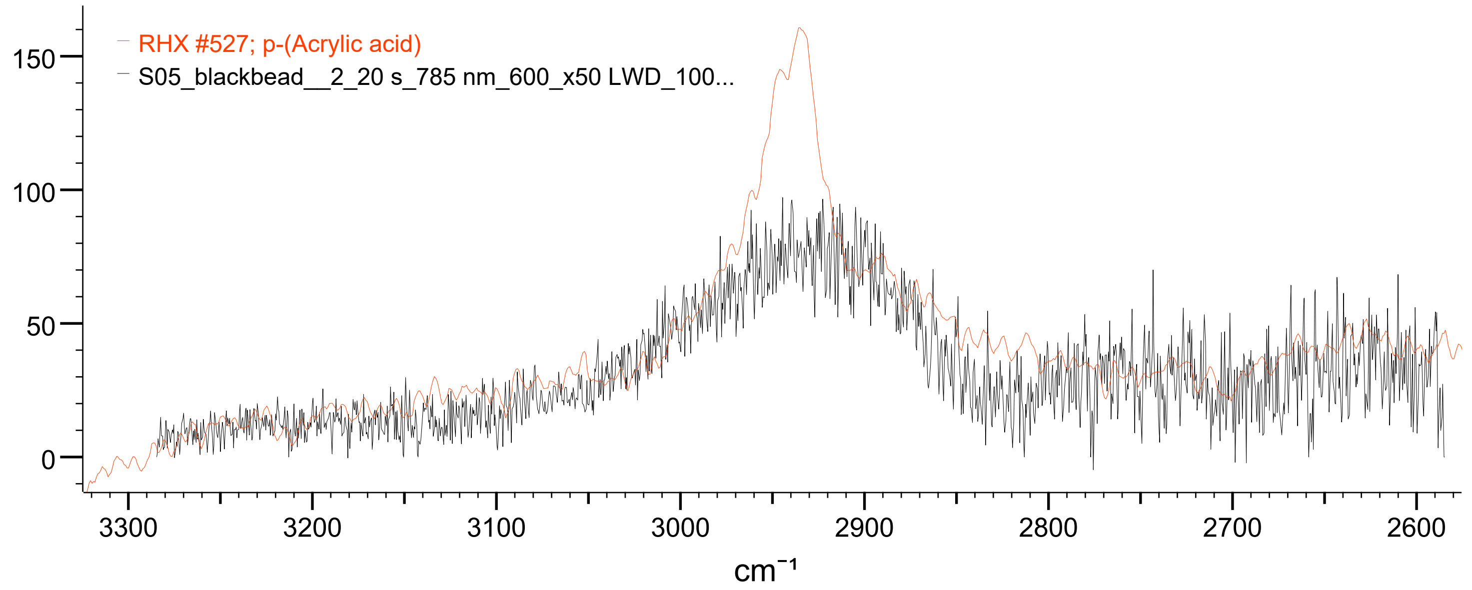

Manuelle Korrekturen: Basislinie
Suchbereiche: Voll
Suchalgorithmus: Korrelation
Pfad des Suchspektrums: C:\Users\installuser\Desktop\Bachelorarbeit\Microplastic Bachelorarbeit [work]\Raman\Bubl\Kugeln\S05_schwarze Kugel\schwarzeKugel1\S05_blackbead__2_20 s_785 nm_600_x50 ...
LWD_100_100_300.ngs

Name:	Wert
Ergebnis-HQI	96.23
Datenbankabkürzung	RHX
Datenbanktitel	Raman - Forensic - HORIBA
Datensatzkennung	527
Name:	p-(Acrylic acid)
CAS Registry Number	9003-01-4
Classification	polymer
Comments	MW 4 000 000; powder
Formula	C3H4O2
Instrument Name	HORIBA
Laser Power	632.8
Source of Sample	Jobin Yvon
Source of Spectrum	HORIBA Scientific
Substance Type	p-(acryl)

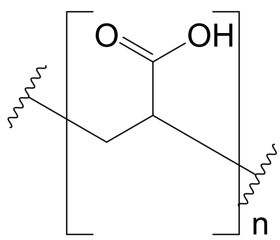

Bio-Rad Laboratories
Informatics Division

07.07.2018 11:22

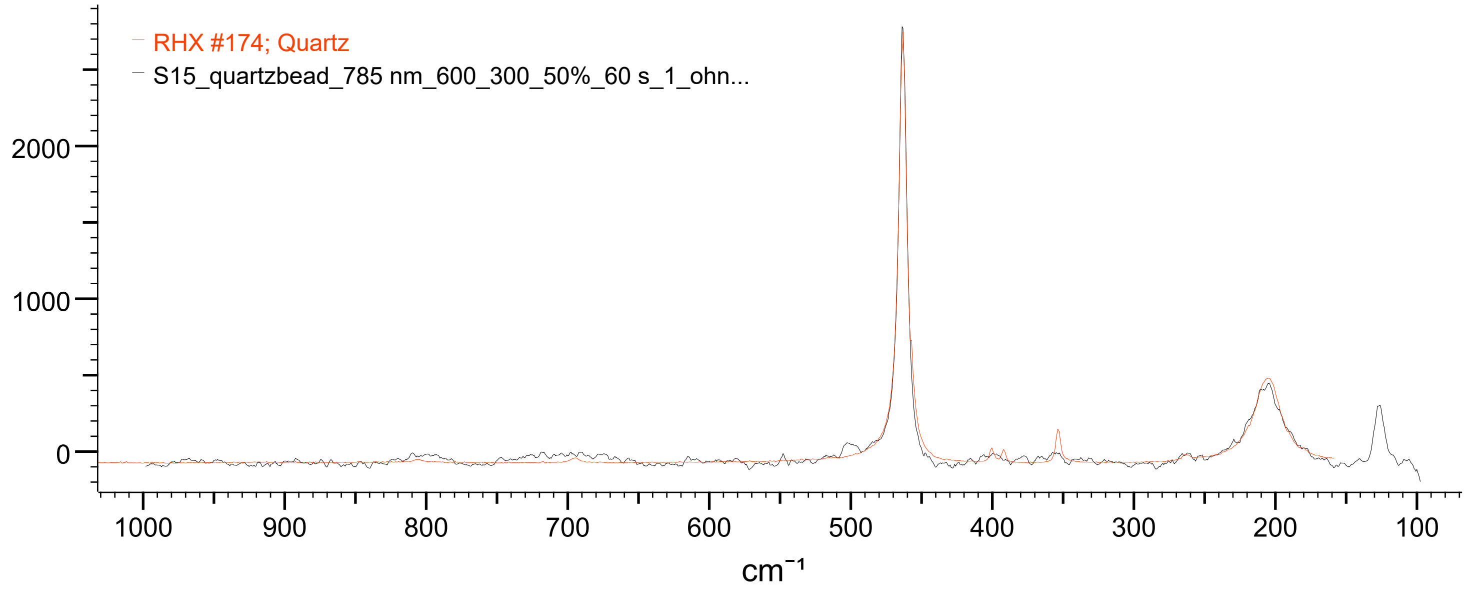

Manuelle Korrekturen: Keine
Suchbereiche: Voll
Suchalgorithmus: Korrelation
Pfad des Suchspektrums: C:\Users\installuser\Desktop\Bachelorarbeit\Microplastic Bachelorarbeit [work]\Raman\Bubl\Kugeln\fertig\S15\Kugel durchsichtig\S15_quartzbead_785 nm_600_300_50%_60 ...
s_1_ohneB_smoo l6s

Name:	Wert
Ergebnis-HQI	98.52
Datenbankabkürzung	RHX
Datenbanktitel	Raman - Forensic - HORIBA
Datensatzkennung	174
Name:	Quartz
CAS Registry Number	14808-60-7
Classification	mineral
Comments	Ghiare Berceto, Italy
Formula	SiO2
Instrument Name	HORIBA LabRAM
Laser Power	632.8
Source of Sample	Bersani, Parma, Italy
Source of Spectrum	HORIBA Scientific
Substance Type	tectosilicate; silicon oxide
Synonyms	C.I. Generic name: Pigment White 27; PW27; Gems: Rock crystal - Citrine - Morion - Girasol - Prasiolit - Hematoid - Ametyste

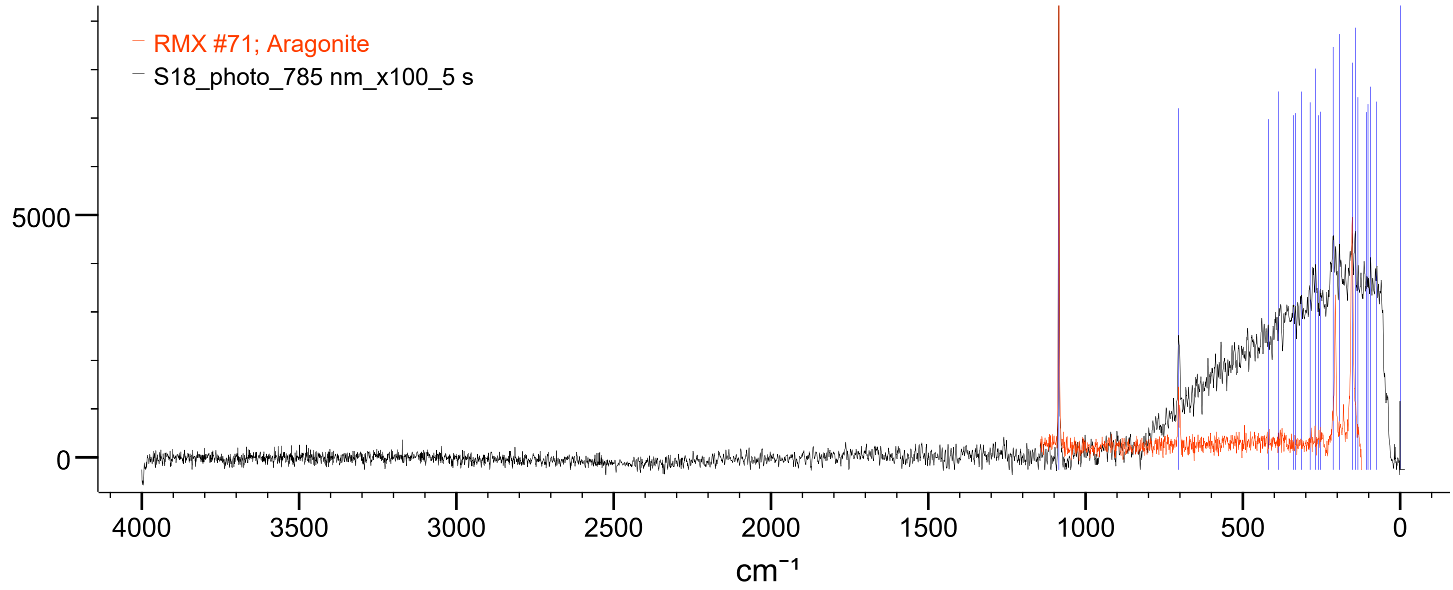

Manuelle Korrekturen: Basislinie, Rauschen

Suchbereiche: Voll

Suchalgorithmus: Korrelation

Pfad des Suchspektrums: C:\Users\installuser\Desktop\Bachelorarbeit\Microplastic ...

Klassifikation	Gruppe	Bindur	Bereich	Intensität	Modus	Bemerkungen
Copolymers-	Acrylonitrile/Butadiene					

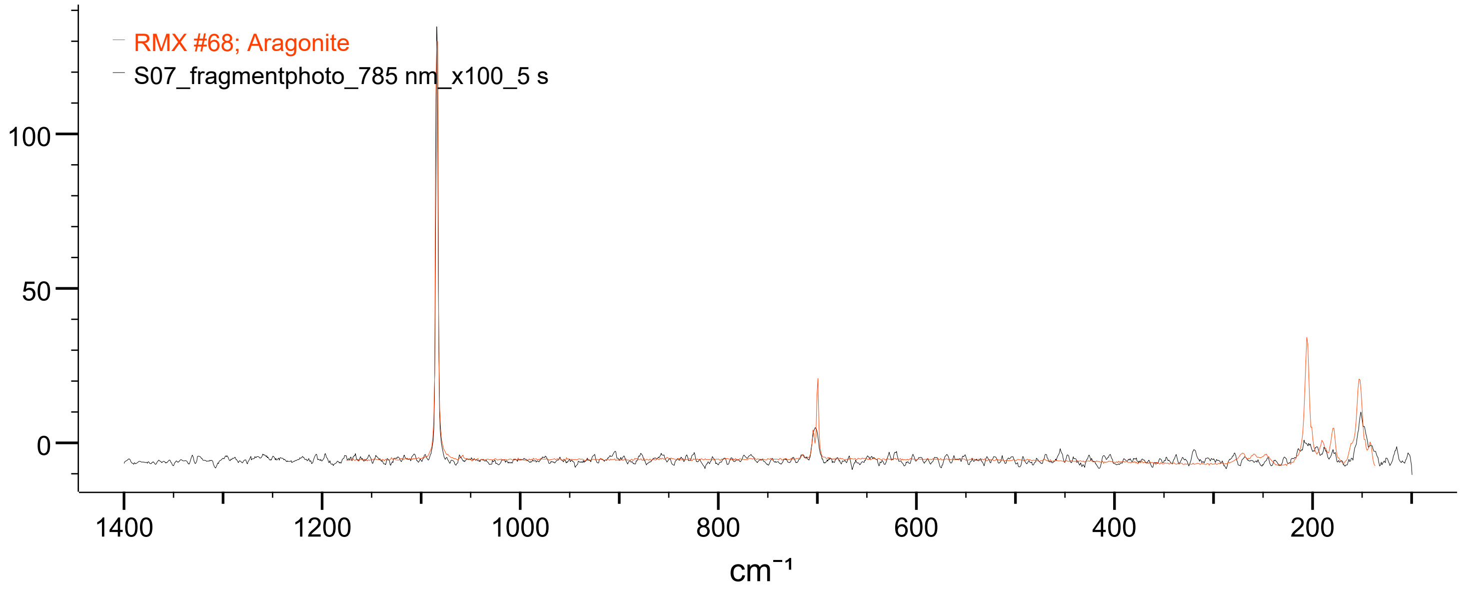

Manuelle Korrekturen: Keine
Suchbereiche: Voll
Suchalgorithmus: Korrelation
Pfad des Suchspektrums: C:\Users\installuser\Desktop\Bachelorarbeit\Microplastic Bachelorarbeit [work]\Raman\Bubl\Fragmente\QtiPlot\Aragonit\S07\weißklein\S07_fragmentphoto_785 nm_x100_5 s.l6s

Name:	Wert
Ergebnis-HQI	88.82
Datenbankabkürzung	RMX
Datenbanktitel	Raman - Minerals - HORIBA
Datensatzkennung	68
Name:	Aragonite
Classification	carbonate
Formula	CaCO3
Instrument Name	HORIBA
Laser Power	632.8
Source of Spectrum	HORIBA Scientific

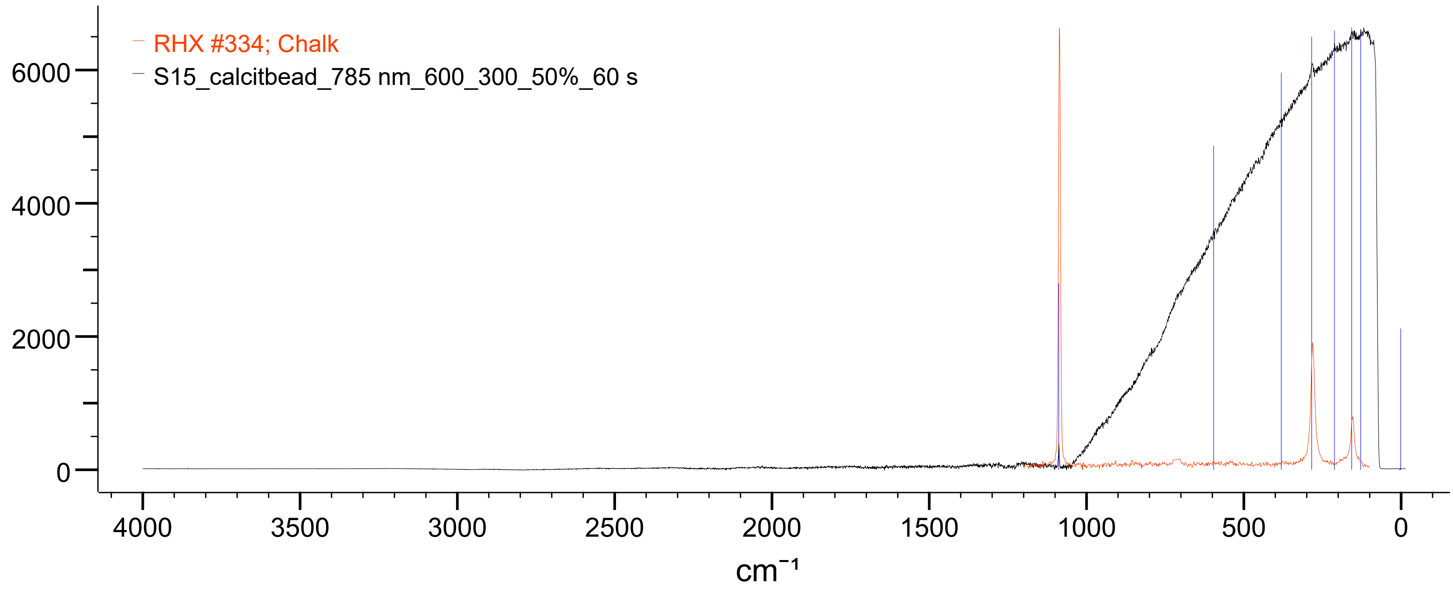

Manuelle Korrekturen: Basislinie
Suchbereiche: Voll
Suchalgorithmus: Korrelation
Pfad des Suchspektrums: C:\Users\installuser\Desktop\Bachelorarbeit\Microplastic ...

Klassifikation	Gruppe	Bindun	Bereich	Intensität	Modus	Bemerkungen
Halogens	C-Cl					

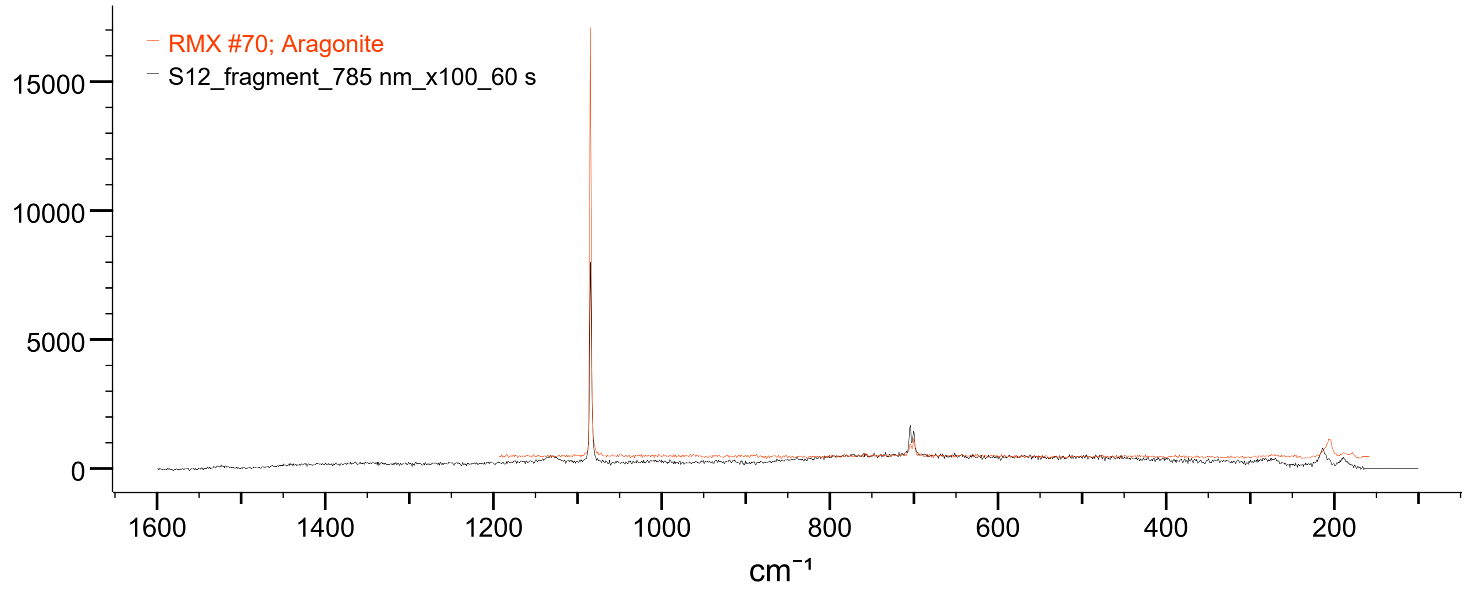

Manuelle Korrekturen: Basislinie
Suchbereiche: Voll
Suchalgorithmus: Korrelation
Pfad des Suchspektrums: C:\Users\installuser\Desktop\Bachelorarbeit\Microplastic Bachelorarbeit [work]\Raman\Bubl\Folie\fertig\S12 rechterwinkelteil\S12_fragment_785 nm_x100_60 s.ngs

Name:	Wert
Ergebnis-HQI	91.52
Datenbankabkürzung	RMX
Datenbanktitel	Raman - Minerals - HORIBA
Datensatzkennung	70
Name:	Aragonite
Classification	carbonate
Comments	Val Manubiola, Italy
Formula	CaCO3
Instrument Name	HORIBA LabRAM
Laser Power	632.8
Source of Sample	Bersani, Parma, Italy
Source of Spectrum	HORIBA Scientific

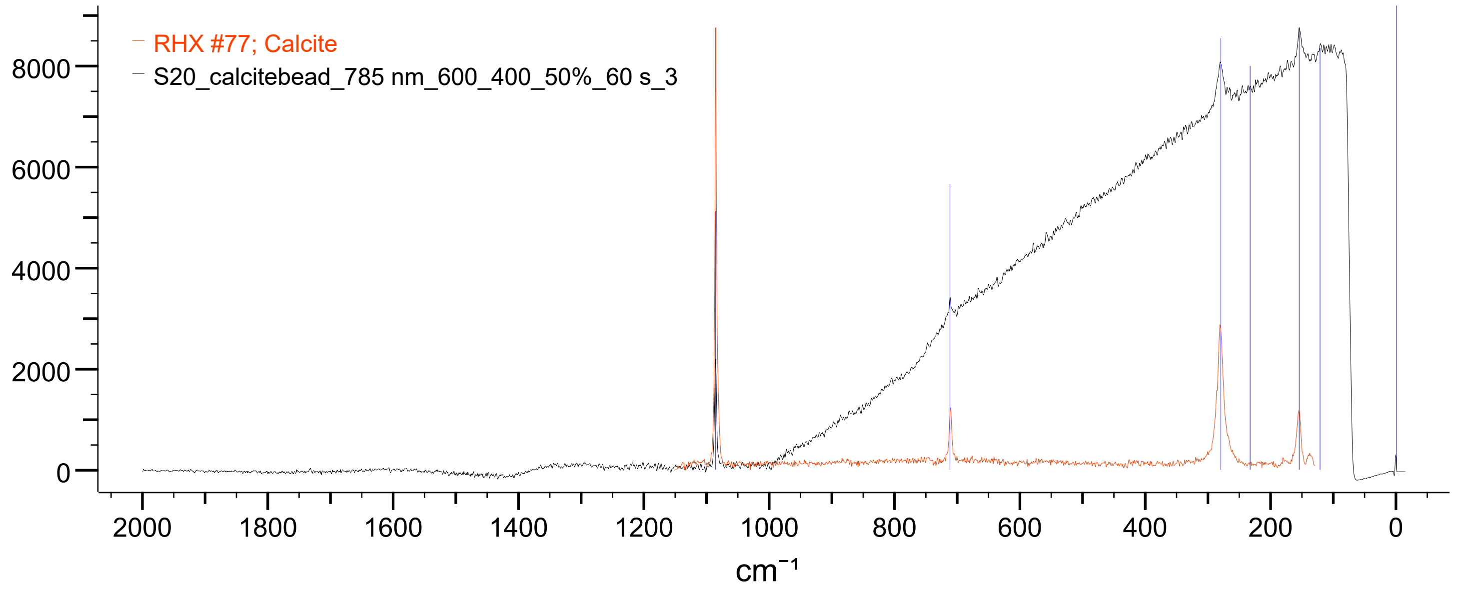

Manuelle Korrekturen: Basislinie, Rauschen

Suchbereiche: Voll

Suchalgorithmus: Korrelation

Pfad des Suchspektrums: C:\Users\installuser\Desktop\Bachelorarbeit\Microplastic ...

Klassifikation	Gruppe	Bindun	Bereich	Intensität	Modus	Bemerkungen
Ethers	RCH_2-O-CH_2R					

Bio-Rad Laboratories
Informatics Division

07.07.2018 12:02

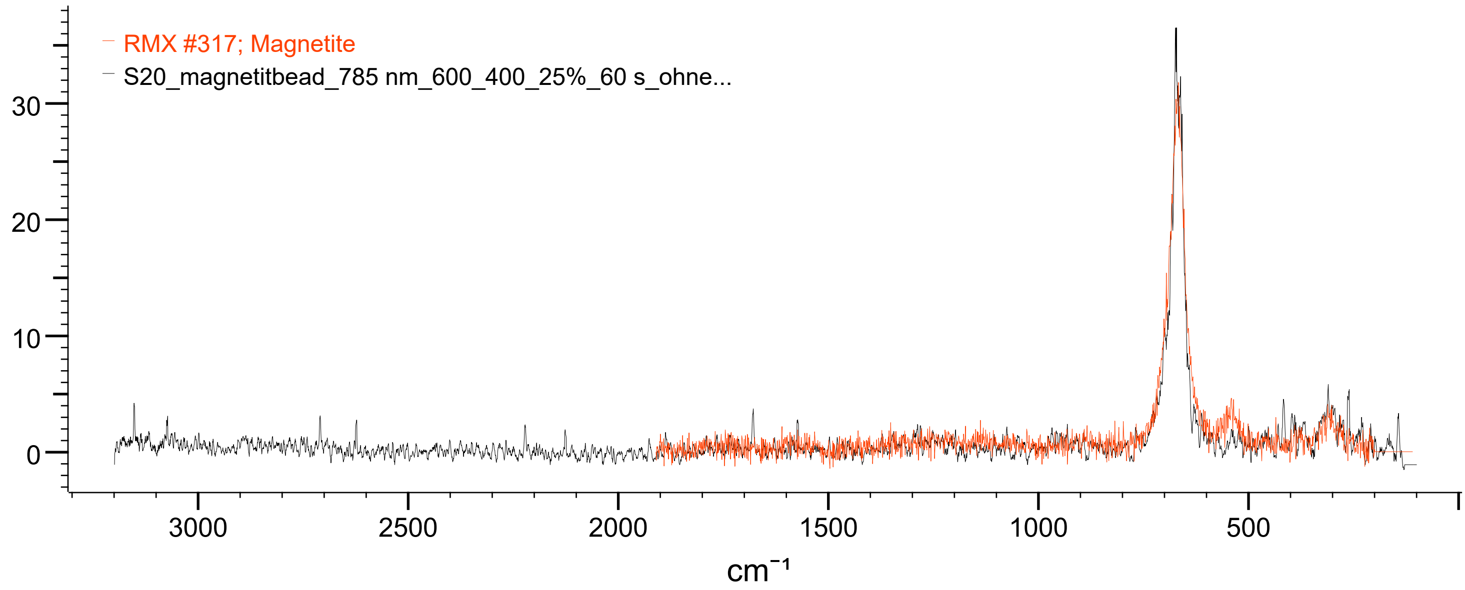

Manuelle Korrekturen: Keine
Suchbereiche: Voll
Suchalgorithmus: Korrelation
Pfad des Suchspektrums: C:\Users\installuser\Desktop\Bachelorarbeit\Microplastic Bachelorarbeit [work]\Raman\Bubl\Kugeln\fertig\SBE\Kugel Schwarz kleinste\S20_magnetitbead_785 nm_600_400_25%_60 ...
s_ohneB_smoo l6s

Name:	Wert
Ergebnis-HQI	92.94
Datenbankabkürzung	RMX
Datenbanktitel	Raman - Minerals - HORIBA
Datensatzkennung	317
Name:	Magnetite
Classification	oxide
Comments	with D.O.2
Formula	Fe3O4
Instrument Name	HORIBA LabRAM
Laser Power	632.8
Source of Spectrum	HORIBA Scientific

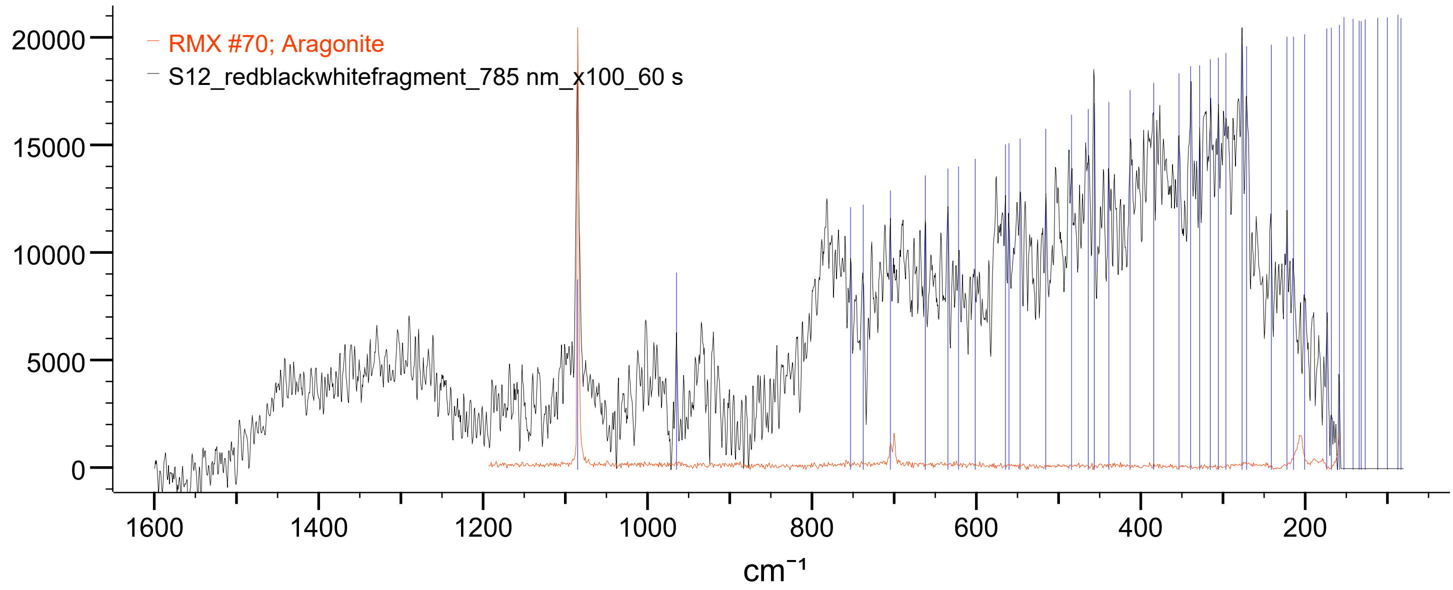

Manuelle Korrekturen: Basislinie, Rauschen
Suchbereiche: Voll
Suchalgorithmus: Korrelation
Pfad des Suchspektrums: C:\Users\installuser\Desktop\Bachelorarbeit\Microplastic ...

Klassifikation	Gruppe	Bindun	Bereich	Intensität	Modus	Bemerkungen
Aromatics	m-disubstituted ring					

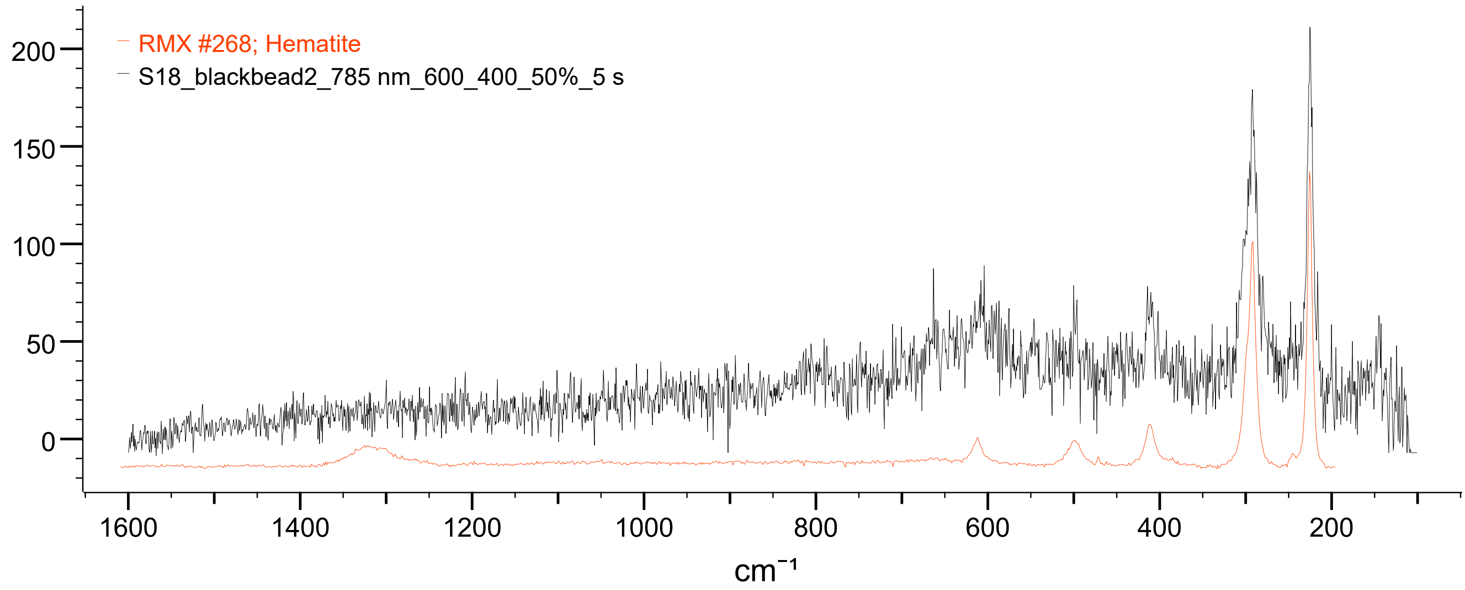

Manuelle Korrekturen: Basislinie
Suchbereiche: Voll
Suchalgorithmus: Korrelation
Pfad des Suchspektrums: C:\Users\installuser\Desktop\Bachelorarbeit\Microplastic Bachelorarbeit [work]\Raman\Bubl\Kugeln\fertig\S18\2. Kugel schwarz etwas kleiner\S18_blackbead2_785 nm_600_400_50%_5 s.ngs

ereinstimmu	Info	Gewicht	Name:	Chemische Struktur	Spektrum
		0.41	Hematite		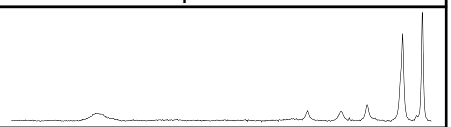

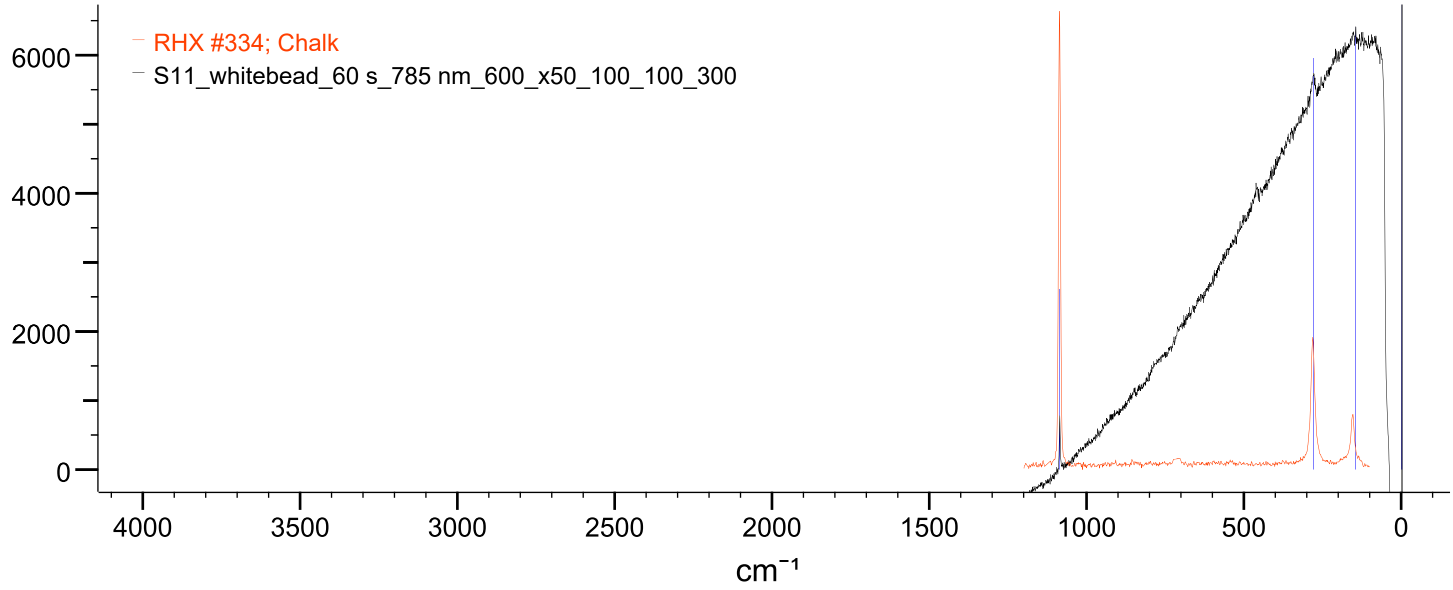

Manuelle Korrekturen: Keine

Suchbereiche: Voll

Suchalgorithmus: Korrelation

Pfad des Suchspektrums: C:\Users\installuser\Desktop\Bachelorarbeit\Microplastic ...

Klassifikation	Gruppe	Bindun	Bereich	Intensität	Modus	Bemerkungen
Ethers	RCH_2-O-CH_2R					

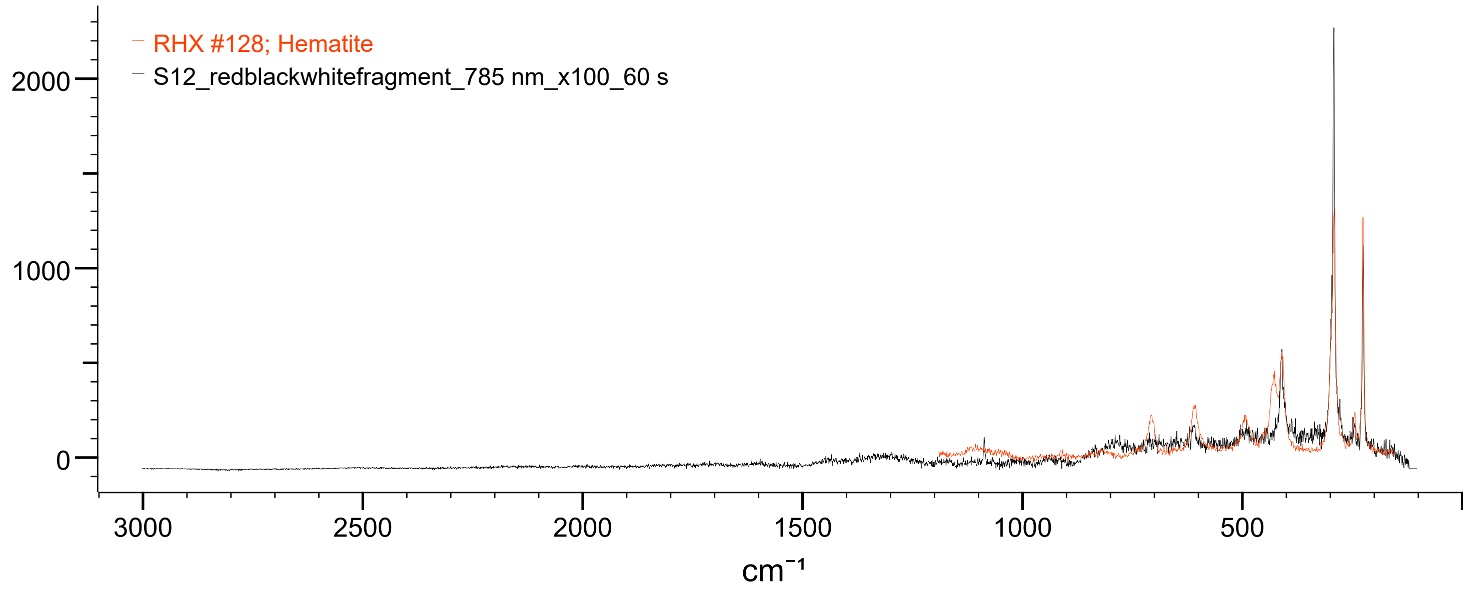

Manuelle Korrekturen: Basislinie
Suchbereiche: Voll
Suchalgorithmus: Korrelation
Pfad des Suchspektrums: C:\Users\installuser\Desktop\Bachelorarbeit\Microplastic Bachelorarbeit [work]\Raman\Bubl\Fragmente\fertig\S12 rotweißschwarz\rote Stelle\S12_redblackwhitefragment_785 nm_x100_60 ... s.ngs

Name:	Wert
Ergebnis-HQI	82.49
Datenbankabkürzung	RHX
Datenbanktitel	Raman - Forensic - HORIBA
Datensatzkennung	128
Name:	Hematite
CAS Registry Number	1317-60-8
Classification	mineral
Comments	varieties: Oligiste - Specularite
Formula	alpha-Fe2O3
Instrument Name	HORIBA LabRAM
Laser Power	632.8
Source of Sample	Bersani, Parma, Italy
Source of Spectrum	HORIBA Scientific
Synonyms	C.I. Generic name: Pigment Red 101; PR101; C.I. Constitution No: 77491; Iron oxide

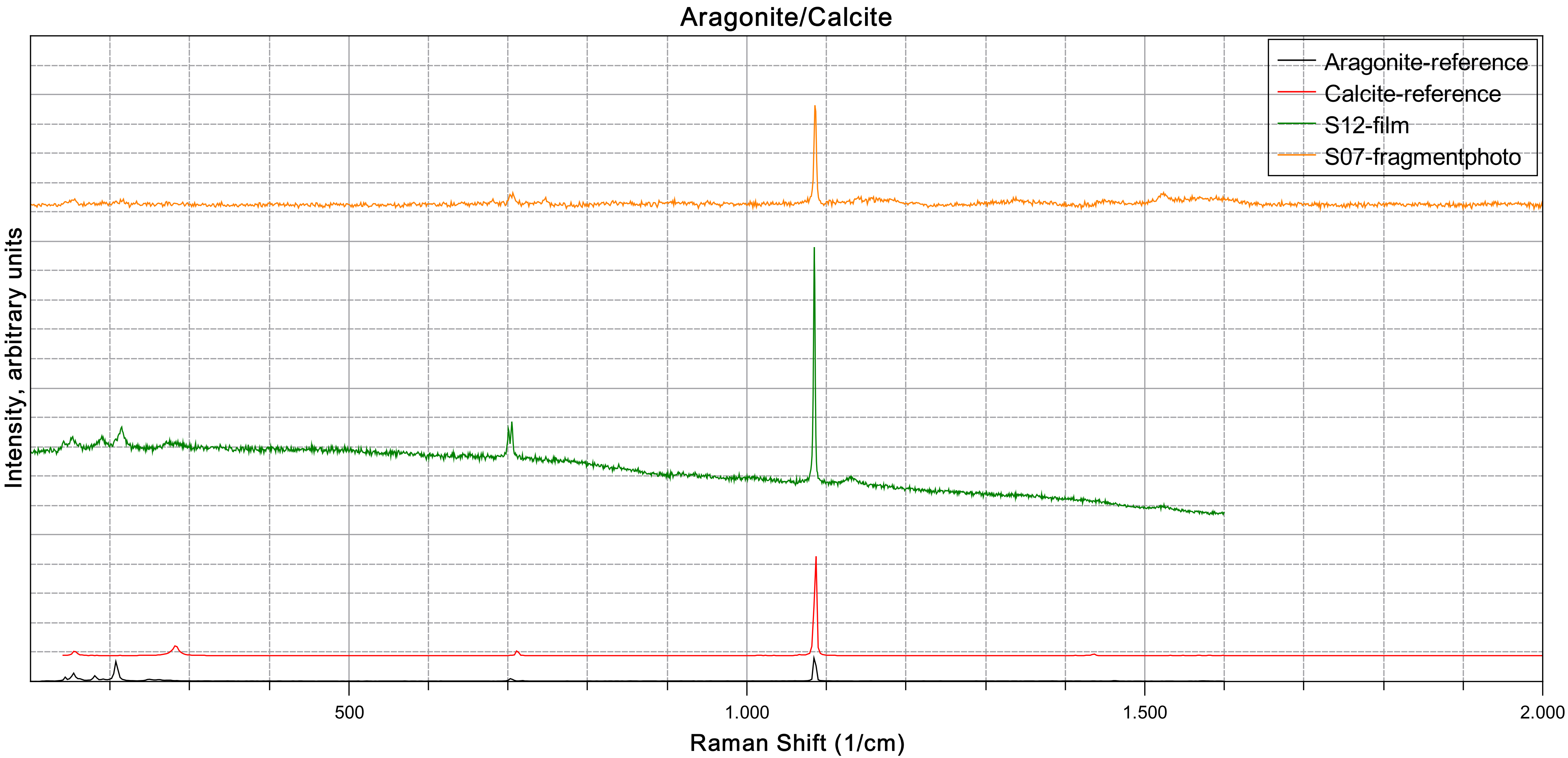

Aragonite/Calcite
Aragonite-reference
Calcite-reference
S12-film
S07-fragmentphoto
Intensity, arbitrary units
500
1.000
1.500
2.000
Raman Shift (1/cm)

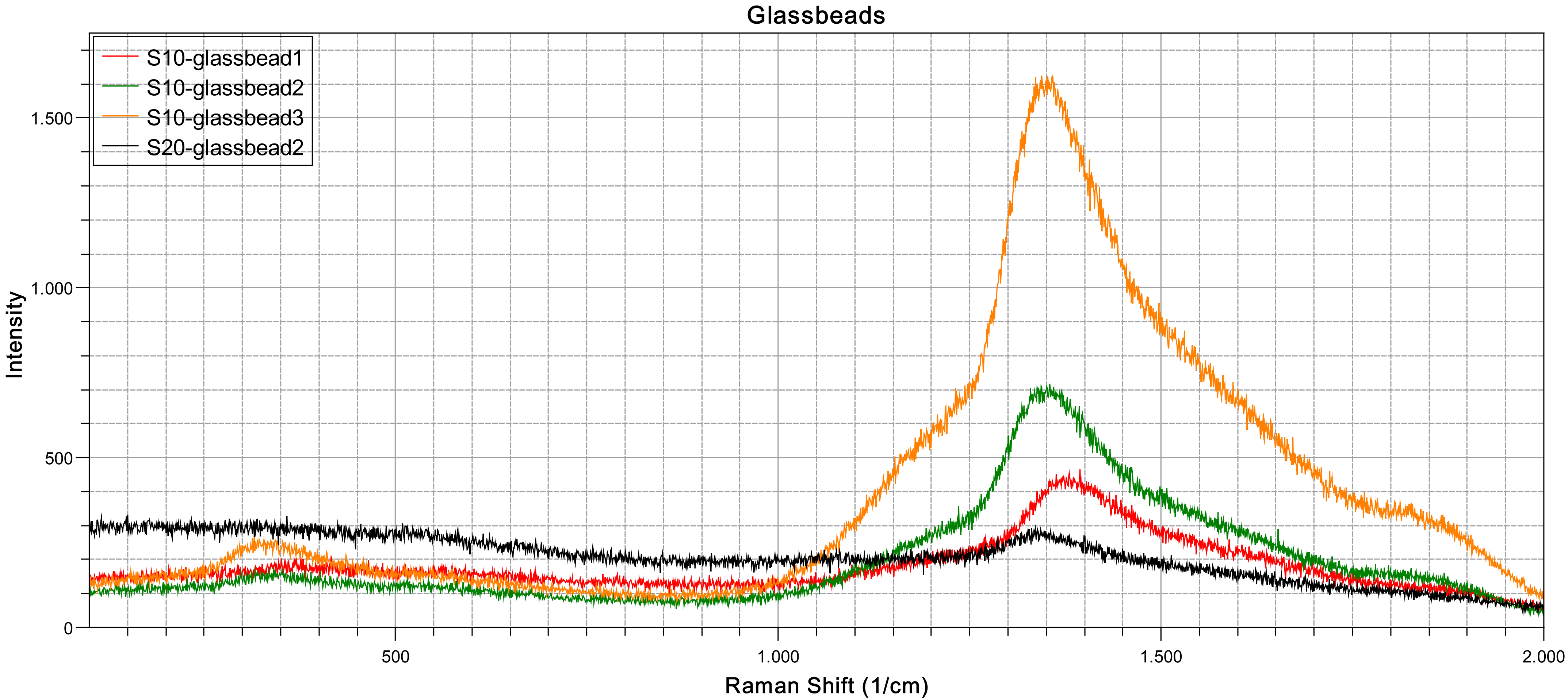

Glassbeads
S10-glassbead1
S10-glassbead2
S10-glassbead3
S20-glassbead2
Intensity
0
500
1.000
1.500
Raman Shift (1/cm)
500
1.000
1.500
2.000

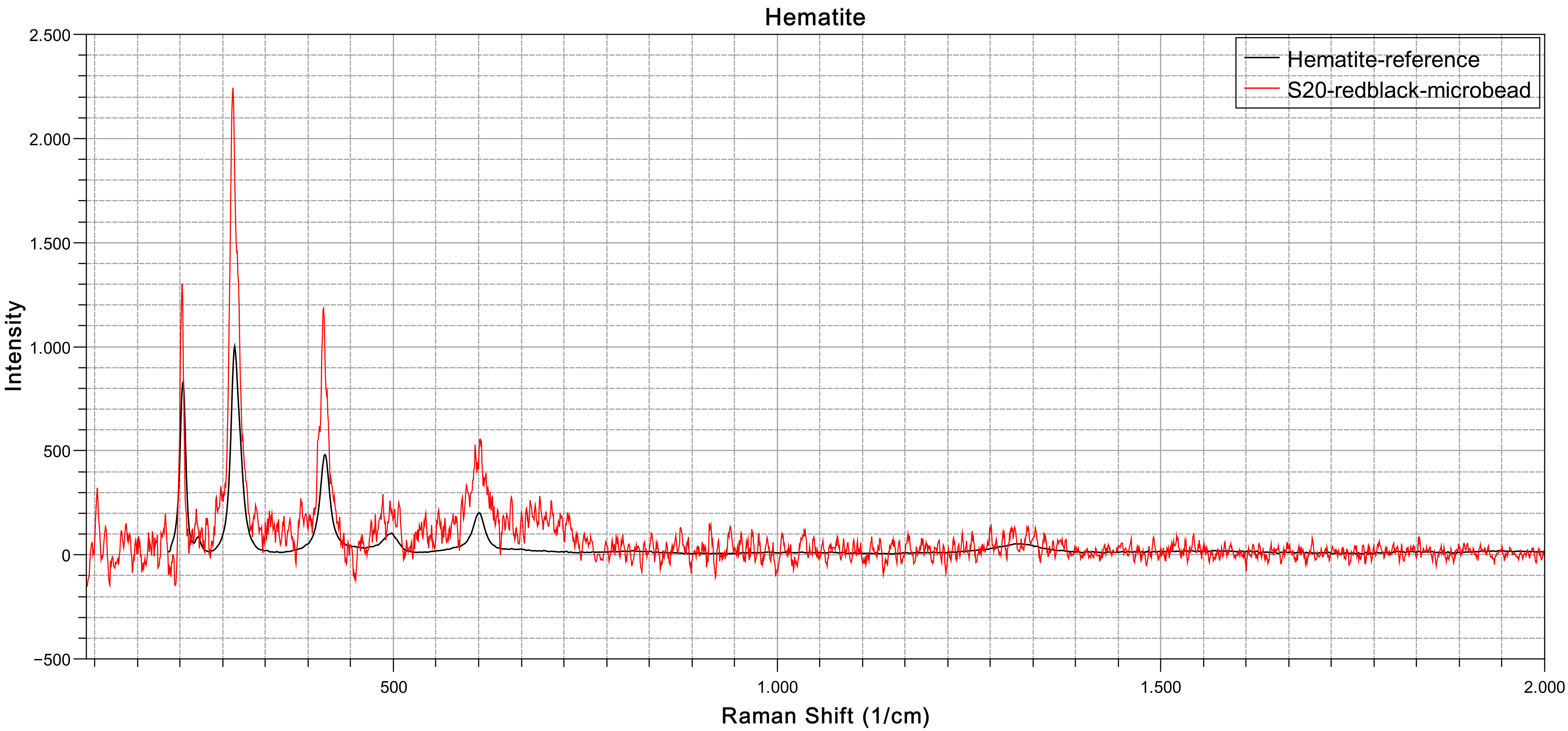

Hematite
Hematite-reference
S20-redblack-microbead
Intensity
2.500
2.000
1.500
1.000
500
0
−500
500
1.000
1.500
2.000
Raman Shift (1/cm)

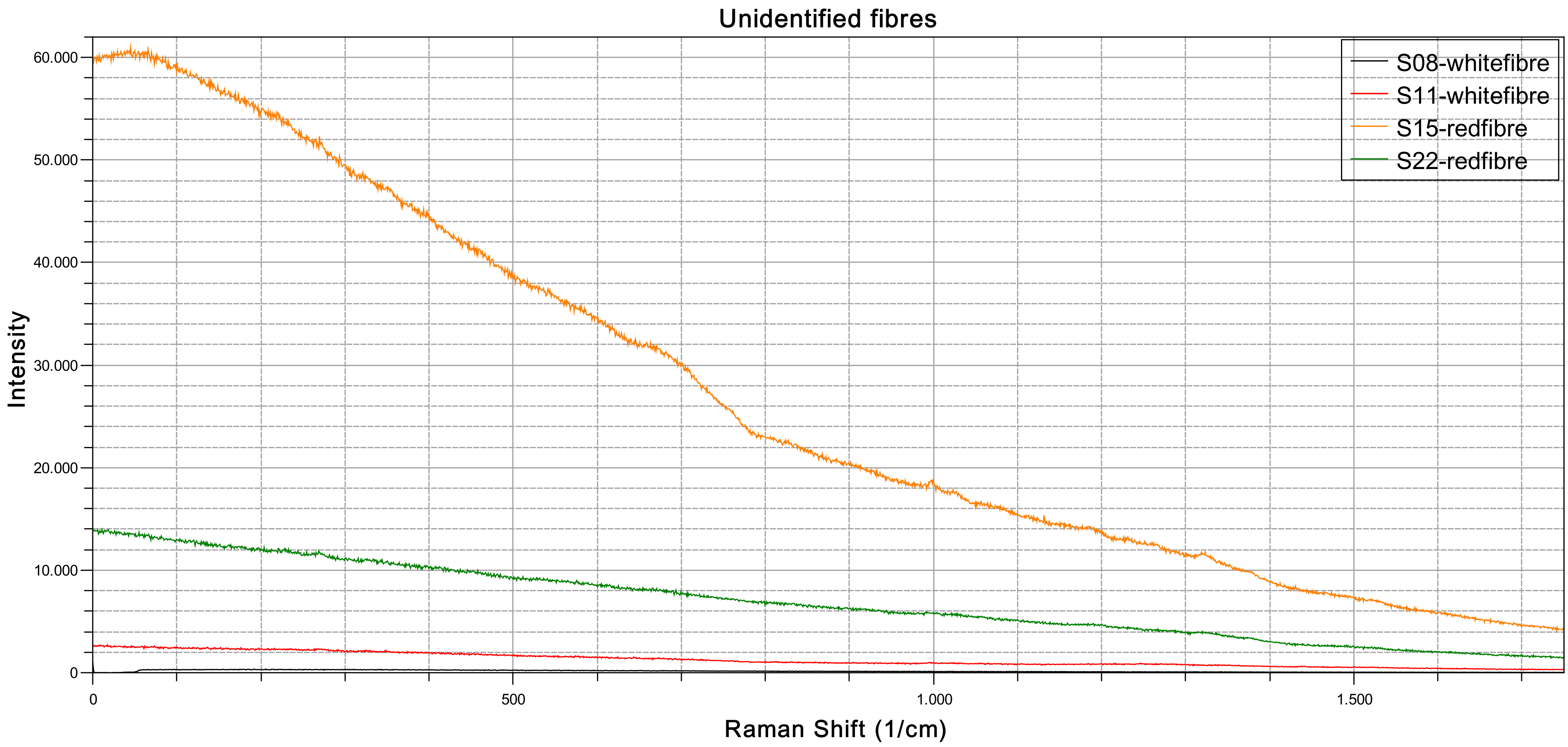

Unidentified fibres
S08-whitefibre
S11-whitefibre
S15-redfibre
S22-redfibre
Intensity
60.000
50.000
40.000
30.000
20.000
10.000
0
500
1.000
1.500
Raman Shift (1/cm)

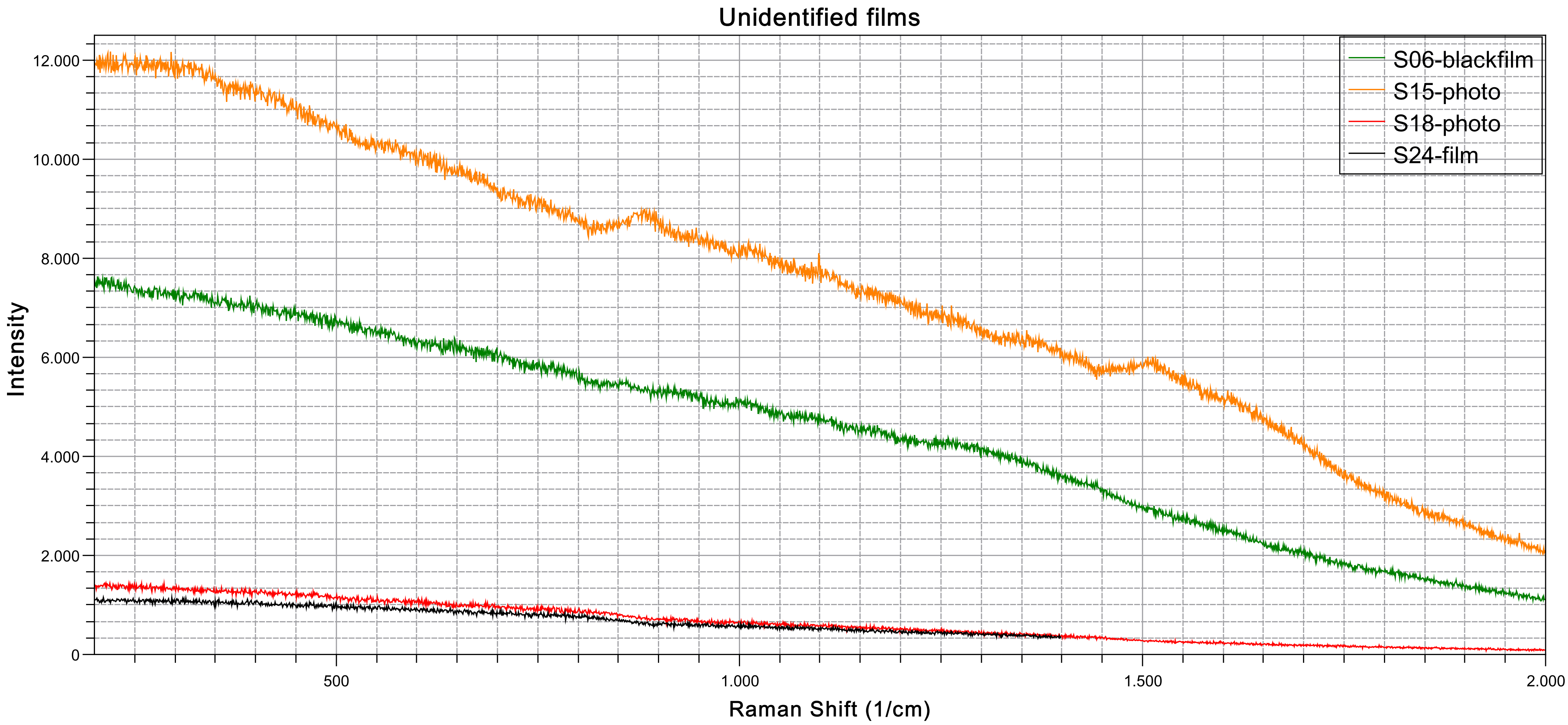
Unidentified films
Intensity
12.000
10.000
8.000
6.000
4.000
2.000
0
500
1.000
1.500
2.000
Raman Shift (1/cm)
S06-blackfilm
S15-photo
S18-photo
S24-film

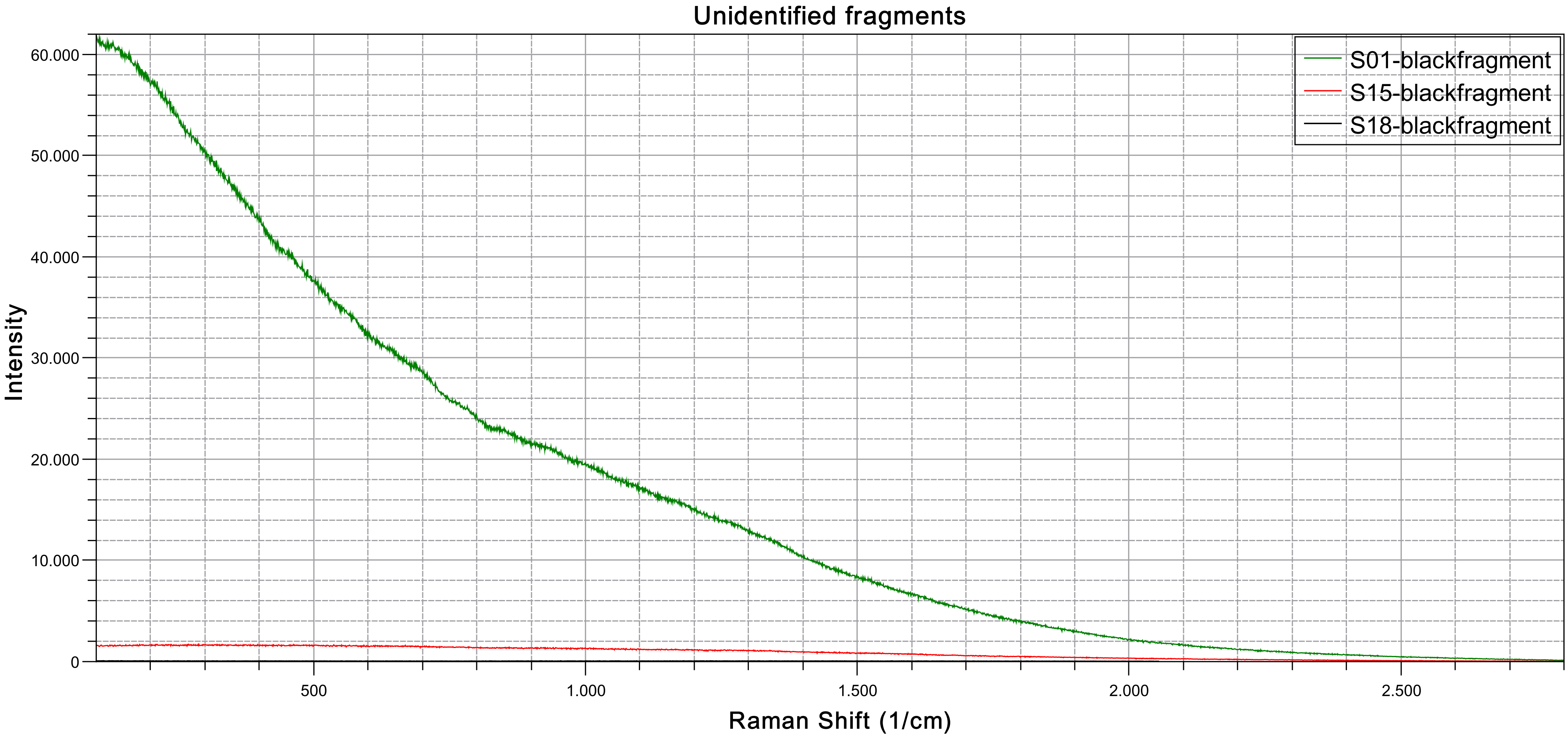
Unidentified fragments
S01-blackfragment
S15-blackfragment
S18-blackfragment
Intensity
60.000
50.000
40.000
30.000
20.000
10.000
0
500
1.000
1.500
2.000
2.500
Raman Shift (1/cm)

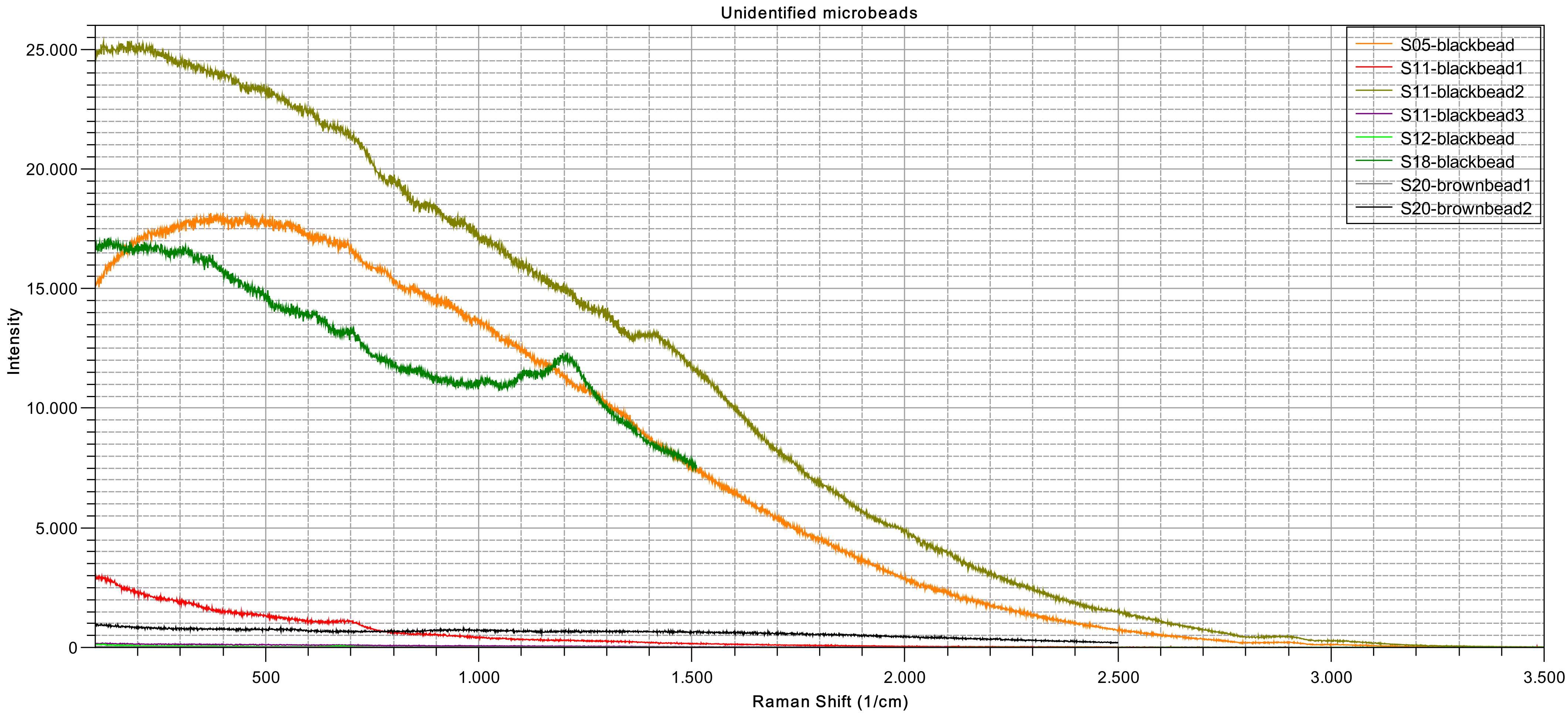
Unidentified microbeads
Intensity
25.000
20.000
15.000
10.000
5.000
0
500
1.000
1.500
2.000
2.500
3.000
3.500
Raman Shift (1/cm)
S05-blackbead
S11-blackbead1
S11-blackbead2
S11-blackbead3
S12-blackbead
S18-blackbead
S20-brownbead1
S20-brownbead2

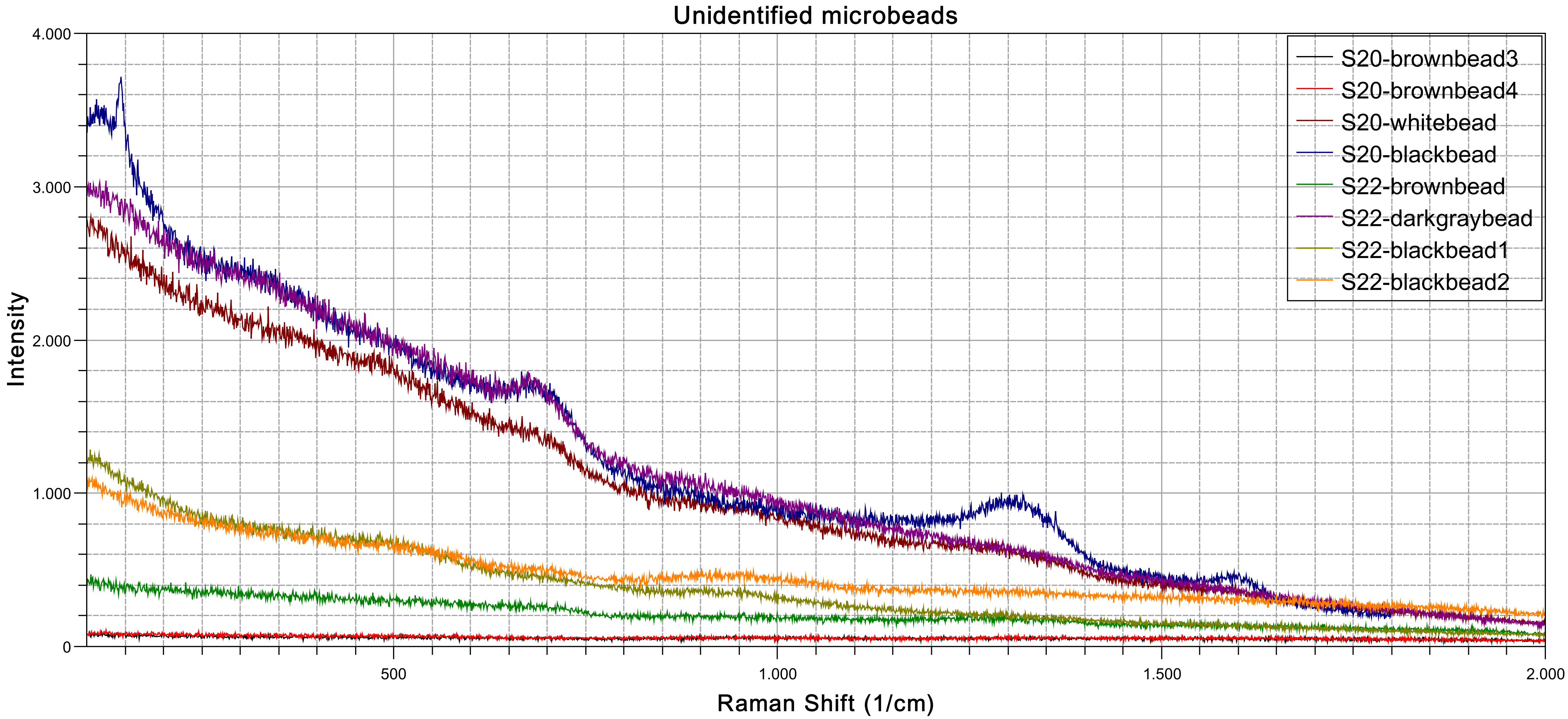
Unidentified microbeads
Intensity
Raman Shift (1/cm)
0
1.000
2.000
3.000
4.000
500
1.000
1.500
2.000
S20-brownbead3
S20-brownbead4
S20-whitebead
S20-blackbead
S22-brownbead
S22-darkgraybead
S22-blackbead1
S22-blackbead2

SAMPLE STATISTICS

		S01
	ANALYST AND DATE:	Mario Bubl, 5/30/2018
	SIEVING ERROR:	9,2%
	SAMPLE TYPE:	Polymodal, Poorly Sorted
	TEXTURAL GROUP:	Sandy Gravel
	SEDIMENT NAME:	Sandy Very Fine Gravel
METHOD OF MOMENTS Arithmetic (μm)	MEAN $(\bar{x}_a)$:	1449,3
	SORTING (σ_a):	957,7
	SKEWNESS (Sk_a):	-0,176
	KURTOSIS (K_a):	1,269
METHOD OF MOMENTS Geometric (μm)	MEAN $(\bar{x}_g)$:	945,3
	SORTING (σ_g):	2,968
	SKEWNESS (Sk_g):	-0,868
	KURTOSIS (K_g):	2,470
METHOD OF MOMENTS Logarithmic (ϕ)	MEAN $(\bar{x}_\phi)$:	0,081
	SORTING (σ_ϕ):	1,570
	SKEWNESS (Sk_ϕ):	0,868
	KURTOSIS (K_ϕ):	2,470
FOLK AND WARD METHOD (μm)	MEAN (M_G):	966,8
	SORTING (σ_G):	2,769
	SKEWNESS (Sk_G):	-0,483
	KURTOSIS (K_G):	0,661
FOLK AND WARD METHOD (ϕ)	MEAN (M_Z):	0,049
	SORTING (σ_I):	1,470
	SKEWNESS (Sk_I):	0,483
	KURTOSIS (K_G):	0,661
FOLK AND WARD METHOD (Description)	MEAN:	Coarse Sand
	SORTING:	Poorly Sorted
	SKEWNESS:	Very Fine Skewed
	KURTOSIS:	Very Platykurtic
	MODE 1 (μm):	2400,0
	MODE 2 (μm):	1200,0
	MODE 3 (μm):	302,5
	MODE 1 (ϕ):	-1,243
	MODE 2 (ϕ):	-0,243
	MODE 3 (ϕ):	1,747
	D_{10} (μm):	157,5
	D_{50} (μm):	1328,1
	D_{90} (μm):	2609,2
	(D_{90} / D_{10}) (μm):	16,56
	$(D_{90} - D_{10})$ (μm):	2451,7
	(D_{75} / D_{25}) (μm):	6,677
	$(D_{75} - D_{25})$ (μm):	1995,5
	D_{10} (ϕ):	-1,384
	D_{50} (ϕ):	-0,409
	D_{90} (ϕ):	2,666
	(D_{90} / D_{10}) (ϕ):	-1,927
	$(D_{90} - D_{10})$ (ϕ):	4,050
	(D_{75} / D_{25}) (ϕ):	-1,225
	$(D_{75} - D_{25})$ (ϕ):	2,739

% GRAVEL:	47,7%
% SAND:	52,3%
% MUD:	0,0%
% V COARSE GRAVEL:	0,0%
% COARSE GRAVEL:	0,0%
% MEDIUM GRAVEL:	0,0%
% FINE GRAVEL:	0,0%
% V FINE GRAVEL:	47,7%
% V COARSE SAND:	14,9%
% COARSE SAND:	12,1%
% MEDIUM SAND:	12,3%
% FINE SAND:	8,3%
% V FINE SAND:	4,8%
% V COARSE SILT:	0,0%
% COARSE SILT:	0,0%
% MEDIUM SILT:	0,0%
% FINE SILT:	0,0%
% V FINE SILT:	0,0%
% CLAY:	0,0%

S02	S04
Mario Bubl, 5/30/2018	Mario Bubl, 5/30/2018
14,7%	20,5%
Trimodal, Moderately Sorted	Polymodal, Poorly Sorted
Slightly Gravelly Sand	Gravelly Sand
Slightly Very Fine Gravelly Fine Sand	Very Fine Gravelly Medium Sand
242,4	874,1
304,9	847,2
4,960	1,021
32,20	2,400
176,3	528,7
1,942	2,745
1,282	0,161
5,480	1,929
2,504	0,920
0,957	1,457
-1,282	-0,161
5,480	1,929
161,1	572,1
1,931	2,978
0,182	0,109
1,295	0,797
2,634	0,806
0,949	1,575
-0,182	-0,109
1,295	0,797
Fine Sand	Coarse Sand
Moderately Sorted	Poorly Sorted
Coarse Skewed	Coarse Skewed
Leptokurtic	Platykurtic
152,5	302,5
302,5	2400,0
76,50	605,0
2,737	1,747
1,747	-1,243
3,731	0,747
76,70	146,5
155,2	511,2
348,3	2388,3
4,542	16,30
271,6	2241,8
2,020	4,647
133,6	980,6
1,521	-1,256
2,688	0,968
3,705	2,771
2,435	-2,206
2,183	4,027
1,529	-5,897
1,015	2,216

1,2%	21,2%
98,8%	78,8%
0,0%	0,0%
0,0%	0,0%
0,0%	0,0%
0,0%	0,0%
0,0%	0,0%
1,2%	21,2%
2,2%	11,4%
5,6%	18,7%
19,1%	30,1%
53,8%	15,5%
18,1%	3,2%
0,0%	0,0%
0,0%	0,0%
0,0%	0,0%
0,0%	0,0%
0,0%	0,0%
0,0%	0,0%

S05	S06	S07
Mario Bubl, 5/30/2018	Mario Bubl, 5/30/2018	Mario Bubl, 5/30/2018
11,7%	18,4%	1,6%
Polymodal, Poorly Sorted	Polymodal, Poorly Sorted	Bimodal, Moderately Well Sorted
Sandy Gravel	Sandy Gravel	Sandy Gravel
Sandy Very Fine Gravel	Sandy Very Fine Gravel	Sandy Very Fine Gravel
1267,3	1133,5	1922,0
1025,4	1032,9	726,2
0,100	0,325	-1,064
1,145	1,229	2,574
704,7	563,3	1650,5
3,417	3,754	1,906
-0,361	-0,187	-2,238
1,579	1,491	8,531
0,505	0,828	-0,723
1,773	1,908	0,930
0,361	0,187	2,238
1,579	1,491	8,531
740,3	564,8	1816,9
3,390	3,615	1,610
-0,429	-0,085	-0,677
0,654	0,563	0,991
0,434	0,824	-0,861
1,761	1,854	0,687
0,429	0,085	0,677
0,654	0,563	0,991
Coarse Sand	Coarse Sand	Very Coarse Sand
Poorly Sorted	Poorly Sorted	Moderately Well Sorted
Very Fine Skewed	Symmetrical	Very Fine Skewed
Very Platykurtic	Very Platykurtic	Mesokurtic
2400,0	2400,0	2400,0
302,5	302,5	1200,0
152,5	76,50	
-1,243	-1,243	-1,243
1,747	1,747	-0,243
2,737	3,731	
135,1	80,13	636,7
1063,8	575,1	2184,8
2590,3	2565,6	2664,5
19,17	32,02	4,185
2455,2	2485,5	2027,8
8,858	14,02	1,998
2044,6	2089,8	1235,3
-1,373	-1,359	-1,414
-0,089	0,798	-1,128
2,887	3,641	0,651
-2,103	-2,679	-0,461
4,261	5,001	2,065
-1,612	-2,255	0,236
3,147	3,809	0,998

43,2%	38,5%	67,8%
56,8%	61,5%	32,2%
0,0%	0,0%	0,0%
0,0%	0,0%	0,0%
0,0%	0,0%	0,0%
0,0%	0,0%	0,0%
0,0%	0,0%	0,0%
43,2%	38,5%	67,8%
8,3%	5,4%	19,7%
7,6%	10,1%	8,1%
17,9%	16,3%	2,2%
16,5%	14,8%	1,5%
6,5%	14,8%	0,8%
0,0%	0,0%	0,0%
0,0%	0,0%	0,0%
0,0%	0,0%	0,0%
0,0%	0,0%	0,0%
0,0%	0,0%	0,0%
0,0%	0,0%	0,0%

S08	S10	S11
Mario Bubl, 5/30/2018	Mario Bubl, 5/30/2018	Mario Bubl, 5/30/2018
2,7%	2,8%	8,0%
Polymodal, Poorly Sorted	Polymodal, Poorly Sorted	Polymodal, Poorly Sorted
Sandy Gravel	Sandy Gravel	Sandy Gravel
Sandy Very Fine Gravel	Sandy Very Fine Gravel	Sandy Very Fine Gravel
1634,7	1284,6	988,0
923,3	885,6	1045,0
-0,496	0,278	0,578
1,433	1,372	1,383
1187,2	918,6	451,6
2,544	2,407	3,682
-1,073	-0,478	0,276
2,959	2,274	1,422
-0,248	0,123	1,147
1,347	1,267	1,881
1,073	0,478	-0,276
2,959	2,274	1,422
1210,3	937,6	455,7
2,534	2,372	3,526
-0,807	-0,214	0,350
0,812	0,675	0,543
-0,275	0,093	1,134
1,342	1,246	1,818
0,807	0,214	-0,350
0,812	0,675	0,543
Very Coarse Sand	Coarse Sand	Medium Sand
Poorly Sorted	Poorly Sorted	Poorly Sorted
Very Fine Skewed	Fine Skewed	Very Coarse Skewed
Platykurtic	Platykurtic	Very Platykurtic
2400,0	2400,0	2400,0
605,0	605,0	152,5
302,5	1200,0	302,5
-1,243	-1,243	-1,243
0,747	0,747	2,737
1,747	-0,243	1,747
281,6	280,3	125,4
2089,0	1073,8	293,1
2640,7	2549,7	2542,3
9,379	9,097	20,28
2359,1	2269,4	2416,9
4,066	4,196	14,70
1823,7	1687,6	2049,9
-1,401	-1,350	-1,346
-1,063	-0,103	1,770
1,828	1,835	2,996
-1,305	-1,359	-2,226
3,229	3,185	4,342
-0,588	-0,803	-2,410
2,024	2,069	3,878

57,4%	35,9%	34,8%
42,6%	64,1%	65,2%
0,0%	0,0%	0,0%
0,0%	0,0%	0,0%
0,0%	0,0%	0,0%
0,0%	0,0%	0,0%
0,0%	0,0%	0,0%
57,4%	35,9%	34,8%
10,7%	17,8%	1,9%
13,5%	25,1%	2,1%
12,6%	16,5%	20,5%
4,3%	3,6%	30,9%
1,5%	1,0%	9,8%
0,0%	0,0%	0,0%
0,0%	0,0%	0,0%
0,0%	0,0%	0,0%
0,0%	0,0%	0,0%
0,0%	0,0%	0,0%
0,0%	0,0%	0,0%

S12	S14
Mario Bubl, 5/30/2018	Mario Bubl, 5/30/2018
10,3%	14,1%
Trimodal, Moderately Sorted	Polymodal, Moderately Sorted
Slightly Gravelly Sand	Slightly Gravelly Sand
Slightly Very Fine Gravelly Fine Sand	Slightly Very Fine Gravelly Medium Sand
199,7	349,2
186,0	431,4
8,998	4,002
105,2	19,05
167,7	248,8
1,666	2,035
0,688	0,830
5,775	5,030
2,576	2,007
0,737	1,025
-0,688	-0,830
5,775	5,030
160,9	234,0
1,716	1,777
0,020	-0,333
0,929	1,208
2,636	2,095
0,779	0,829
-0,020	0,333
0,929	1,208
Fine Sand	Fine Sand
Moderately Sorted	Moderately Sorted
Symmetrical	Very Fine Skewed
Mesokurtic	Leptokurtic
152,5	302,5
302,5	152,5
76,50	76,50
2,737	1,747
1,747	2,737
3,731	3,731
78,32	88,30
157,1	274,0
320,0	561,8
4,085	6,362
241,6	473,5
2,007	2,134
133,4	173,2
1,644	0,832
2,670	1,868
3,674	3,501
2,235	4,209
2,030	2,670
1,526	1,676
1,005	1,093

0,5%	3,7%
99,5%	96,3%
0,0%	0,0%
0,0%	0,0%
0,0%	0,0%
0,0%	0,0%
0,0%	0,0%
0,5%	3,7%
0,0%	0,9%
1,0%	8,2%
28,4%	50,5%
53,6%	26,2%
16,4%	10,6%
0,0%	0,0%
0,0%	0,0%
0,0%	0,0%
0,0%	0,0%
0,0%	0,0%
0,0%	0,0%

S15	S16
Mario Bubl, 5/30/2018	Mario Bubl, 5/30/2018
8,9%	1,0%
Trimodal, Moderately Sorted	Polymodal, Poorly Sorted
Slightly Gravelly Sand	Sandy Gravel
Slightly Very Fine Gravelly Fine Sand	Sandy Very Fine Gravel
308,8	1195,5
468,4	947,5
4,040	0,386
18,15	1,296
206,3	792,0
2,034	2,555
1,602	0,002
6,988	1,472
2,277	0,337
1,025	1,354
-1,602	-0,002
6,988	1,472
192,1	763,5
1,753	2,434
0,327	0,227
1,195	0,492
2,380	0,389
0,810	1,283
-0,327	-0,227
1,195	0,492
Fine Sand	Coarse Sand
Moderately Sorted	Poorly Sorted
Very Coarse Skewed	Coarse Skewed
Leptokurtic	Very Platykurtic
152,5	2400,0
302,5	302,5
76,50	605,0
2,737	-1,243
1,747	1,747
3,731	0,747
86,08	268,8
169,5	643,1
342,0	2554,4
3,973	9,504
255,9	2285,7
2,126	7,071
156,7	1911,0
1,548	-1,353
2,560	0,637
3,538	1,896
2,286	-1,401
1,990	3,249
1,619	-1,445
1,088	2,822

4,6%	36,7%
95,4%	63,3%
0,0%	0,0%
0,0%	0,0%
0,0%	0,0%
0,0%	0,0%
0,0%	0,0%
4,6%	36,7%
0,2%	8,0%
1,4%	18,9%
36,3%	33,3%
46,2%	2,8%
11,4%	0,3%
0,0%	0,0%
0,0%	0,0%
0,0%	0,0%
0,0%	0,0%
0,0%	0,0%
0,0%	0,0%

S17	S18
Mario Bubl, 5/30/2018	Mario Bubl, 5/30/2018
1,2%	5,6%
Bimodal, Moderately Well Sorted	Polymodal, Poorly Sorted
Slightly Gravelly Sand	Sandy Gravel
Slightly Very Fine Gravelly Medium Sand	Sandy Very Fine Gravel
361,3	955,6
261,9	1021,2
5,915	0,658
45,18	1,505
317,9	447,4
1,520	3,566
1,242	0,297
9,092	1,484
1,653	1,160
0,604	1,834
-1,242	-0,297
9,092	1,484
339,9	457,7
1,475	3,498
0,285	0,345
2,557	0,547
1,557	1,128
0,561	1,806
-0,285	-0,345
2,557	0,547
Medium Sand	Medium Sand
Moderately Well Sorted	Poorly Sorted
Coarse Skewed	Very Coarse Skewed
Very Leptokurtic	Very Platykurtic
302,5	2400,0
605,0	152,5
	302,5
1,747	-1,243
0,747	2,737
	1,747
250,9	126,4
302,8	297,2
580,1	2525,0
2,312	19,97
329,2	2398,5
1,265	14,27
71,33	2010,7
0,786	-1,336
1,723	1,751
1,995	2,983
2,539	-2,233
1,209	4,320
1,218	-2,447
0,339	3,835

1,2%	32,5%
98,8%	67,5%
0,0%	0,0%
0,0%	0,0%
0,0%	0,0%
0,0%	0,0%
0,0%	0,0%
1,2%	32,5%
0,4%	2,8%
14,6%	3,5%
74,6%	21,8%
8,7%	30,2%
0,5%	9,1%
0,0%	0,0%
0,0%	0,0%
0,0%	0,0%
0,0%	0,0%
0,0%	0,0%
0,0%	0,0%

S20	S22
Mario Bubl, 5/30/2018	Mario Bubl, 5/30/2018
2,4%	13,2%
Polymodal, Poorly Sorted	Trimodal, Moderately Sorted
Sandy Gravel	Slightly Gravelly Sand
Sandy Very Fine Gravel	Slightly Very Fine Gravelly Fine Sand
1286,2	219,0
1008,9	239,4
0,101	6,288
1,141	53,94
769,5	168,6
3,071	1,884
-0,303	0,753
1,535	4,365
0,378	2,568
1,619	0,914
0,303	-0,753
1,535	4,365
879,5	157,1
2,778	1,911
-0,334	0,086
0,587	1,026
0,185	2,671
1,474	0,934
0,334	-0,086
0,587	1,026
Coarse Sand	Fine Sand
Poorly Sorted	Moderately Sorted
Very Fine Skewed	Symmetrical
Very Platykurtic	Mesokurtic
2400,0	152,5
302,5	302,5
152,5	76,50
-1,243	2,737
1,747	1,747
2,737	3,731
156,5	72,74
1084,5	156,7
2590,6	335,1
16,55	4,606
2434,0	262,3
8,058	2,237
2019,3	154,9
-1,373	1,578
-0,117	2,674
2,675	3,781
-1,948	2,397
4,049	2,204
-1,498	1,633
3,010	1,162

43,3%	0,7%
56,7%	99,3%
0,0%	0,0%
0,0%	0,0%
0,0%	0,0%
0,0%	0,0%
0,0%	0,0%
43,3%	0,7%
8,9%	0,8%
6,7%	3,6%
26,2%	29,3%
12,8%	40,7%
2,1%	24,8%
0,0%	0,0%
0,0%	0,0%
0,0%	0,0%
0,0%	0,0%
0,0%	0,0%
0,0%	0,0%

S23	S24	
Mario Bubl, 5/30/2018	Mario Bubl, 5/30/2018	
1,5%	5,2%	
Trimodal, Poorly Sorted	Trimodal, Poorly Sorted	
Sandy Gravel	Sandy Gravel	
Sandy Very Fine Gravel	Sandy Very Fine Gravel	
1643,9	1600,0	
829,5	1012,7	
-0,360	-0,542	
1,431	1,383	
1329,2	997,7	
2,041	3,243	
-0,998	-0,862	
3,061	2,108	
-0,411	0,003	
1,029	1,698	
0,998	0,862	
3,061	2,108	
1437,6	1110,8	
2,015	2,836	
-0,719	-0,836	
0,732	0,605	
-0,524	-0,152	
1,011	1,504	
0,719	0,836	
0,732	0,605	
Very Coarse Sand	Very Coarse Sand	
Poorly Sorted	Poorly Sorted	
Very Fine Skewed	Very Fine Skewed	
Platykurtic	Very Platykurtic	
2400,0	2400,0	
1200,0	302,5	
605,0	152,5	
-1,243	-1,243	
-0,243	1,747	
0,747	2,737	
513,6	150,5	
2028,2	2119,1	
2625,1	2648,2	
5,112	17,60	
2111,5	2497,8	
3,423	7,940	
1686,9	2129,1	
-1,392	-1,405	
-1,020	-1,083	
0,961	2,732	
-0,690	-1,945	
2,354	4,137	
-0,417	-1,327	
1,775	2,989	

52,2%	60,4%	
47,8%	39,6%	
0,0%	0,0%	
0,0%	0,0%	
0,0%	0,0%	
0,0%	0,0%	
0,0%	0,0%	
52,2%	60,4%	
21,9%	5,7%	
17,3%	2,2%	
7,9%	16,2%	
0,6%	11,3%	
0,2%	4,3%	
0,0%	0,0%	
0,0%	0,0%	
0,0%	0,0%	
0,0%	0,0%	
0,0%	0,0%	
0,0%	0,0%	

Triangular Diagram

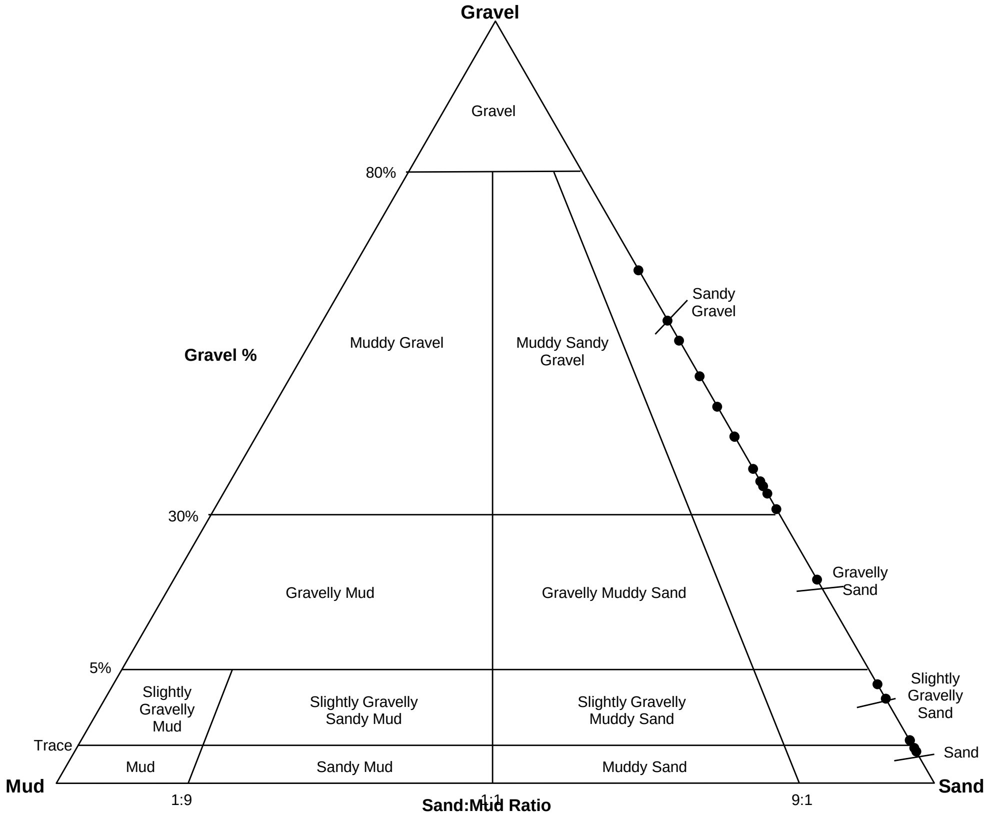

Triangular Diagram

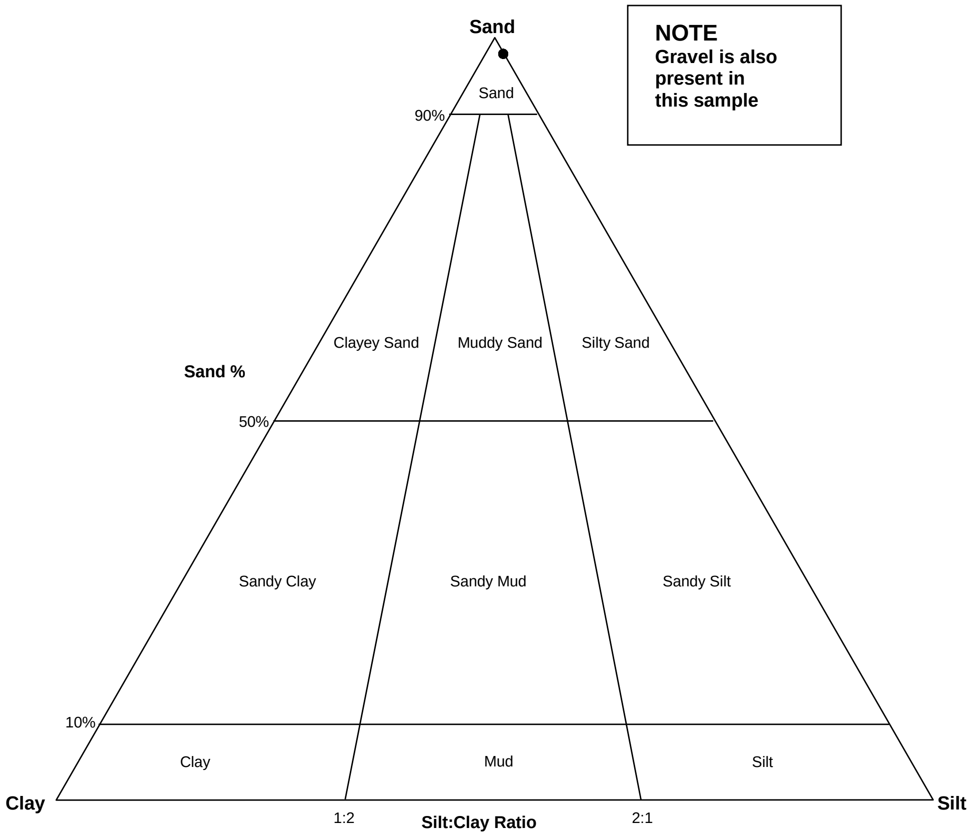

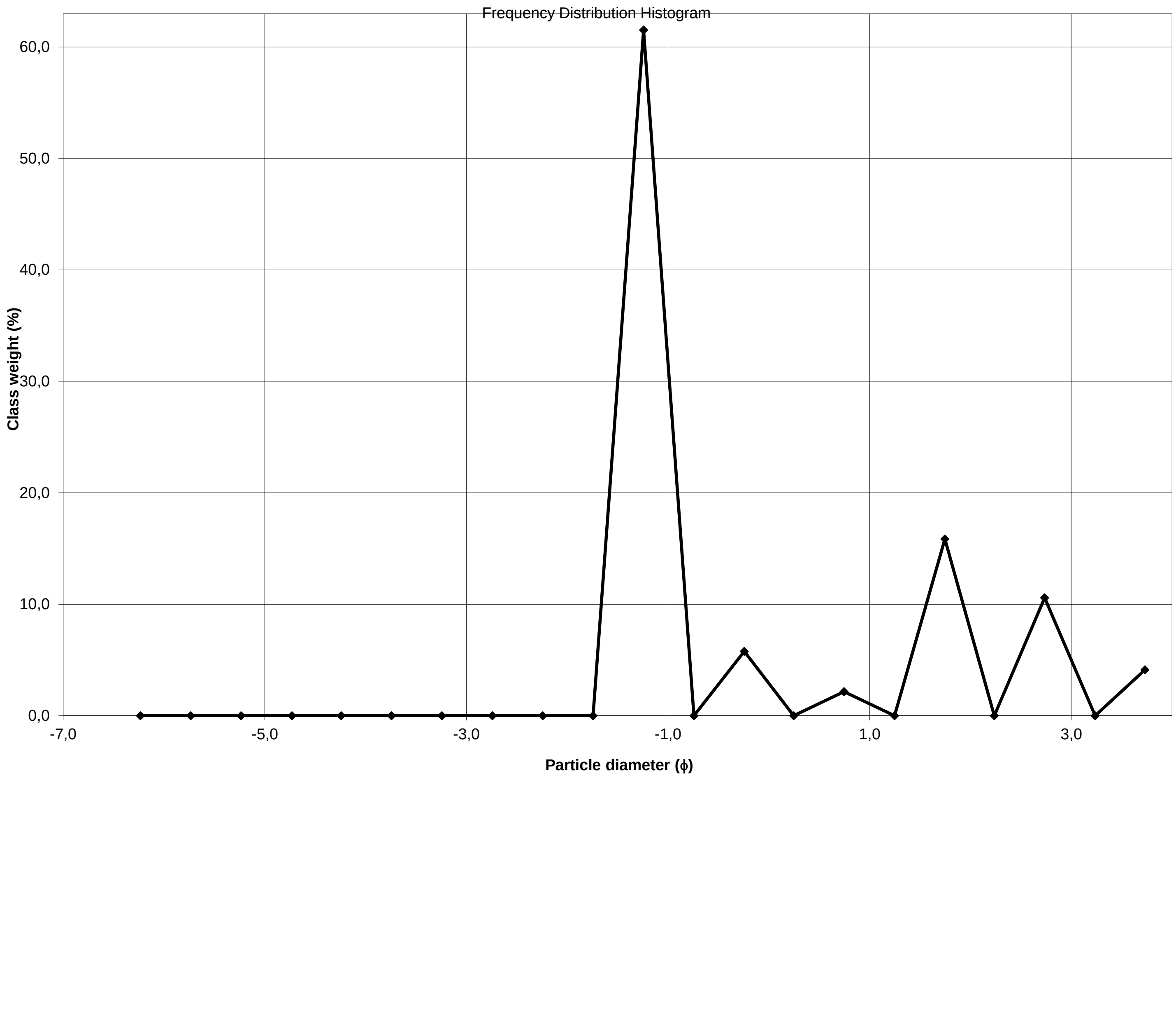
Frequency Distribution Histogram
Class weight (%)
60,0
50,0
40,0
30,0
20,0
10,0
0,0
-7,0
-5,0
-3,0
-1,0
1,0
3,0
Particle diameter (ϕ)

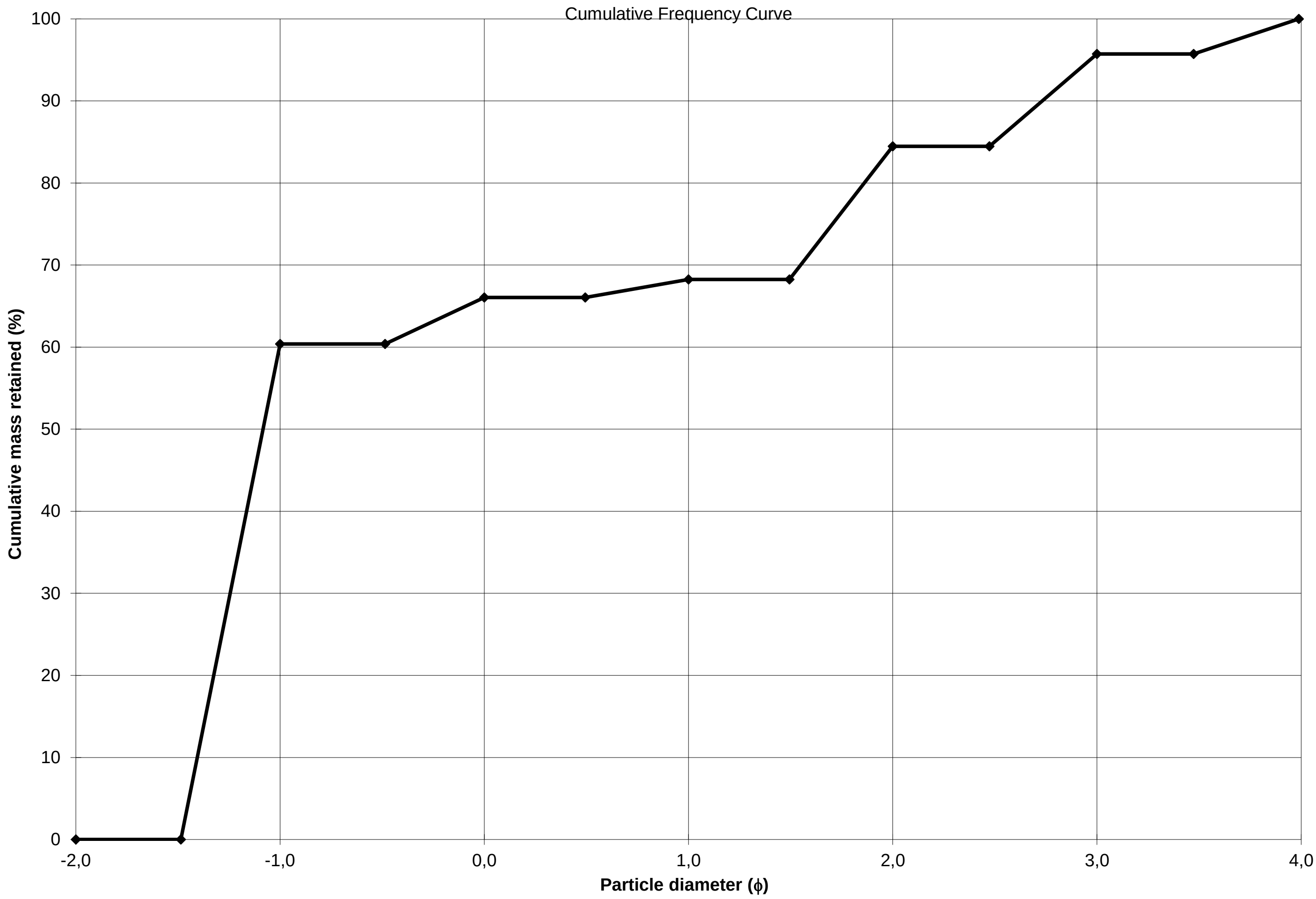
Cumulative Frequency Curve
100
90
80
70
60
50
40
30
20
10
0
Cumulative mass retained (%)
-2,0
-1,0
0,0
1,0
2,0
3,0
4,0
Particle diameter (ϕ)

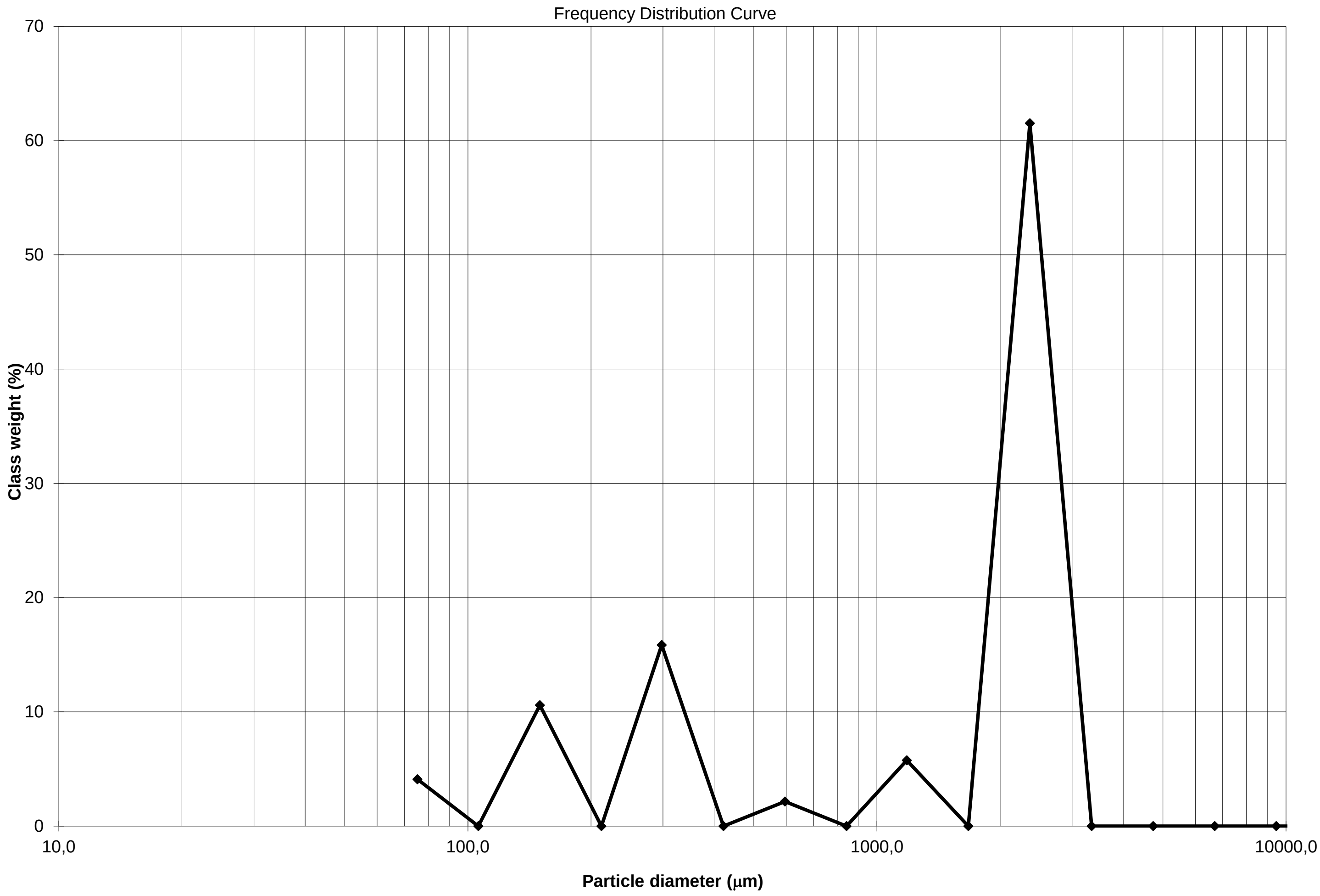
Frequency Distribution Curve
Class weight (%)
70
60
50
40
30
20
10
0
10,0
100,0
1000,0
10000,0
Particle diameter (μm)

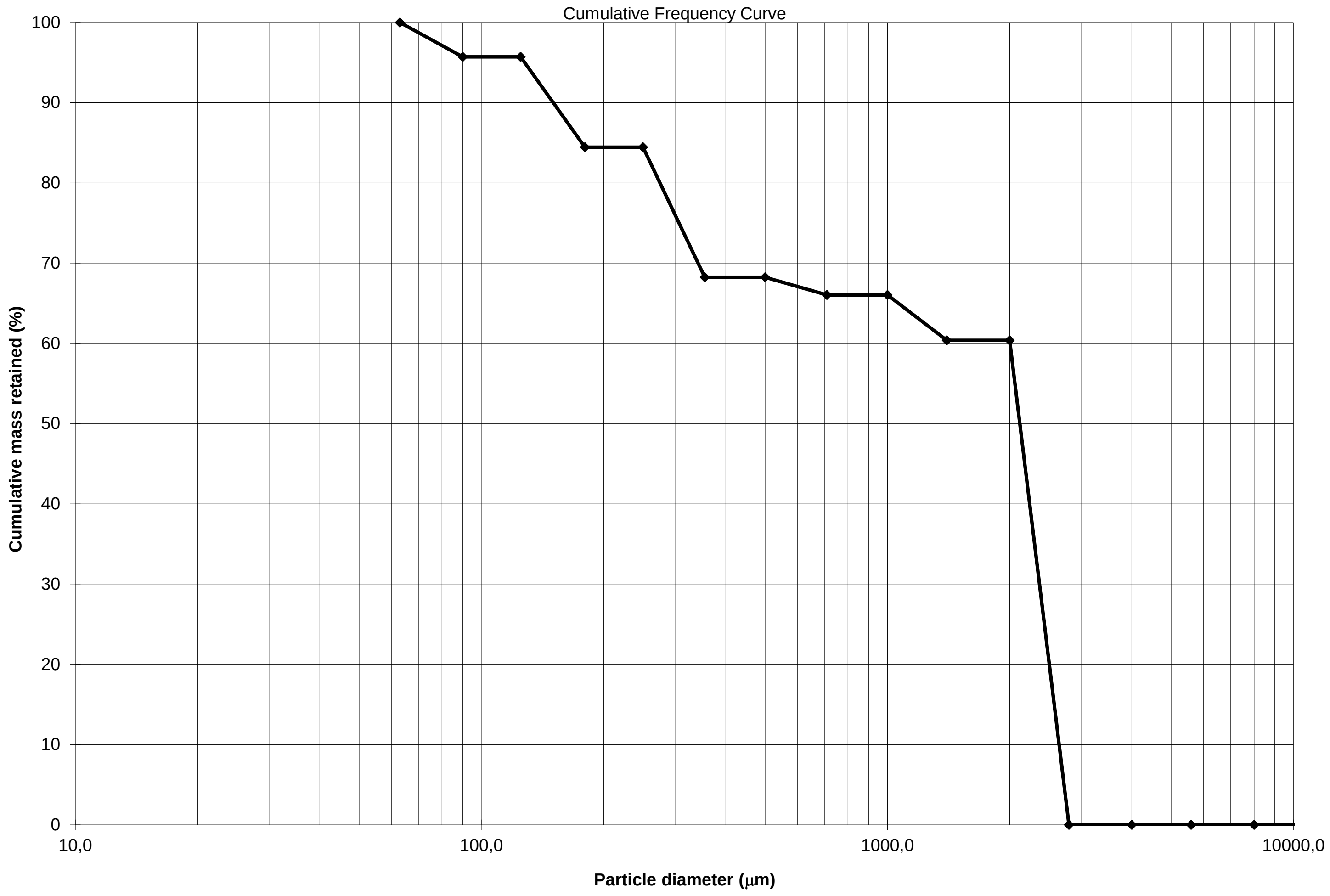
Cumulative Frequency Curve
Cumulative mass retained (%)
100
90
80
70
60
50
40
30
20
10
0
10,0
100,0
1000,0
10000,0
Particle diameter (μm)

Regierung von Oberbayern

Regierung von Oberbayern ◆ 80534 München

Herrn
Mario Bubl
Feldstraße 3
84503 Altötting

Bearbeitet von	Telefon / Fax	Zimmer	E-Mail
Sigrid Rossiwal	+49 (89) 2176-2875 / -402875	2214	Sigrid.Rossiwal@reg-ob.bayern.de
Ihr Zeichen	**Ihre Nachricht vom**	**Unser Geschäftszeichen**	**München,**
	01.08.2017	55.1-8693-AÖ-2-2017	04.08.2017

Naturschutzgesetze;
Befreiung von den Verboten der Verordnung über das Naturschutzgebiet (NSG) „Untere Alz", Landkreis Altötting
Entnahme von Flusssedimentproben des Alzufers

Sehr geehrter Herr Bubl,

wir haben Ihren Antrag vom 01.08.2017 sachlich und rechtlich geprüft und erlassen folgenden

Bescheid:

1. Die naturschutzrechtliche Befreiung von den Verboten der Verordnung über das Naturschutzgebiet „Untere Alz", Landkreis Altötting, für die Entnahme von Flusssedimentproben vom Alzufer im Rahmen Ihrer Bachelorarbeit wird erteilt.

2. Für die unter Nr. 1 erteilte naturschutzrechtliche Befreiung werden folgende Nebenbestimmungen festgesetzt:

2.1 Die naturschutzrechtliche Befreiung wird befristet bis zum **31.12.2017**.

2.2 Die Befreiung ist jederzeit widerrufbar und mit folgenden Auflagen verbunden:

2.2.1 Die untere Naturschutzbehörde am Landratsamt Altötting ist vorab über die genauen Befahrungstermine zu informieren.

2.2.2 Publikationen/Berichte und die Bachelorarbeit, die sich aus den Untersuchungen ergeben, sind der Regierung von Oberbayern kostenfrei zu übermitteln. Die Übermittlung ist auch elektronisch möglich.

2.2.3 Dieser Bescheid ist vor Ort mitzuführen und berechtigten Personen auf Verlangen vorzuzeigen.

2.3 Die Regierung von Oberbayern behält sich die nachträgliche Aufnahme, Änderung oder Ergänzung von Auflagen vor.

3. Sie haben als Antragssteller die Kosten des Verfahrens zu tragen.

4. Es werden keine Kosten erhoben.

Hinweis:
In den Naturschutzgebietsverordnung „Untere Alz“ sind keine Befahrungsregelungen/-einschränkungen für Boote enthalten.

Gründe:

I.

Mit Email vom 01.08.2017 beantragten Sie die entsprechende naturschutzrechtliche Befreiung von den Verboten der Naturschutzgebietsverordnung „Untere Alz“.

An der Universität Wien, Erdwissenschaften, arbeiten Sie an Ihrer Bachelorarbeit, in welcher Sie Mikroplastik in den Flusssedimenten der Alzufer entlang des gesamten Flussverlaufs nachweisen möchten. Im Rahmen dieses Projekts wollen Sie Flusssedimentproben entnehmen und dazu die Alz mit einem unmotorisierten Schlauchboot befahren. Die Befahrung mit soll im Zeitraum 09.08. bis 09.09.2017 stattfinden.

Von einer Mitwirkung der anerkannten Naturschutzvereinigungen im Rahmen des naturschutzrechtlichen Verfahrens gem. § 63 Abs. 2 Nr. 5 BNatSchG wurde abgesehen, da bei Einhaltung der Auflagen nur geringfügige Auswirkungen auf Natur und Landschaft zu erwarten sind, vgl. § 63 Abs. 4 BNatSchG i.V.m. Art. 45 Satz 1 BayNatSchG.

II.

1. Die Regierung von Oberbayern ist zur Entscheidung über die Befreiung gemäß § 6 der Naturschutzgebietsverordnung „Untere Alz“ i.V.m. Art. 56 Satz 1 BayNatSchG sachlich zuständig. Die örtliche Zuständigkeit ergibt sich aus Art. 3 Abs. 1 Nr. 1 des Bayer. Verwaltungsverfahrensgesetzes - BayVwVfG -.

2. Das geplante Vorhaben liegt in dem Naturschutzgebiet „Untere Alz“, worin es nach § 4 Abs. 1 Nr. 2 der NSG-VO verboten ist, Bodenbestandteile abzubauen, Aufschüttungen, Ablagerungen, Grabungen, Sprengungen oder Bohrungen vorzunehmen oder die Bodengestalt in sonstiger Weise zu verändern.

Da Ausnahmen nach § 5 Abs. 1 der Naturschutzgebietsverordnung hier nicht zutreffen, ist eine Befreiung nach § 6 der Naturschutzgebietsverordnung i. V. m. Art. 56 BayNatSchG und § 67 BNatSchG erforderlich.

Die Regierung von Oberbayern erteilt in vorliegendem Einzelfall die naturschutzrechtliche Befreiung von dem in den NSG-VO angeführten Verbot, da dies aus Gründen des überwiegenden öffentlichen Interesses notwendig ist, § 67 Abs. 1 Satz 1 Nr. 1 BNatSchG.
Die Untersuchungen im Rahmen Ihrer Bachelorarbeit liegen im öffentlichen Interesse und überwiegende Gründe des allgemeinen Wohls sind unter Berücksichtigung der festgelegten Auflagen und der dadurch verbleibenden geringen und zeitlich befristeten Auswirkungen des Projekts zu bejahen. Zudem sind die Bruten der Flussregenpfeifer bereits abgeschlossen, sodass Störungen ausgeschlossen sind.

3. Für das örtliche FFH-Gebiet 7742-371 „Inn und Untere Alz“ sind unter Beachtung der Auflagen erhebliche Beeinträchtigungen ausgeschlossen. Artenschutzrechtliche Verbote des § 44 BNatSchG werden ebenfalls nicht verwirklicht.

4. Die Zulässigkeit von Nebenbestimmungen ergibt sich aus § 67 Abs. 3 Satz 1 BNatSchG i. V. m. Art. 36 Abs. 2 BayVwVfG.

4.1 Die Befristung, zulässig nach § 67 Abs. 3 Satz 1 BNatSchG i. V. m. Art. 36 Abs. 2 Nr. 1 BayVwVfG ist notwendig, da eine Nutzung nur für die Laufzeit des Forschungsprojektes befreit werden kann und für eine darüber hinaus gehende Befreiung Gründe des öffentlichen Interesses derzeit nicht erkennbar sind.

4.2 Die Zulässigkeit der Auflagen ergibt sich aus § 67 Abs. 3 Satz 1 BNatSchG i.V.m. Art. 36 Abs. 2 Nr. 4 BayVwVfG. Sie sind notwendig, geeignet und erforderlich, damit die Beeinträchtigung von Natur und Landschaft in dem Naturschutzgebiet „Untere Alz“ soweit wie möglich vermieden werden kann.

4.3 Die Zulässigkeit des Auflagenvorbehalts ergibt sich aus § 67 Abs. 3 Satz 1 BNatSchG i.V.m. Art. 36 Abs. 2 Nr. 5 BayVwVfG. Er ist notwendig, da nicht mit Sicherheit ausgeschlossen werden kann, dass mit dem Vorhaben und seinen Begleiterscheinungen Natur und Landschaft, in einer Weise beeinträchtigt werden, die nicht mehr hinnehmbar ist. Tritt dieser Fall ein, so ist mit einer nachträglichen Aufnahme, Änderung oder Ergänzung von Auflagen zu rechnen.

4.4 Der Widerrufsvorbehalt stützt sich auf § 67 Abs. 3 Satz 1 BNatSchG i. V. m. Art. 36 Abs. 2 Nr. 3 BayVwVfG. Die Befreiung wird widerrufen, wenn auch durch die nachträgliche Aufnahme, Änderung oder Ergänzung von Auflagen etwaige Beeinträchtigungen für Natur und Landschaft nicht auf ein annehmbares Maß reduziert werden können.

5. Diese Befreiung gilt nur für die vorgenannten naturschutzrechtlichen Verbote. Anderweitige Erlaubnisse und Rechte Dritter (z. B. Grundeigentümer) werden dadurch nicht berührt.

6. Die Kostenentscheidung beruht auf Art. 1, 2, und 4 des Kostengesetzes (KG).

<u>Rechtsbehelfsbelehrung</u>

Gegen diesen Bescheid können Sie **Klage** erheben. Die Klage müssen Sie **innerhalb eines Monats nach Bekanntgabe dieses Bescheides** beim

Bayerischen Verwaltungsgericht München,
Bayerstraße 30, 80335 München
(Postanschrift: Postfach 20 05 43, 80005 München),

schriftlich oder zur Niederschrift des Urkundsbeamten der Geschäftsstelle dieses Gerichts erheben. Die Klage kann beim Bayerischen Verwaltungsgericht München auch **elektronisch** nach Maßgabe der der Internetpräsenz der Verwaltungsgerichtsbarkeit (www.vgh.bayern.de) zu entnehmenden Bedingungen erhoben werden. **In der Klage müssen Sie den Kläger, den Beklagten** (Freistaat Bayern) **und den Gegenstand des Klagebegehrens bezeichnen**, ferner sollen Sie einen bestimmten Antrag stellen und die zur Begründung dienenden Tatsachen und Beweismittel angeben. Der Klageschrift sollen Sie diesen Bescheid beifügen (in Urschrift, in Abschrift oder in Ablichtung), ferner zwei Abschriften oder Ablichtungen der Klageschrift für die übrigen Beteiligten.

Hinweise zur Rechtsbehelfsbelehrung

- Die Einlegung eines Rechtsbehelfs per einfacher E-Mail ist nicht zugelassen und entfaltet keine rechtliche Wirkungen!
- Nähere Informationen zur elektronischen Klageerhebung sind der Internetpräsenz der Bayerischen Verwaltungsgerichtsbarkeit (www.vgh.bayern.de) zu entnehmen.
- Kraft Bundesrechts ist bei Prozessverfahren vor den Verwaltungsgerichten grundsätzlich ein Gebührenvorschuss zu entrichten.

Mit freundlichen Grüßen

Gez.
Efimenko
Regierungsrätin